ISSN 1028-8546

Azərbaycan Milli Elmlər Akademiyası
Fizika-Riyaziyyat və Texnika Elmləri Bölməsi
Fizika İnstitutu

1-2

Fizika

Cild
XII
2006

Bakı ✵ Elm

INFLUENCE OF Ga PARTIAL SUBSTITUTION IN $TlGaS_2$ FOR Mn ON DIELECTRIC PROPERTIES

S.N. MUSTAFAEVA, Sh.D. ALIZADE
Institute of Physics, Azerbaijan National Academy of Sciences
Baku AZ-1143, H.Javid av., 33

Frequency dependence of the dissipation factor $tan\delta$, the permittivity ε, and the ac conductivity σ_{ac} across the layers in the frequency range $f = 5\cdot10^4 \div 3{,}5\cdot10^7$ Hz was studied in layered $TlGa_{1-x}Mn_xS_2$ single crystals (x = 0,01; 0,03). In the alternate electric fields, the ac conductivity obeyed the $f^{0,8}$ law at $f = 5\cdot10^4 \div 3{,}5\cdot10^7$ Hz. It was established that the mechanism of the ac charge transport across the layers in $TlGa_{1-x}Mn_xS_2$ single crystals is hopping over localized states near the Fermi level. Estimations yielded the following values of the parameters: the density of states at the Fermi level $N_f = 9{,}9\cdot10^{18}$ $eV^{-1}\cdot cm^{-3}$ for $TlGa_{0,99}Mn_{0,01}S_2$ and $8{,}1\cdot10^{18}$ $eV^{-1}\cdot cm^{-3}$ for $TlGa_{0,97}Mn_{0,03}S_2$; the average time of charge carrier hopping between localized states $\tau = 5{,}7\cdot10^{-2}$μs; average hopping distance R = 77Å for both crystals.

Introduction

$TlGaS_2$ single crystals are representatives of layered wide-band semiconductors with high electric resistivity ($\rho \approx 10^{10}$Ohm·cm at 300K) [1]. In [1] it is established by experiments that at $T \le 200$K in $TlGaS_2$ single crystals along C-axis in dc electric field hopping conductivity with alternating length of jump in localized states near the Fermi level is taken place. In ac electric fields frequency dispersion of dielectric coefficients of $TlGaS_2$ single crystals was observed [2]. In [3] the influence of γ-radiation on dielectric permittivity and electric conductivity of $TlGaS_2$ crystals was investigated at $10^2 \div 10^6$ Hz. The influence of intercalation of $TlGaS_2$ with lithium ions on dielectric properties of obtained crystals was studied in [4].

The aim of the present paper is to study the influence of Ga partial substitution in $TlGaS_2$ for Mn on dielectric properties of obtained crystals in alternate electric fields.

Sample preparation and experimental technique

Synthesis of $TlGa_{1-x}Mn_xS_2$ (x = 0,01; 0,03) produced in quartz ampoules, evacuated to the pressure 10^{-3} Pa. Synthesis of samples has been carried out at interaction of initial elements (Tl, Ga, Mn, S) of high purity degree. Technology of growth of these single crystals has been worked out. Synthesized samples and their single crystals were exposed to roentgenphase analysis, which was carried out at diffractometer DRON-3M in $Cu_{K\alpha}$ emission (Ni filter, λ_α = 1,5418Å). Diffractogramms were recorded continuously, diffraction angles were determined by method of measurement according peak of intensity. Errors of reflection angles determination did not exceed 0,02°. X-ray analysis showed that $TlGa_{1-x}Mn_xS_2$ single crystals are crystallized in tetragonal structure with elementary cell parameters a = 7,2692Å; c = 29,8981Å; $\rho_x = 5{,}684 g/cm^3$ for x = 0,01 and a = 7,2658Å; c = 29,9392Å; $\rho_x = 5{,}676 g/cm^3$ for x = 0,03.

Samples from $TlGa_{1-x}Mn_xS_2$ for measurements are obtained by spalling along C-axis of the natural spall from massive crystal and have a thickness $(2.0\div 2.5)\cdot10^{-2}$ cm. $TlGa_{1-x}Mn_xS_2$ samples formed flat capacitors whose plane was perpendicular to the crystalline C-axis. The capacitor plate area was $6\cdot10^{-2} \div 8\cdot10^{-2}$ cm^2. Ohmic contacts of samples are made by Ag paste.

Measurements of the dielectric coefficients of $TlGa_{1-x}Mn_xS_2$ single crystals were performed at fixed frequencies in the range $5\cdot10^4 \div 3.5\cdot10^7$ Hz by the resonant method using a TESLA BM 560 Q-meter. For electrical measurements, the samples were placed in a specially constructed screened cell. An ac electric field was applied across the natural layers of $TlGa_{1-x}Mn_xS_2$ single crystals. The amplitude of the applied fields corresponded to the Ohmic region of the current-voltage characteristics of $TlGa_{1-x}Mn_xS_2$ samples. All measurements were performed at T = 300K. The accuracy in determining the resonance capacitance and the quality factor $Q = 1/tan\delta$ of the measuring circuit was limited by errors related to the resolution of the device readings. The accuracy of the capacitor graduation was ±0.1pF. The reproducibility of the resonance position was ± 0.2pF in capacitance and ± (1.0 – 1.5) scale divisions in quality factor.

We measured the electric capacitance of $TlGa_{1-x}Mn_xS_2$ samples in the frequency range $5\cdot10^4 – 3{,}5\cdot10^7$Hz. Using the measured capacities of samples, we calculated the permittivity ε at different frequencies.

Results and discussion

Fig.1 shows the experimental frequency dependences of the dielectric permittivity for $TlGa_{1-x}Mn_xS_2$ (x = 0; 0,01; 0,03). It is seen from Fig.1 that for $TlGaS_2$ single crystal (curve 1) significant variation of ε was not observed at studied interval of frequencies (ε = 26 ÷ 30). At Ga partial substitution in $TlGaS_2$ for Mn ε of obtained samples decreased with the rise of frequency from $5\cdot10^4$ to $3{,}5\cdot10^7$Hz. For example, ε of $TlGa_{1-x}Mn_xS_2$ single crystal decreased by 5 times for x = 0,01 and 2.5 times for x = 0,03.

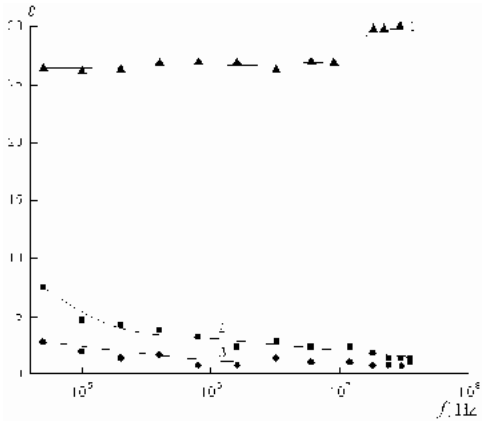

Fig.1. Frequency dispersion of the permittivity of $TlGaS_2$ (1); $TlGa_{0,99}Mn_{0,01}S_2$ (2) and $TlGa_{0,97}Mn_{0,03}S_2$ (3) at T=300K.

Observed in experiments monotonic decrease of ε with rise of frequency (Fig.1, curves 2 and 3) is evidence of relaxation dispersion.

Experimental frequency dependences of the dissipation factor tanδ for $TlGa_{1-x}Mn_xS_2$ (x = 0,01; 0,03) were characterized with presence of maximums (Table)

Table

tanδ values vs frequency for $TlGa_{1-x}Mn_xS_2$ single crystals

f, Hz	*tanδ* ·10^4	
	x = 0,01	x = 0,03
5·10^4	1052	2449
10^5	1660	2750
2·10^5	1602	3024
4·10^5	1478	2130
8·10^5	1427	3550
1,6·10^6	1791	3058
3,2·10^6	1252	1586
6·10^6	1299	1695
1,2·10^7	1150	1519
1,8·10^7	1618	2180
2,4·10^7	1877	1938
3,0·10^7	1937	2335
3,5·10^7	1917	1438

The maximums on *tanδ(f)* – dependences also confirm the fact of presence of relaxation losses.

Fig.2 shows the dependences of dielectric permittivity of $TlGa_{1-x}Mn_xS_2$ single crystals on their composition at various frequencies of alternate electric field: 5·10^4; 10^5; 3,2·10^6 and 3,0·10^7 Hz (curves 1-4). It is seen from Fig.2 that introduction of Mn to $TlGaS_2$ crystals leads to significant decrease of their dielectric permittivity at all pointed frequencies.

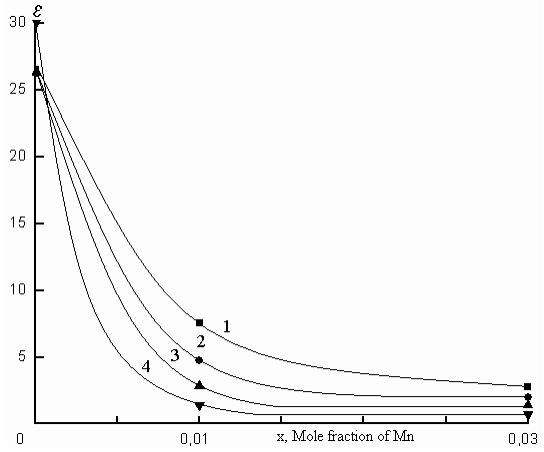

Fig.2. Dependence of the permittivity on composition of $TlGa_{1-x}Mn_xS_2$ single crystals at various frequencies of alternate electric field f, Hz: 1 - 5·10^4; 2 – 10^5; 3 – 3,2·10^6; 4 - 3·10^7.

Frequency dependence of $\varepsilon'' = \varepsilon \cdot tan\delta$ for $TlGa_{1-x}Mn_xS_2$ crystals is given in Fig.3. As it is seen from Fig.3 Ga partial substitution in $TlGaS_2$ crystals for Mn leads to modification of dispersion curves *ε″(f).* In $TlGaS_2$ the *ε″(f)* curve has two branches: a weakly descending one at f = 5·10^4 – 10^{6}Hz and a rising one at f >10^{6}Hz. In $TlGa_{1-x}Mn_xS_2$ frequency dependences of ε'' differ from *ε″(f)* curve in $TlGaS_2$; they were characterized by significant descending up to 10^{7}Hz, after that ε″ values are practically independent on frequency.

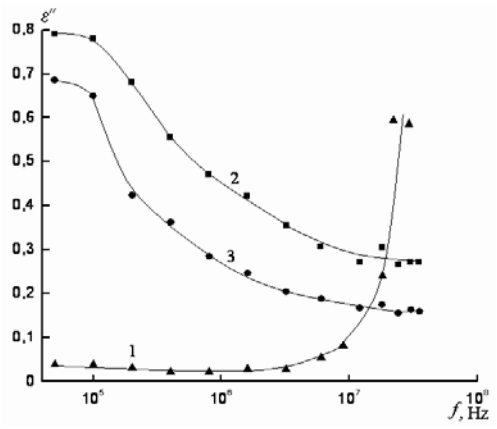

Fig.3. Frequency dependence of ε'' for $TlGaS_2$ (1); $TlGa_{0,99}Mn_{0,01}S_2$ (2) and $TlGa_{0,97}Mn_{0,03}S_2$ (3).

Fig.4 shows the experimentally measured frequency dependence of the ac conductivity of $TlGa_{1-x}Mn_xS_2$ single crystals at T = 300K. The ac conductivity σ_{ac} of $TlGaS_2$ varies as $f^{0,8}$ in the frequency range 5·10^4 – 10^{6}Hz (curve 1). At high frequencies (f = 10^6 ÷ 3·10^{7}Hz) σ_{ac} of $TlGaS_2$ obeyed the f^2 – law. As it was shown in [5] the conductivity proportional to f^2 is related to optical transitions in semiconductors and is dominant at high frequencies.

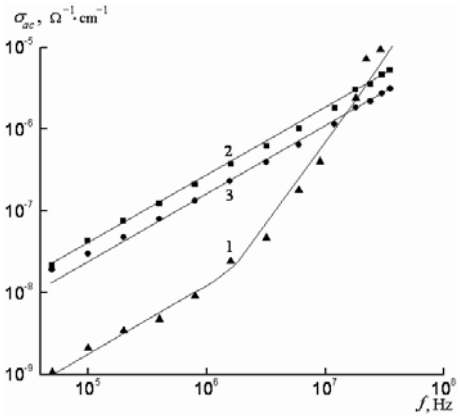

Fig.4. Frequency - dependent *ac* conductivities of $TlGa_{1-x}Mn_xS_2$ single crystals at room temperature: curve 1 – x = 0; 2 – x = 0,01; 3 – x = 0,03.

Dispersion curves $\sigma_{ac}(f)$ of $TlGa_{1-x}Mn_xS_2$ samples (Fig.4, curves 2 and 3) were characterized by $f^{0,8}$ – law at all investigated frequencies. The $\sigma_{ac} \sim f^{0,8}$ dependence indicates that the mechanism of charge transport in $TlGa_{1-x}Mn_xS_2$ single crystals in the frequency range 5·10^4 – 3,5·10^{7}Hz is hopping over localized states near the Fermi level. This charge transport mechanism is characterized by the following expression obtained in [6]:

$$\sigma_{ac}(f) = \frac{\pi^3}{96} \cdot e^2 kTN_F^2 a^5 f \left[\ln \frac{\nu_{ph}}{f} \right]^4, \qquad (1)$$

where e is the elementary charge, k is the Boltzmann constant, N_F is the density of localized states near the Fermi

level, $a = 1/\alpha$ is the localization length, α is the decay parameter of the wave function of a localized charge carrier, $\psi \sim e^{-\alpha r}$, and ν_{ph} is the phonon frequency.

Using expression (1), we can calculate the density of states at the Fermi level from the measured values of the conductivity $\sigma_{ac}(f)$. Calculated values of N_F for $TlGa_{1-x}Mn_xS_2$ (x = 0; 0,01; 0,03) single crystals were equal to $2{,}1\cdot10^{18}$; $9{,}9\cdot10^{18}$ and $8{,}1\cdot10^{18}$ $eV^{-1}\cdot cm^{-3}$, correspondingly (localization radius chosen as 14Å, in analogy with the GaS single crystal [7], which is a double analog of $TlGaS_2$).

The theory of ac hopping conductivity provides an opportunity to determine the average time τ of charge carrier hopping from one localized state to another using the formula [5]:

$$\tau^{-1} = \nu_{ph} \exp(-2R\alpha), \qquad (2)$$

where R is the average hopping distance,

$$R = \frac{1}{2\alpha} \ln \frac{\nu_{ph}}{f} \qquad (3)$$

Calculated values of τ and R for both $TlGa_{1-x}Mn_xS_2$ (x = 0,01; 0,03) single crystals were equal to $5{,}7\cdot10^{-2}$μs and 77Å, correspondingly. For $TlGaS_2$ R = 103Å [2].

Knowing N_F and R from [5]:

$$\frac{4\pi}{3} R^3 N_F \cdot \frac{\Delta E}{2} = 1 \qquad (4)$$

we estimate scattering of trap states near the Fermi level: ΔE = 0,11eV for $TlGa_{0,99}Mn_{0,01}S_2$ and 0,13eV for $TlGa_{0,97}Mn_{0,03}S_2$ single crystals.

By formula:

$$N_t = N_F \cdot \Delta E \qquad (5)$$

we can determine the concentration of deep traps in $TlGa_{1-x}Mn_xS_2$: $N_t \approx 10^{17} cm^{-3}$ for both compositions x = 0,01 and 0,03.

Conclusions

Thus, the results of high-frequency dielectric measurements on $TlGa_{1-x}Mn_xS_2$ single crystals provided an opportunity to determine the mechanisms of dielectric losses and charge transport, and also to evaluate the density of states at the Fermi level; the average time of charge carrier hopping between localized states, average hopping distance, scattering of trap states near the Fermi level; concentration of deep traps.

[1] *S.N. Mustafaeva, V.A.Aliev, M.M.Asadov*. FTT, 1998, v.40, № 4, p.612.
[2] *S.N. Mustafaeva*. FTT, 2004, v.46, № 6, p.979.
[3] *A.U. Sheleg, K.V. Iodkovskaya, N.F. Kurilovich*, FTT, 2003, v.45, № 1, p. 68.
[4] *S.N. Mustafaeva*. Power Engineering Problems. 2004, № 2, p.70.
[5] *N.Mott, E.Davis*. Electron processes in noncrystalline materials. Clarendon Press, Oxford, 1971.
[6] *M.Pollak*. Phil. Mag., 1971, v.23, p.519.
[7] *V.Augelli, C.Manfredotti, R.Murri, et.al*, Nuovo Cimento, 1977, v. 38, № 2, p.327.

S.N. Mustafayeva, Ş.D. Əlizadə

$TlGaS_2$-DƏ Ga-UN QİSMƏN Mn-LA ƏVƏZ EDİLMƏSİNİN DİELEKTRİK XASSƏLƏRİNƏ TƏSİRİ

$TlGa_{1-x}Mn_xS_2$ ($0 \le x \le 0{,}03$) monokristallarında $f = 5\cdot10^4 \div 3{,}5\cdot10^7$Hs tezlik intervalında dielektrik nüfuzluğunun həqiqi (ε) və xəyali (ε'') toplananları və laylara perpendikulyar istiqamətdə (σ_{ac}) keçiricilik öyrənilmişdir. $TlGa_{1-x}Mn_xS_2$ monokristalında relaksasiya dispersiyasının mövcudluğu müəyyən edilmişdir. $TlGaS_2$ monokristalında Ga ionlarının qismən Mn ionları ilə əvəz edilməsi onun dielektrik nüfuzluğunun azalmasına və dispersiya əyrilərinin $\varepsilon''(f)$ modifikasiya olunmasına səbəb olur. $TlGa_{1-x}Mn_xS_2$ monokristalı üçün ölçülən tezlik intervalında ac- keçiriciliyi $\sigma_{ac} \sim f^{0,8}$ qanunauyğunluğa tabe olur ki, bu da Fermi səviyyəsinə yaxın hallarda lokallaşmış yükdaşıyıcıların sıçrayışla hərəkət etməsinin xarakterik xüsusiyyətidir. Fermi səviyyəsi ətrafında yerləşən halların sıxlığı (N_F), enerjisi (ΔE), sıçrayışlar arası məsafə və orta sıçrayış vaxtı təyin edilmişdir.

С.Н. Мустафаева, Ш.Д. Ализаде

ВЛИЯНИЕ ЧАСТИЧНОГО ЗАМЕЩЕНИЯ Ga НА Mn В $TlGaS_2$ НА ДИЭЛЕКТРИЧЕСКИЕ СВОЙСТВА

В слоистых монокристаллах $TlGa_{1-x}Mn_xS_2$ ($0 \le x \le 0{,}03$) исследована частотная дисперсия тангенса угла диэлектрических потерь ($tg\delta$), действительной (ε) и мнимой (ε'') составляющих комплексной диэлектрической проницаемости, ac - проводимости (σ_{ac}) поперек слоев в области частот $f = 5\cdot10^4 \div 3{,}5\cdot10^7$Гц. Установлено, что в изученных монокристаллах $TlGa_{1-x}Mn_xS_2$ имеет место релаксационная дисперсия. Частичное замещение галлия в монокристаллах $TlGaS_2$ марганцем приводит к уменьшению их диэлектрической проницаемости и модифицированию дисперсионных кривых $\varepsilon''(f)$. Во всем изученном диапазоне частот ac-проводимость монокристаллов $TlGa_{1-x}Mn_xS_2$ подчинялась закономерности $\sigma_{ac} \sim f^{0,8}$, характерной для прыжкового механизма переноса заряда по локализованным вблизи уровня Ферми состояниям. Оценены плотность (N_F) и разброс (ΔE) состояний, лежащих в окрестности уровня Ферми, среднее время и расстояние прыжков.

Received: 20.12.05

$(SnSe)_{1-x}(GdSe)_x(0,0\leq x\leq 2,0)$ SİSTEM BƏRK MƏHLULLARININ RENTGENOQRAFİK TƏDQİQİ VƏ FİZİKİ PARAMETRLƏRİN TƏRKİB ASILILIĞI

M.S. MURQUZOVA, B.A. TAHİROV
AMEA Fizika İnstitutu
Azərbaycan, Bakı, Az-1143, H. Cavid pr., 33

M.İ. MURQUZOV, Ş.S. İSMAYILOV, C.İ. HÜSEYNOV
Azərbaycan Dövlət Pedaqoji Universiteti,
Bakı, Az-1000, U.Hacıbəyov küç,. 4

Diferensial termik, rentgen faza və mikrobərkliyin tədqiqi öyrənilməsi yolu ilə $(SnSe)_{1-x}(GdSe)_x(0,0\leq x\leq 2,0)$ bərk məhlulları tədqiq edilmişdir. Müəyyən olunmuşdur ki, bu tərkiblər SnSe birləşməsi əsasında qalayın (Sn) qismən qadalinium (Gd) atomlarıyla əvəz olunması ilə kristallaşır. Otaq temperaturunda termo e.h.q. (α); elektrik keçiriciliyi (σ); Xoll əmsalı (R_x) və yükdaşıyıcıların Xoll yürüklüyünün (U_x) tərkib asılılıqları tədqiq edilmişdir. Tədqiq etdiyimiz nümunələr qismən kompensasiya olunmuş *p* tip yarımkeçiricidirlər.

Elm və texnikanın müxtəlif sahələrinin sürətli inkişafı geniş spektrli fiziki xassələrə malik yeni perspektiv materialların alınması və tədqiqinə böyük stimul yaradır. Nadir torpaq metallarının iştirakı ilə olan bərk məhlullar da bu qəbildəndir. Çünki bu metal atomlarının 4*f* elektron səviyyələrinin mövcudluğu və *4f-5d* hallarının yaxınlığı onların iştirakı ilə alınan ərinti və birləşmələri maraqlı tədqiqat obyektinə çevirir [1-3]. Müəyyən edilmişdir ki, $(SnSe)_{1-x}(GdSe)_x$ sisteminin bərk məhlullarından bəzi tərkiblərin Xoll əmsalının R_x; xüsusi müqavimətinin ρ və maqnit müqavimətinin $\frac{\Delta\rho}{\rho_c}$ temperatur asılılığında T=285÷310 K-də anomal dəyişmələr müşahidə olunmuşdur. Bu dəyişmələrin səbəbini və SnSe birləşməsinin quruluşunda olan məxsusi defektlərlə bağlılığı aydın deyil. Məhz ona görə bu sistemin bərk məhlullarının geniş konsentrasiya intervalında tədqiqinə, kristallik quruluşun öyrənilməsi və fiziki-kimyəvi analizinə, tərkib - xassə arasındakı qanunauyğunluğun aşkar edilməsinə ehtiyac vardır.

İşdə $(SnSe)_{1-x}$-$(GdSe)_x$ sistem bərk ərintilərindən x=0,1; 0,25; 0,50; 1,00; 1,50 və 2,00 mol%-li tərkiblər sintez edilmiş və onların fiziki-kimyəvi analizi, kinetik parametrlərdən: termo e.h.q. - α, elektrik keçiriciliyi - σ, Xoll əmsalı - R_x və yükdaşıyıcıların Xoll yürüklüyünün tərkib asılılıqları öyrənilmişdir. Rentgen faza analizi DPOH-3 markalı rentgen difraktometrində aparılmışdır. $(SnSe)_{1-x}$-$(GdSe)_x$ sistem ərintilərinin ana maddə olan SnSe-də olduğu kimi ortorombik sinqoniyada kristallaşdığı təsdiq olunmuş, uyğun qəfəs parametrləri hesablanmışdır. Differensial termik analiz alçaq tezlikli NTR-73 markalı pirometrdə yerinə yetirilmişdir. Pirometrin sobası 9°S/dəq. sürətlə qızdırılmışdır. Sintez edilmiş ərintilərin mikrobərkliyi PMT-3 markalı metalloqrafik mikroskopla aparılmışdır.

Cədvəl 1

$(SnSe)_{1-x}(GdSe)_x$ $(0,0\leq x\leq 2)$ tərkibli kristalların difraktoqramları (şüalanma CuK$\alpha\lambda$=1,5418Å filtr Ni, 35 kV, 10 mA)

	x=0,5				x=1,0				x=2,0			
№	θ	intensivlik I	$d_{təcr}$	d_{hesab}	θ	intensivlik I	$d_{təcr}$	d_{hesab}	θ	intensivlik I	$d_{təcr}$	d_{hesab}
1	6,87	10	6,4450	-	7,75	15	5,7166	5,7166	6,5	8	6,810	-
2	7,76	13	5,7162	5,7083	9,30	14	4,7702	4,7351	7,70	17	5,7535	3,7259
3	8,50	7	5,2154	-	12,65	10	3,5201	3,4627	12,76	17	3,5154	3,7259
4	10,25	7	4,3322	4,3315	13,25	4	3,3634	-	13,35	7	3,3634	-
5	12,66	13	3,5201	3,4586	14,07	17	3,1710	3,1927	14,00	10	3,1865	3,2042
6	13,25	7	3,3634	-	14,80	4	3,0178	3,0758	14,80	7	3,0178	2,9852
7	14,00	13	3,1865	3,1994	15,66	100	2,8571	2,8571	15,65	100	2,8663	2,8630
8	15,60	100	2,8550	2,8548	19,00	20	2,3678	2,3850	19,00	21	2,3678	2,3918
9	17,90	6	2,5081	-	21,75	12	2,0704	2,0677	19,78	4	2,2791	2,2893
10	19,00	20	2,3678	2,3649	22,24	10	2,0368	2,0327	21,65	10	2,0895	2,0992
11	19,60	6	2,2981	2,2839	23,16	8	1,9600	1,9451	22,20	10	2,0102	2,0129
12	20,75	7	2,1759	2,1652	24,94	19	1,8282	1,8315	23,75	10	1,9140	1,9087
13	21,85	9	2,0613	2,0567	26,08	8	1,7535	1,7536	24,98	17	1,8254	1,8248
14	22,25	9	2,0359	2,0203	27,25	7	1,1702	-	26,00	8	1,7505	1,7479
15	23,76	11	1,9140	1,9035	28,35	4	1,6289	1,6239	27,30	7	1,6807	1,6829
16	24,90	14	1,8309	1,8227	29,00	4	1,5800	1,5802				
17	26,00	7	1,7585	1,7658								
18	26,35	6	1,7429	1,7426								
19	27,30	6	1,6807	1,6791								

Cədvəl 2

SnSe-GdSe sistem ərintilərinin fiziki-kimyəvi parametrləri

№	Tərkib mol%		Termiki qızma effektləri	Xüsusi çəki 10^3q/sm^3		Mikro-bərkliyi, MPa	Qəfəs parametrləri Å		
	SnSe	GdSe		ρ_{pikn}	P_{rent}		*a*	*b*	*c*
1	100	0,0	880	6,18	-	480	4,46	4,19	11,57
2	99,6	0,4	880	6,20	6,40	500	4,73	4,33	11,42
3	99	1,0	875	6,21	6,42	570	4,735	4,34	11,42
4	98	2,0	790,875	6,22	6,41	590	4,736	4,35	11,45
5	97	3,0	760,870	6,23	6,42	650	4,738	4,37	11,47
6	96	4,0	725,865	6,24	6,43	720	4,74	4,38	11,51
7	95	5,0	715,850	6,25	6,43	780	4,75	4,40	11,54

Nümunələrin sıxlığı piknometrik üsulla ölçülmüş və rentgenoqrafik nəticələr əsasında hesablanmışdır.

Nümunələrin fiziki parametrlərini ölçmək üçün onlar həndəsi ölçüləri (3,0x5,0) 20 mm^3 olan paralelepiped şəklində hazırlanmışdır. Ölçmələr kompensasiya üsulu ilə aparılmışdır. Sabit UİP-1 və B5-49 cərəyan mənbəyindən, gərginlik düşgüsünü ölçmək üçün B7-21 və B7-30 markalı universal voltmetrdən, cərəyanı ölçmək üçün Ş4313 markalı, kombinasiyalı cihazdan istifadə olunmuşdur. Nümunələrdən keçən cərəyanın qiyməti maksimum 2,0 mA, nümunə boyunca olan temperatur qradiyenti isə $\Delta T=6\div10$ dərəcə təşkil etmişdir. Xoll əmsalını təyin edərkən sabit elektromaqnitdən istifadə olunmuşdur (H=11000Ers). Termo e.h.q.-ni ölçərkən buraxılan xəta ~2,4%, elektrik keçiriciliyini və Xoll əmsalını təyin edərkən isə 2,7% olmuşdur.

$(SnSe)_{1-x}$-$(GdSe)_x$ sistem ərintilərinin kompleks fiziki-kimyəvi analizinin nəticələri 1-ci cədvəldə verilmişdir. Cədvəldən göründüyü kimi bərk məhlullarda GdSe-nin faizlə miqdarı artıqca kristal qəfəsin elementar özəyinin parametrlərinin zəif artımı, ərintinin ərimə temperaturunun isə azalması müşahidə olunur.

Tərkibdə GdSe-nin 0,0÷3,0 mol% intervalında olduqda rentgenoqrammalardakı xətlərin sürüşməsi SnSe əsasında bərk məhlulların əmələ gəldiyini göstərir. SnSe-ə GdSe-nin əlavə olunması qəfəs parametrlərinin və elementar özəyin həcminin artmasına səbəb olur. Elementar özəyə düşən atomların sayı isə dəyişməz qalır. Elementar özəyin müşahidə olunan genişlənməsi Sn atomlarının qismən böyük radiuslu Gd atomları ilə əvəz edilməsi ilə yaxşı uzlaşması və Veqard qanunun ödənilməsi SnSe əsasında əvəzetmə tipli bərk məhlulların yarandığını söyləməyə imkan verir [4].

2-ci cədvəldə termik qurma effektlərin, xüsusi çəkilərin (piknometrik və rentgenoqrafik), mikrobərkliyin və qəfəs parametrlərinin tərkib asılılıqları verilmişdir. Cədvəldən göründüyü kimi tərkiblərin xüsusi çəkiləri bir o qədərdə dəyişməmişdir. Lakin mikrobərkliyi isə Gd-un miqdarının artması ilə mütənasib artdığı müşahidə olunur. Qəfəs sabitlərinin dəyişməsi isə onu göstərir ki, alınan kristallar qismən deformasiya olunmuş ortorombik quruluşda kristallaşır. Şəkildə termo e.h.q.-α; elektrik keçiriciliyi -σ; Xoll əmsalının - R_x və yük daşıyıcıların Xoll yürüklüyünün tərkib asılılıqları verilmişdir. Qrafiklərdən göründüyü kimi tərkiblərdə GdSe-nin miqdarı artıqca σ və u - Xoll yürüklüyünün qiymətləri mütənasib olaraq azalır. Xoll əmsalının (R_x) qiyməti isə artır. Termo e.h.q.(α) isə artmaq əvəzinə, azalır.

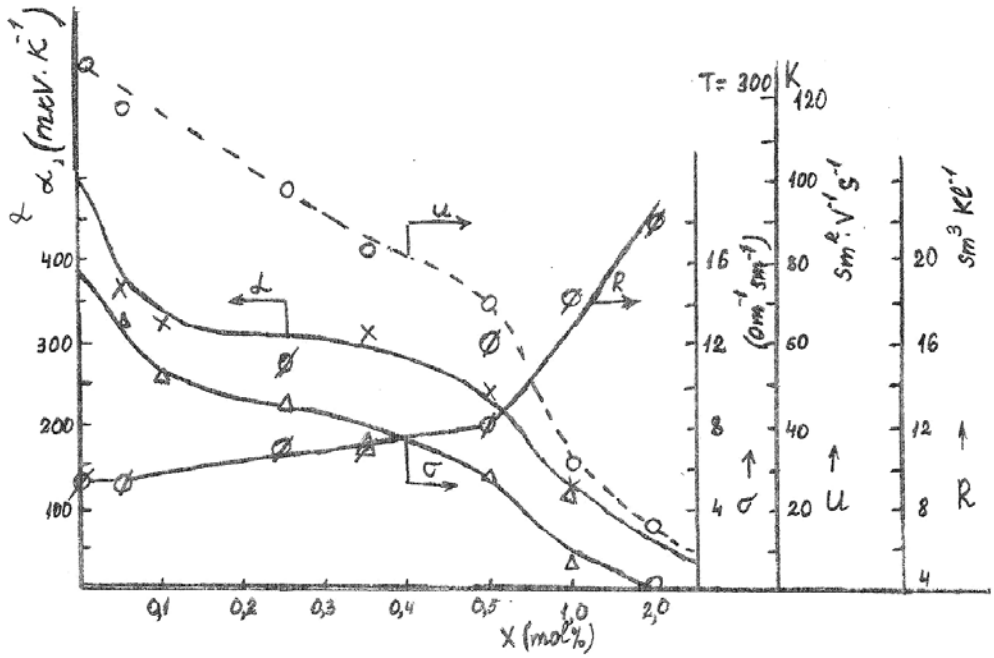

Şəkil 1. $(SnSe)_{1-x}$-$(GdSe)_x$- sistem bərk məhlullarında: 1- termo e.h.q.-(α); 2- elektrik keciriciliyi (σ); 3-Xoll əmsalının – (R_x); 4-Xoll yürüklüyü (U) tərkib asılılığı.T=300K.

TƏCRÜBƏNİN MÜZAKİRƏSİ

Müəyyən olunmuş $(SnSe)_{1-x}$-$(GdSe)_x$ sistem ərintilərinin quruluş xüsusiyyətləri göstərir ki, tədqiq etdiyimiz tərkiblər qalay (Sn) atomlarının qismən qadolinium (Gd) atomları ilə əvəz olunmaqla kristallaşır. Bu əvəz olunma prosesi kristal qəfəsində heterovalent izomorfizm çevrilməsi ilə baş verdiyi ehtimal olunur. Bu halda elektroneytrallığın pozulması üçün eyni valentiyin cəmi saxlanılmaqla ionlar qrupu tərəfidən tənzimlənir [5,6]. İzomorf əvəz olunma prinsipini və kiçik radiuslu ionların polyarizələşməsinin zəifliyini nəzərə alaraq göstərmək olar ki, $(SnSe)_{1-x}$-$(GdSe)_x$ bərk məhlullarının heterovalent əvəzlənməsi valentliyin kompensasiya olunması ilə, xüsusi halda kristal qəfəsi özəklərində yükdaşıyıcıların mübadiləsi hesabına baş verir [6]. Başqa sözlə Gd^{3+} müsbət ionlarının güclü polyarizələşməsi hesabına SnSe quruluşunda Sn^{2+} (ion radiusu $\tau=1,02A^0$) Sn^{4+} (ion radiusu $r=0,74A^0$) ionuna keçməklə tənzimlənir. Bu halda əvəzolunma qrup halında olur, yəni $2(Gd^{3+})$ ionları (Sn^{2+}, Sn^{4+}) ionlarını əvəz edir. Alınan tərkiblər qismən kompensasiya olunmuş yarımkeçirici maddələr olmaqla bərabər onlarda SnSe birləşməsinə məxsus ikiqat defektli quruluşunda ionların yenidən paylanması ilə kristallaşır [3,7].

Elektrik keçiriciliyin (σ) və Xoll əmsalının (R_x) tərkib asılılıqları (şəkil 1) bu göstərilənləri təsdiq edir.

Termo e.h.q.(α)-nin $\alpha=f(x)$ tərkib asılılığında müşahidə olunan qanunauyğunluqdan kənara çıxma isə effektiv kütlənin dəyişməsi və həmdə əlavə zonaların yaranması ilə bağlı olduğu ehtimal olunur [8]. Çünki tərkiblərdə Gd - atomlarının miqdarının artması ilə kompensasiya prosesi getməklə, yükdaşıyıcıların konsentrasiyası azalmasına baxmayaraq α-nın qiyməti azalır. Bu isə zona altı əlavə zonaların yaranması ilə izah oluna bilər.

[1] *A.P.Qurşumov, B.B.Kuliev, A.M.Axmedov i dr*. "Neorqaniçeskiye materialı, 1984, T.20. №7. s.1090-1094. (Rusca)

[2] *M.S.Murquzova, M.İ.Murquzov, Ş.S.İsmayılov*. "Qadolinium elementinin iştirakı ilə SnSe əsasında olan bərk məhlulların qalvanomaqnit xassələri. "Fizika, 2003, jild 9, № 1, səh.59-61.

[3] *M.İ.Murquzov, Ş.S.İsmayılov, R.F.Məmmədova*. "$(SnSe)_{1-x}(LnSe)_x$ (Ln=La,Gd) sistem ərintilərinin bəzi kinetik xassələri". ADPU-nun 2000-ci ildəki konfr. mat., s.64.

[4] *B.F.Ormont*. "Vvedeniye v fiziçeskuyu ximiyu i kristalloximiyu poluprovodnikov. M. 1982, s.528. (Rusca)

[5] *M.İ.Murquzov, A.P.Qurşumov*. "Zakonomernosti vzaimodeystviya v sistemax SnSe-LnSe. Tezisı dokl. V Vsesoyuzn. konf. po fizike i ximii redkozemelnıx poluprovodnikov. Saratov, 1990. (Rusca)

[6] *R.M.Mehra, R.Shyam, P.C.Mathyr*. Magnetoresistence in Amorphous semiconductors. Thin Solid Films. 1983. Vol.100, №2, p.81-109.

[7] *A.P.Qurşumov*. "Fiziko-ximiçeskaya i fiziçeskaya prirodı slojnix poluprovodnikovix materialov na osnove monoselenida olova. Baku, 1991. (Rusca)

[8] *B.M.Askerov*. "Kinetiçeskiy effekti v poluprovodnikax. L., 1971. (Rusca)

М.С. Мургузова, М.И. Мургузов, Ш.С. Исмайылов , Ж.И. Гусейнов, Б.А. Таиров

РЕНТГЕНОГРАФИЧЕСКОЕ ИССЛЕДОВАНИЕ И ИЗУЧЕНИЕ ЗАВИСИМОСТИ ОТ СОСТАВА ФИЗИЧЕСКИХ ПАРАМЕТРОВ СИСТЕМ $(SnSe)_{1-x}(GdSe)_x(0,0\leq x\leq 2,0)$ ТВЕРДЫХ РАСТВОРОВ

Исследованы твердые растворы $(SnSe)_{1-x}(GdSe)_x(0,0\leq x\leq 2,0)$ с помощью анализов: дифференциально-термического, рентгенфазового и микротвердости. Определено, что эти составы на основе соединений SnSe кристаллизуются частично заменой атомов олова атомами гадалиниума (Gd). Исследованы зависимости от состава термо э.д.с.(α), электропроводимости (σ), коэффициента Холла (R_x) и Холловской подвижности (U_x) носителей заряда при комнатной температуре на образцах частично компенсированных полупроводников *p*-типа.

M.S. Murguzova, M.I. Murguzov, Sh.S. Ismayilov, J.I. Guseynov, B.A. Tairov

ROENTGEN RESEARCH AND INVESTIGATION OF COMPOSITION DEPENDENCE OF PHYSICAL PARAMETERS IN SOLID SOLUTIONS OF $(SnSe)_{1-x}(GdSe)_x(0,0\leq x\leq 2,0)$ SYSTEM

The research of $(SnSe)_{1-x}(GdSe)_x(0,0\leq x\leq 2,0)$ solid solutions has been carried out by study of differentially thermal, roentgen-phase and microhardness methods. It have been determined, that these compounds are crystallized due to replacing of Sn partially by Gd on the base SnSe. The composition dependences of thermo-electromotive force (α), electrical conductivity (σ), Hall coefficient (R_x) and Hall mobility of charge carriers have been studied for room temperatures. The studied examples are the partially compensated semiconductors of *p*-type.

Received: 06.03.06

THE OBTAINING AND INVESTIGATION OF PHOTOELECTRIC PROPERTIES OF HETEROJUNCTION ON THE BASE InP – CdS STRUCTURES

A.Z. BADALOV, M.M. EFENDIYEV, L.S. MAHMUDOVA
Mingechaur Politechnical Institute
Mingechaur, Dilara Aliyeva , 21

The technology of epitaxial growth of the layers of CdS on the substrate of InP with the transversal layer p^+InP and without one is developed. The electrical, photoelectrical properties of the obtained heterojunctions are investigated and also the influence of the technological factors on *p*InP – *n*CdS heterostructure properties is studied.

The task of the widening of spectral range of the useable sources and radiation-measuring instrument appears during the development of the semiconductor electronics. As the semiconductor compounds $A^{III}B^{V}$ and the solid solutions on their base can't satisfy the demands of science and technique, so the creation of the "hybrid" heterojunctions, where the layer of $A^{III}B^{V}$ compound is used in the capacity of the one of the components, and the layer of the $A^{II}B^{VI}$ compound is used in the capacity of the another one, is the one of the ways of the task solving.

The heterojunctions InP-CdS′ present the special interest between many different variants, as the compounds, used in the given case, have the small disparity of lattice parameters $\frac{\Delta a}{a} = 0.3\%$ at 25°C, which practically doesn't change with the temperature increase.

Thus, the paper is dedicated to the treatment of the technology of epitaxial growth of the layers of CdS on the substrate of InP with the transversal layer p^+InP, to the investigation of the electrical, photoelectrical properties of the obtained heterojunctions and also it will study the influence of the technological factors on *p*InP – *n*CdS heterostructure properties [1].

The growth from the gas phase with the help of the transport reactions is the main method of the obtaining of the monocrystalline films of CdS nowadays. We prefer the open lubricating system in the equipment design, as the more technological one in the comparison with the soldered ampoule. The open system allows to rule more effectively by the growth and doping processes of the film, and also to carry out several consistent operations in the one installation.

Her main knots are:

1) The systems of purification, stabilization and measurement of helium flow; 2) gas-distribution system with the source of three-chlorine phosphate; 3) quartz reactor with the volume Cd or S; 4) four-band resistance furnace with the system of the regulation and temperature measurement.

The plates by the size $5\times10\times0.5 mm^3$, cut from InP monocrystal on the plane (I I I) with the exactness lower than 1°, were used in the capacity of the substrates.

As it is known, the state of the surface of the semiconductor substrate defines significantly the quality of the produced devices, their longevity and durability. That's why the obtaining of the high-quality surfaces of the semiconductor substrates, maximally perfect by the structure, geometry, homogeneous by the chemical nature and purity, is the especially important condition at the production semiconductor heterostructures.

On the assumption of the above mentioned, the influence of the composition of the isotopic chemical etchant, time and etchant temperature on the substrate was considered by us. It has established, that the best results are obtained in the case of the use of the green etchant on the base of sulphuric acid, hydrogene peroxide and water [1]. It significantly improves the quality the initial polish surface of the substrates, oriented in the planes (111) and (100) in optimal conditions at room temperature at volume ratio H_2SO_4:H_2O_2:H_2O=3:1:1.

The reactor with the sources of CdS, S or Cd and InP was put into cool furnace and the expulsions were carried out by the dosed helium flows, which were directed on the CdS source and flowed around it, the furnace bands were heating till given temperature and it was possible to carry out the growth process.

The special attention was paid to the creation of the fluent temperature gradient between furnace bands, that was the solving factor of the prevention of the spontaneous crystallization of CdS on the reactor walls. The temperature gradient depended on the temperature difference in the bands, but it was constant in all points of the furnace between bands (as at ΔT=50°C the gradient was 3°C/cm). Before the grafting the substrate was fixed in quartz holder and was put into cool corner of the reactor.

After the finishing of the grafting the substrate slowly was moved into cool corner of the reactor, cooled there and taken together with the holder. On this step the experiment was over, but the installation allowed us to carry out several experiments consistently without furnace cooling.

The growth velocity was defined on the results of substrate weighing before and after the experiment on the half-microanalytical weights with delicacy $1\cdot10^5$gr. The estimation of the value of the grown layer CdS was carried out on the formulae $d = \frac{\Delta m}{\rho \cdot S}$, where ρ are densities, Δm is CdS layer mass, S is sample square. In order to consider the decrease of the substrate weight because of the gas etchant, the prior experiments, in which the carry-over of InP from the substrate in the etchant conditions was investigated, were carried out. Further, the obtained average value of carry-over was summed to the all results.

It is established, that in the case of S excess in the gas phase under stoichiometric composition of the morphology, the surfaces of the CdS layer and crystalline structure change. It is shown, that with the help of the type of crystalline structure and morphology of epitaxial films of CdS it's possible to rule by the creation of the chalcogenide excess in

the gas phase at the one and the same temperature of the substrate.

Further, it is shown, that the possibility of the growth of the transversal layer of InP P^+ -type on the interface of *p*InP-*n*CdS heterojunction was foresaw in the device and the corresponding technological mode was chosen with the aim of the exclusion of the possibility of the erosion of surfaces of InP substrates.

For the investigation of the influence of the back *p*-*n*-homojunction on the *p*InP-*n*CdS properties of heterostructures, the technology was treated and *n*InP- *p*InP-*n*CdS heterohomojunctions are prepared by thermal evaporation in the vacuum of the epitaxial layer of CdS on *p*InP-*n*CdS homojunction. Moreover, the new method of obtaining of *p*InP-*n*CdS heterojunctions [2], which includes CdS precipitation in the closed volume at *T*=140-160°C on InP from the source, consisting its second half.

The roentgen-structural analysis showed that films have cubical structure and *p*InP – *n*CdS heterojunctions, prepared by the correspondence of the lattice parameters are close to the "ideal" ones.

The microroentgen-spectral, roentgen-difractional analysis and usual metallographical methods, which show, that the obtaining of *p*InP – *n*CdS structure has the strong heteroborder and mutual diffusion of the constituents is small in the chosen technological mode, are used with the aim of the study of the interface of the prepared heterojunctions, the definition of the composition and character of the distribution of main components in the epitaxial layers [2].

The typical volt-ampere characteristics of *p*InP – *n*CdS heterojunction with the transversal layer in the dynamic mode (*T*=300°K) is given on the fig.1. As it is seen from the fig.1 the investigated structure has the strongly expressed straightening: the rectification factor achieves the value 10^2 at *U=1V*.

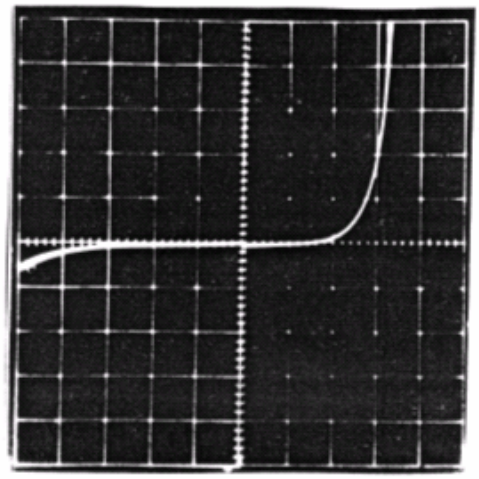

Fig.1. VAC of InP - CdS heterojunctions at *T*=300°K, on the point *J*=2mA; *U*=0.5V.

The volt-ampere characteristics have been investigated in the wide interval of the densities of the current and temperatures (80-300°K). The straight branches of these characteristics in the half-logariphmic scale are shown on the fig. 2. As it is seen the rectilinear regions, proving the exponential dependencies of the direct current on the voltage are observed on the straight branches of VAC at the all studied temperature range.

From the analysis of the tempo volt-ampere characteristics of *p*InP – p^+InP - *n*CdS structures with the transversal layer, investigated in the wide interval of densities of the current and temperatures (150-300K) is followed, that the current passing through in the temperature range 150-190K is explained by the method of the intraband tunneling of the thermally excited carriers. The mechanism of current passing through connects with the generation-recombination processes in the region of the volume charge in the temperature interval 240-300K and forward voltage $\frac{3KT}{q} < U < 0.5V$. The current passing through at the more high voltages (*U>0.5V*) is defined by Zener tunneling of the electrons from the valence band of the narrow-band material InP in the conduction band of wide-band CdS [3].

The volt-ampere characteristics of pInP – nCdS heterojunction at the different intensities of the lightening is shown on the fig.2.

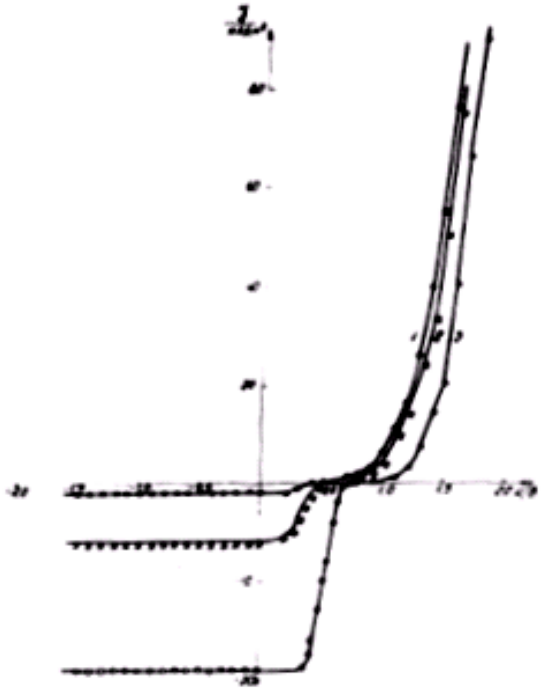

Fig.2. The volt-ampere characteristics of *p*InP - *n*CdS heterojunction with transversal layer at the different powers of the incident light:1 - 10MVt/cm^2; 2 - 25MVt/cm^2; 3-70MVt/cm^2.

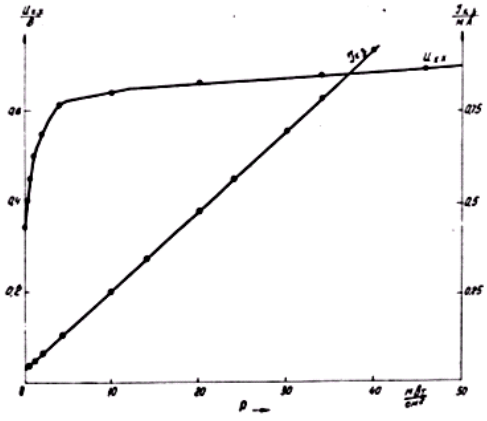

Fig.3. The dependence of open-circuit voltage U_{xx} and short-circuit photocurrent I_{sc} on the lightening.

The dependences of the open-circuit voltage U_{xx} (I) and short-circuit photocurrent density $J_{s.c.}$ (2) on the power of the fallen white light on the sample are shown on the fig.3. It is shown, that short-circuit photocurrent density linearly increase and the open-circuit voltage achieves the saturation with the increase of the power of the incident light.

The investigation of the open-circuit voltage dependence (U_{xx}) on the temperature showed, that the voltage (U_{xx}) in the range 77÷300K linearly decreases with the increase of the temperature coefficient $2 \cdot 10^{-3}$V/grad.

The open-circuit voltage and short-circuit photocurrent density for the best samples are U=750÷780mV and $J_{s.c.}$=30÷32mA/cm at the lightening of heterojunctions with the transversal layer by the white light of the power 90mV/cm^2.

The value of the open-circuit voltage and short-circuit photocurrent density are correspondingly equal to 740÷770mV and 15-17mA/cm^2 for *p*InP – *n*CdS heterojunction without transversal layer at the lightening by the light of the power 70mV/cm^2.

It is shown, that the strongly slump of the quantum output value in the short-wave region of the spectrum (λ<0.55mkm) is caused by the light absorption in the "thick" layer of CdS (5 mcm), the slow slump is observed at the decrease of the photon energy of recombination losses and at the increase of the scattering from the generation place of electron-hole till interface.

The photoelectric properties of *n* – Cd - *p*InP – *n*InP heterohomojunctions have also investigated.

The accumulation of the photocurrent sign and the appearance of the strongly negative maximum at the photon energy, which is equal to 1.35eV is characteristic for the samples with *n*InP – *p*InP - *n*CdS heterohomojunction. Moreover, the positive short-wave maximum saves (fig.4). As it is seen, the strong junction from maximal positive value till minimal negative value on the narrow region of the spectrum is observed in spectral characteristics, and the region of the sign change of short-circuit photocurrent is linear in the dependence on the wave length of fallen radiation. The analogical results have obtained for the spectral dependence of the photo-electromotive force also. The negative and positive maximums at photon energy 1,4eV are caused by two different competitive mechanisms. Whereas the negative maximum connects only with the separation of electron-hole couples on *p*InP - *n*InP homojunction, the positive maximum is caused by the accumulation in the conditional *n*CdS - *p*InP heterojunction. For the confirmation of the above mentioned the experiment, in which the spectral distribution of photocurrent of the sample with *p-n*-homojunction after co-polishing of CdS of main *p*InP - *n*CdS heterojunction was carried out. Moreover, the positive short-wave maximum disappears and negative maximum at 1,4 eV saves and doesn't change the sign. The analogical co-polishing on the samples without *p-n* homojunction has led to the total disappearance of the sensitivity.

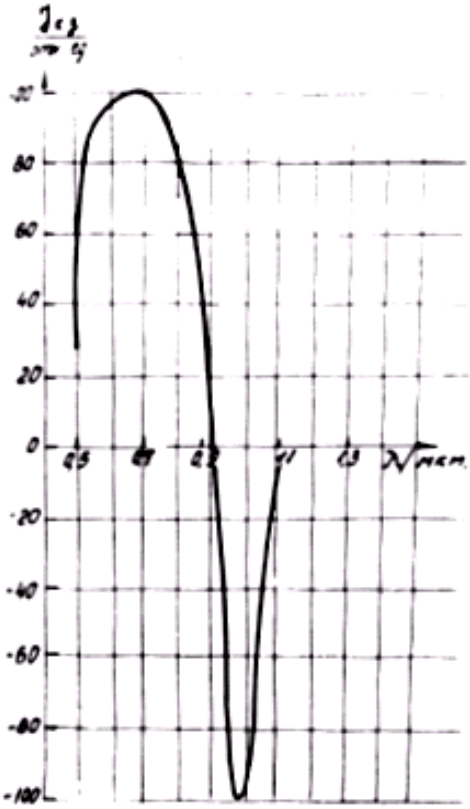

Fig.4. The spectral distribution of I_{sc} *n*InP - *p*InP - CdS heterohomojunction.

The energy band diagram of *p*InP - *n*CdS prepared heterojunctions with transversal layer on the interface and without it has constructed on the base of the experimental data. It is shown, that they describe Andersen midship, in which breaches of conduction band ΔE_c and valence band ΔE_g are equal to ΔE_c =-0.12eV; ΔE_g =1.26eV for the structure with transversal layer and ΔE_c =-0.06eV and ΔE_g - 1.20eV for the structure without transversal layer and energy "beam" is absent in the conduction band.

The main electrical and photoelectrical parameters (non-ideality coefficient of VAC, short-circuit photocurrent density, saturation current, surface recombination velocity, quantum efficiency, transformation efficiency of solar energy in electrical one) in *p*InP – p^+InP - *n*CdS heterostructures with transversal layer are better on 15-50% than in *p*InP – *n*CdS heterostructures without transversal layer. It is shown, that the improvement of the parameters of heterojunctions with transversal layer is caused by the decrease of the density of the recombination (defect) centers on the interface of *p*InP - *n*CdS structure, and also by the increase of contact electric field strength.

[1] *A.Z. Badalov, I.A. Guseinov*. Obrabotka poverkhnosti podlojek fosfida indiya. Vsesoyuzniy seminar po "Poluprovodnikovie strukturi s dielektricheskoy izolyatsiey I integralnie skhemi na ikh osnove", Svetlovodsk, 1983. (in Russian)

[2] *G.B. Abdullayev, T.D. Dzjafarov, I.A. Guseinov, A.Z. Badalov, A.Sh. Mekhtiev*. Sposob polucheniya clove sulfide kadmiya. Avt. Svid. №862744.

[3] *T.L.Tanaley.* Heterojunctions properties-In. Sinciconluetors and Senimetals. New York-London Academic Press, 1971

A.Z. Bədəlov, Ş.M. Əfəndiyev, L.C. Mahmudova

InP – CdS STRUKTUR ƏSASLI HETEROKEÇİDLƏRİN ALINMASI VƏ ONLARIN FOTOELEKTRİK XASSƏLƏRİNİN ARAŞDIRILMASI

Fosfid indium altlığı üzərində keçidli p^+InP və keçidsiz laylı kadmiy sulfid laylarının epitaksial yetişdirilmə texnologiyası işlənilmişdir. Alınan heterokeçidlərin elektrik və fotoelektrik xüsusiyyətləri araşdırılmış, həmçinin texnoloji faktorların *p*InP – *n*CdS heterostrukturların xüsusiyyətlərinə təsiri öyrənilmişdir.

А.З. Бадалов, Ш.М. Эфендиев, Л.С. Махмудова

ПОЛУЧЕНИЕ ГЕТЕРОПЕРЕХОДОВ НА ОСНОВЕ InP – CdS СТРУКТУР И ИССЛЕДОВАНИЕ ИХ ФОТОЭЛЕКТРИЧЕСКИХ СВОЙСТВ

Разработана технология эпитаксиального выращивания слоев сульфида кадмия на подложке фосфида индия с переходным слоем p^+InP и без переходного слоя. Исследованы электрические и фотоэлектрические свойства полученных гетеропереходов, а также изучено влияние технологических факторов на свойства *p*InP – *n*CdS гетероструктур.

Received: 14.12.05

OPTICAL PROPERTIES OF Bi_2Te_3-Bi_2Se_3 FILMS

S.I. MEHDIYEVA, N.Z. JALILOV, N.M. ABDULLAYEV, N.R. MEMMEDOV, M.I. VELIYEV, V.Z. ZEYNALOV

Institute of Physics of NAS of Azerbaijan
Baku, AZ-1143, H. Javid ave., 33

The spectrums of film samples Bi_2Te_3-Bi_2Se_3 of p-type with Tb impurity and n-type conductivity with Cl impurity have been investigated by methods of optical reflection (in region 1÷6,5eV) and transmission (in region 1-3,5 eV). The more intensive peaks, showing on the existence of interband transitions, are observed in the dependence of reflectivity factor (R) on energy (E) of incident radiation.

The Bi_2Te_3-Bi_2Se_3 is more effective electron thermoelectric material of refrigeratoring thermoelements and thermogenerators in temperature interval 200-550K. It gives way to the set of medium-temperature materials higher 550K. Firstly thermoelectric material on Bi_2Te_3-Bi_2Se_3 base was synthesized and investigated by S.Sinani [1]. The composition 80% (mol.) Bi_2Te_3 – 20% (mol.) Bi_2Se_3 with the width of prohibited band 0.27eV at room temperature has the best thermoelectric properties [2].

The Bi_2Te_3-Bi_2Se_3 system creates the constant set of solid solutions. This means, that Te atoms in any quantity (from 0 till 100%) can be changed by their analogue - selenium in Te_I-Bi-Te_{II}-Bi-Te_I chains, that is caused to the technology flexibility, moreover firstly Se atoms are changed by all Te_{11} atoms, and further Te_1 atoms. The Bi_2Te_3-Bi_2Se_3 (structure of 20%Bi_2Te_3) crystallizes in hexanal structure with lattice parameters a= 4,296Å and c=5,988Å [3]. The calculations of band structure of semiconductors of $A_2^{IV}B_3^{VI}$ type, and also the set of the experiments on the investigation of optical properties show on the fact, that electron spectrum in Bi_2Te_3 has the three-dimensional character [3]. Moreover, the meaning of effective electron mass of the given composition achieves of maximal meaning $m_n^* = 1{,}2m_0$. The relatively big value of prohibited band is the important factor for the use of this material in thermoelements till the temperatures 600-650K.

At the synthesis of poly-crystal samples the initial components with doping additions are melted in quartz ampoules at temperature 1000K [4]. At the doping by Cu, as the long investigations have shown, the sample properties are changing during the time [5].

The investigation of reflection and transmission spectrums of Bi_2Te_3-Bi_2Se_3 films of p- and n-type conductivity, doped by Tb and Cl is the task of the given paper.

The obtaining method of films Bi_2Te_3-Bi_2Se_3 was considered in the ref [6].

The doped binary films by the width of 300Å have been obtained by us by cathode scattering on usual glass, on the glass, covered by carbon film, on mica and NaCl. The films, created on carbon, on the limit (100) of rack salt in range 200-400°C, textured or crystallized in plane (001) parallel to the substrate.

Cl was the main doping addition. This impurity was introduced with the aim of the change of conductivity type of material and increase of its thermoelectric effectiveness. Maximal value $\alpha^2\sigma$ are achieved at the doping of the composition by the Cl till 0,3% (mol.) in $CdCl_2$ form. In the given paper the investigation results on massive samples of p- and n-types Bi_2Te_3 at the normal light falling, directed parallel and perpendicular to chip plane at 300K with the aim of the comparison of the results of the given paper with the results of ref [4], where different minimums of reflection coefficients at 1,11eV, possibly corresponding to three different effective masses are given.

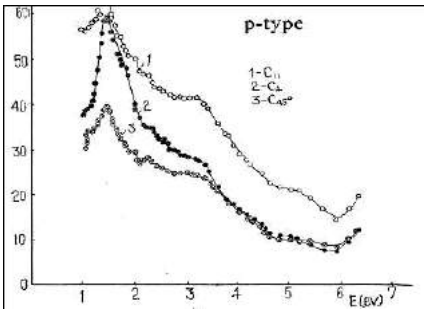

Fig.1. The reflection spectrums of p-Bi_2Te_3 monocrystals: 1 – along ($c_{\parallel}$), 2 – perpendicular to ($c_{\perp}$), 3 – in the direction 45°C to C axes.

The reflection spectrums in [4] were investigating on massive samples Bi_2Te_3 of p-type conductivity, containing the impurity of terbium and n-type conductivity ones containing the impurity of chlorine. In the dependence of reflectivity factor (R) on energy of falling radiation, as p-, so n-type conductivity along ($c_{\parallel}$) perpendicular ($c_{\perp}$) and in the direction 45° to the axes of C crystal at 1,1 and 1.45eV the more intensive peaks are observed. The reflection spectrums of film samples Bi_2Te_3-Bi_2Se_3 of p-type conductivity, consisting terbium impurity and n-type conductivity, consisting Cl impurity have been also investigated in the paper. The intensive peaks are observed in the dependence of reflectivity factor (R) of Bi_2Te_3-Bi_2Se_3 films on radiation energy for n-type conductivity (fig.2), at 1,1eV and 1.45eV. The repeating splitting at 1,1eV and 1.45eV in Bi_2Te_3 spectrum the authors interpret as spin-orbital scattering of valence band and conductivity band. The peaks are observed for the n-type films at 3,8 eV. This fact corresponds with the data of ref [4], showing on the existence in Bi_2Te_3-Bi_2Se_3 films in 0,2-1,8eV interval of strong interband transitions.

The dependence of reflection spectrum of film Bi_2Te_3-Bi_2Se_3 p-type conductivity, doped by Tb, and n-type conductivity with Cl impurity on the wave length, are given on the fig.2.

The texture was changed on the disorder oriented polycrystal with increase of film width up to 3 mcm at temperature higher, than 500K at the evaporation. The doped polycrystal of film width 0,30; 0,35; 0,40mcm have been

obtained by us. Thus, the weak and more intensive peaks, which are connected with transfers in critic points of Brillouin band were observed at the investigation of reflection spectrums of Bi_2Te_3-Bi_2Se_3 monocrystals as *p*-type with Tb impurities, so *n*-type with $CdCl_2$ impurity.

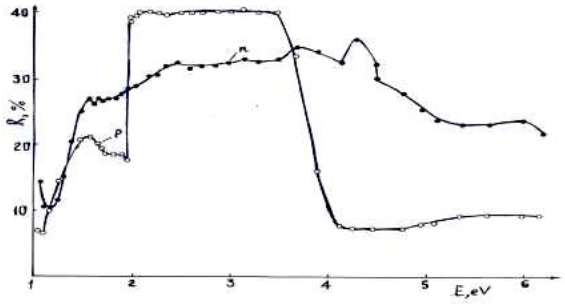

Fig.2. The reflection spectrums of film polycrystal *p*-Bi_2Te_3-Bi_2Se_3 with Tb impurity; *n*- Bi_2Te_3-Bi_3Se_3 with Cl impurity.

From the dependence of absorption coefficients (*T*) of Bi_2Te_3-Bi_2Se_3 films of *p*-and *n*-types of conductivity, given on the figure 3 it is seen, that in the region 1 eV the films Bi_2Te_3-Bi_2Se_3 of *p*-type absorb the light energy on 16%, and of *n*-type conductivity absorb on 10%. These films can be used for the production of thermobatteries.

It is known, that at the production of film thermobatteries the special coverings with big coefficients of transmission are needed.

For the decrease of oxygen influence on the films at the high temperatures in the process of its exploitation and also in exclusion of electric shorting of thermoelectric branches at the creation of manylayered compact batteries the following demands are needed for such coverings: high electric density, low heat conductivity, thermostability at the widths less, than 1mcm. The polymer coverings, widely used in microelectronics in the capacity of passivation and insulating coverings, have high disruptive pressure (more than 10^6V/sm), specific resistance (more than 10^{10}Om·cm), low specific heat conductivity ($æ$=(3-4)10^{-3}Vt/cm K)) [7], high density of elastic deformation, high chemical stability to the different inorganic dissolvents. The polymer coverings are profitable on the given properties, than inorganic dielectric materials (CuO_2, MgF_2, etc.).

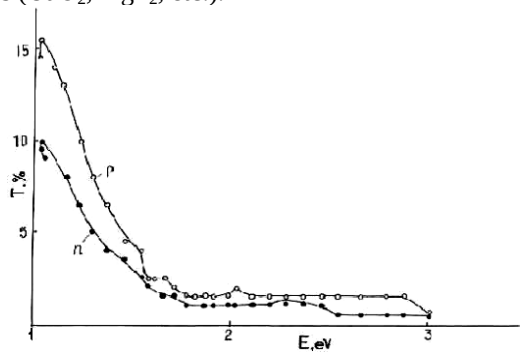

Fig. 3. The transmission spectrums of film polycrystal *p*-Bi_2Te_3-Bi_2Se_3 with Tb impurity; *n*- Bi_2Te_3-Bi_3Se_3 with Cl impurity.

In the conclusion we can say, that the intensive peaks, showing on the existence of interband transitions in the films in the interval 0,2-1,8 eV are observed in dependence of reflectivity factor (*R*) of *p*-Bi_2Te_3-Bi_2Se_3 films on radiation energy for *p*-type conductivity at 1,1 and 1.45 eV, for *n*-type conductivity at 3,8 eV. The repeating splitting 1,1eV and 1.45eV in the spectrum are interpreted as spin-orbital splitting of valence band and conductivity band. From the dependence of absorption coefficients (*T*) of Bi_2Te_3-Bi_2Se_3 films of *p*- and *n*-type conductivity it is seen, that in region 1eV the Bi_2Te_3-Bi_2Se_3 films of *p*-type conductivity absorb the light energy on 16%, and *n*-type conductivity ones absorb on 10%.

[1] *S.S. Sinani, G.N. Gordjakova.* JTF 1956, 2398,10, 26.

[2] *E.K. Iordanishvili.* Semiconductor thermoelectric materials, Leningrad, 1963, p.16.

[3] *B.M. Goltsman, V.A. Kudinov, I.A. Smirnov.* Semiconductor thermoelectric materials on the basis Bi_2Te_3, "Nauka", Moscow 1972, p.320, 229,234.

[4] *S.I. Mehdiyeva, N.Z. Jalilov, N.M. Abdullayev, M.I Veliyev, V.Z Zeynalov., N.R. Memmedov*. Spectra of reflection monocrystals Bi_2Te_3. Materials of international conference, devoted to the 85-anniversary from birthday of academician G.B. Abdullayev. Baku - 2003.

[5] *A.G. Abdullayev, E.I. Veliulin, S.S. Kahramanov.* Influence doping and intercalation on properties chalcogenides bismuth. Pre-print, Baku, 1991, p.25.

[6] *D.I. Ismailov, G.M. Ahmedov, R.B. Shafizadeh.* Electronografic research of the binary films Bi_2Te_3. Reports Of The Academy Of Sciences Azerbaijan SSR, XLV, #4, 1989, p.6-10

[7] *L.V. Gregor*. Drawing dielectric of the films from a gas phase. Physics thin films. Under red. G. Hassa, R.E. Tuna. M, 1968. T.3.

S.İ. Mehdiyeva, N.Z. Cəlilov, N.M. Abdullayev, N.R. Məmmədov, M.İ. Vəliyev,V.Z. Zeynalov

Bi_2Te_3-Bi_2Se_3 TƏBƏQƏLƏRİNİN OPTİK XASSƏLƏRİ

Optik əksolma (1-6 eV intervalında) və buraxılma (1-3,5 eV intervalında) metodu ilə Tb ilə aşqarlanmış *p*-tip və Cl ilə aşqarlıanmış *n*-tip Bi_2Te_3-Bi_2Se_3 əsasında alınmış nazik təbəqələr tədqiq olunmuşlar. Əksolma əmsallarının(*R*) düşən şüalanmanın enerjisindən (*E*) asılı olaraq, 1,1 və 1,45 eV-də zonalararası keçidlərin mövcudluğunu göstərən daha intensiv piklər müşahidə olunmuşdur.

С.И. Мехтиева, Н.З. Джалилов, Н.М. Абдуллаев, Н.Р. Меммедов, М.И. Велиев, В.З. Зейналов

ОПТИЧЕСКИЕ СВОЙСТВА ПЛЁНОК Bi_2Te_3-Bi_2Se_3

Методами оптического отражения (в области 1÷6,5эВ*)* и пропускания (в области 1-3,5 эВ*)* исследованы спектры плёночных образцов Bi_2Te_3-Bi_2Se_3 *p*-типа с примесью Tb и *n*-типа проводимости с примесью Cl. Зависимость коэффициента отражения *(R)* от энергии подающего излучения *(E*) показывает, что при значениях *E* равных 1,1эВ и 1,45эВ наблюдаются более интенсивные пики, указывающие на наличие межзонных переходов.

Received: 22.12.05

THE INFLUENCE OF γ-RADIATION ON RELAXING PROPERTIES OF DOPED VANADIUM CRYSTALS $TlInS_2$

F.T. SALMANOV
Institute of Radiational Problem of NAS of Azerbaijan
AZ 1143, Baku c., H.Javid av., 31a

The influence of γ-radiation on relaxing properties of $TlInS_2$<V> compound has been studied. It has been established, that the Fogel-Fulcher temperature T_f shifts to the side of low temperatures in this compound, and Bernce temperature T_d shifts to the side of high temperatures. In the result, the temperature interval of existence of relaxing state becomes wider on ~40K.

Our previous investigations [1-5] show, that doping of $TlInS_2$ crystal by the some impurities leads to the strong relaxation of dielectric receptivity in the region of disproportionate phase. It has been established, the appearance of nano-sized polar domains, leading to the fact, that the state of dipole and ferroelectric glass precedes the ordered phase. The doping atoms, leading to the appearance of the relaxing state, create the capture levels in the forbidden band of semiconductor ferroelectric $TlInS_2$. The charge carriers, settling these levels, are spatially limited and in as the result the conductivity in this case is carried out by the tunneling through the potential barriers. This was observed at the investigation of the process of charge transfer in crystals $TlInS_2$, doped by atoms Fe, Mn, Cr, B, V, i.e. in these crystals in region of disproportionate phase the non-activated, temperature-independent hopping had been established.

In given paper the results of the investigations of the influence of γ-radiation on relaxing properties of $TlInS_2$<V> compound, where V – 0,3 atm.% are presented.

$TlInS_2$<V> monocrystals had been grown by the modified method of Bridgmen-Stockberger. The measurements were carried out on the borders, cut perpendicularly to polar axes. The borders had been polishing and covering by the silver paste.

The dielectric constant ε was measured with the help of the bridges of alternating current E7-8 (1 kHz) and E7-12 (1 MHz) in the temperature interval 150-250K. The velocity of temperature scanning was 0,1 K/min. The radiation of the samples (Co^{60}) was carried out at the room temperature. The radiation dose was accumulated in the one and the same sample and was 400 Mrad. The measurements $\varepsilon(T)$ were carried out after each radiation.

The temperature dependencies of dielectric constant $\varepsilon(T)$ of $TlInS_2$<V> crystal are given on the fig.1. The investigation of frequency dispersion was carried out on two frequencies of measured field. The shifting of degraded maximum $\varepsilon(T)$ in $TlInS_2$<V> crystal at the frequency increase was ~3K (fig.1, curves 1-2). As we suppose, the condition of the appearance of relaxing behavior in $TlInS_2$<V> crystal is the coincidence of the temperature of phase transition with temperature region of heat filling of local centers. The relaxing properties can be significantly changed by the introduction even the insignificant impurity quantity, influence on charge state of the compound [1,5]. Moreover, the temperature shift of maximum of dielectric constant can achieve the several degrees.

The important peculiarity of ferroelectrics with degraded phase transition is the fact, that the dielectric constant in them higher the T_m temperature changes not on Curie-Weis law, but on law $\varepsilon^{-1/2} = A + B(T - T_0)$. The dependence $\varepsilon^{-1/2}(T)$ for the compound $TlInS_2$<V> is also given on the fig.1 (curves 3,4). It crosses the temperature axes at T_f=170K from the side of the high-temperature phase. At this temperature the phase transition from relaxing (nano-domain) state macro-domain (ferroelectric) state is carried out. Also at the temperature T_d=212K (Berns temperature) the phase transition from paraelectric into relaxing state is carried out.

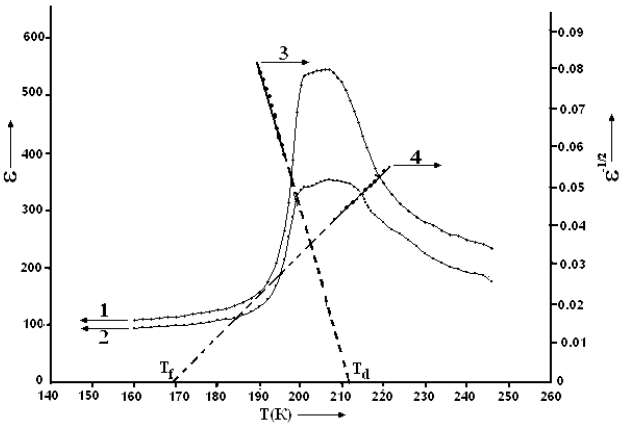

Fig. 1. The temperature dependence of dielectric constant $\varepsilon(T)$ of $TlInS_2$<V> crystal, measured on the frequencies: 1kHz (curve 1); 1 MHz (curve 2). Curve 3,4 – temperature dependence $\varepsilon^{-1/2}(T)$ for $TlInS_2$<V> (without radiation).

The temperature dependencies of dielectric constant $\varepsilon(T)$ at the radiation dose 400 Mrad is given on the fig.2. The radiation doses up to 200Mrad weakly influence on the dependence $\varepsilon(T)$, leading only to the decrease of maximum value of investigated dependence. These radiation doses of γ-radiation for these crystals are only slight ionizing radiation and plays the role of activating factor for such processes as the migration of point defects, impurities, domain borders and transitions of metastable states into stable ones. By other words, the radiation-stimulated senescence of the samples, not leading to the temperature changes of phase transitions and energetic spectrum of the crystal [7-8] is observed. At the achievement of the expositional dose in 400 Mrad the radical change of $\varepsilon(T)$ dependency is observed. The strong degradation of the $\varepsilon(T)$ curve in temperature interval T_f -T_d and its widening in as the high temperature region, so the low one are observed (fig.2).

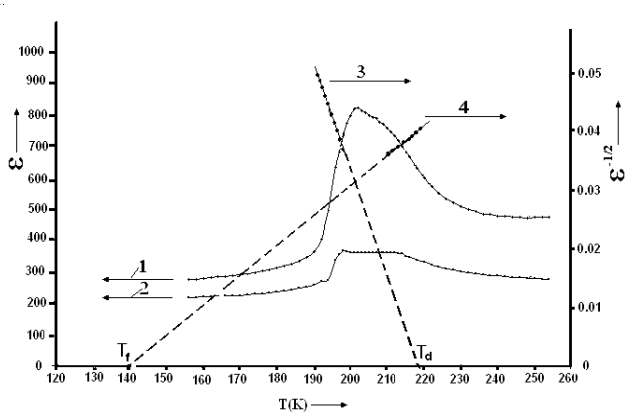

Fig. 2. The temperature dependency of dielectric constant $\varepsilon(T)$ of $TlInS_2$<V> crystal, measured on the frequency 1kHz (curve 1); 1 MHz (curve 2). Curve 3,4 – temperature dependence $\varepsilon^{-1/2}(T)$ for $TlInS_2$<V> (radiation by the dose 400 Mrad).

As it is known [8-9], the depredated character of $\varepsilon(T)$ dependency is the necessary condition of the existence of relaxing state. The enough condition is the fact that $\varepsilon^{-1/2}(T)$ dependency changes on linear law. This dependence is demonstrated by the fig.2. As it is seen from the figure, $\varepsilon^{-1/2}(T)$ dependence crosses the temperature axes at the T_f=140K (fig.2, curve 3) and at T_d=220K (fig.2, curve 4) in radiated crystal with high-temperature and low-temperature correspondingly, relatively to the temperature of maximum of $\varepsilon(T)$ curve. In relaxing ferroelectrics, this temperature is that one, at which the freezing of polar dipoles takes place and crystal from the state of ferroelectric glass transforms into ordered ferroelectric state. This temperature is also characterized by the fact, that at this the temperature filling of trap centers and localized charged impurities are neutral ones.

As it is known [8], the existence of disordered distribution of the charges in the crystal is the main cause, leading to the degradation of phase transition. The increase of degradation at the radiation by the dose 400 Mrad shows on the fact that the dipole charge centers appear in crystal volume at the radiation. On the given stage of the investigation we can make the supposition about the nature of these dipole centers. These can be the radiation defects, created because of the energy of electron excitements, created by the radiation. On our opinion, the most probable mechanism of the creation of radiation defects in $TlInS_2$<V> compound is repeated ionization of boron impurity atom. The created defect increases the energy levels in forbidden crystal band, the heat filling of this level carries out at the more low temperature, in the comparison with non-radiated compound, i.e. the region of the existence of the ferroelectric glass widens.

In the ref [11] the influence of γ-radiation on dielectric constant of Rb_2ZnCl_4 and Pb_2ZnBr_4 crystals in the region of the incommensurate-commensurable phase transition had been investigated. It is shown, that the value of the peak of dielectric constant for both crystals decreases, and their value increases with the increase of the radiation dose. It is established, that the temperature of phase transition for Rb_2ZnCl_4 decreases, and for Pb_2ZnBr_4 it increases and widens with the increase of the radiation dose. The defects of ionizing type (charged defects), which appear in the result of γ-radiation, play in these processes the dominating role. The degradation of the phase transition probably is carried out because of the interaction of polar defects with spontaneous polarization of initial crystal [12]. According to [13], the decrease of the temperature of the phase transition with the increase of radiation dose is caused by the decrease of the concentration of ferroelectric active dipoles in crystal.

The influence of γ-radiation on dielectric and electric properties of $TlInS_2$ crystals in the region of incommensurable-commensurable phase transition [14] had been studied by us earlier and the possibility of the obtaining of relaxing state in these compounds had been established. It is shown, that the anion atom is charged positively and its normal position in the nod, surrounded by cations, is unstable at two (or more) divisible ionization. In the result of electrostatic interaction with positively charged cations, such positively charged anion is pushed into interstice, where further is neutralized.

Analyzing the literature data and results of own experiments we can say, that γ-radiation strongly influences on relaxing state of $TlInS_2$<V> compound and widens the temperature interval of its existence. It is also shown, that Fogel-Fulcher T_f temperature shifts to low temperature region and Berns T_d temperature shifts to the high temperature region.

[1] *R.M.Sardarli, O.A.Samedov, I.Ş.Sadigov, V.A.Aliev*. FTT. t.45, v.6, 2003, s.1067.

[2] *R.M. Sardarli, O.A. Samedov, A.I.Nadjafov, I.Sh. Sadigov.* FTT, t.45, v.6, 2003, s.1085.

[3] *R.M.Sardarli, O.A.Samedov, I.Sh.Sadigov.* Neorganicheskie materiali. t.40, №10, 2004, s.1163.

[4] *A.Sardarli, I.M.Filanovsky, R.M.Sardarli, O.A. Samedov, I.Sh.Sadigov, I.I.Aslanov.* Proceedings of International Conference on MEMS, NANO and Smart Systems. Banff, Alberta, Canada, July 20 to July 23, 2003, p.159.

[5] *O.A.Samedov.* Azerbaijan MEA Kheberleri. Fiz.-riyaz. ve texnika elmleri ser., 2003, N2, s.60.

[6] *A.U.Sheleq, K.V.Iodkovskaya, N.F.Kurilovich*. FTT. t.40, v.7, 1998, s.1328.

[7] *A.U.Sheleq, K.V.Iodkovskaya, N.F.Kurilovich*. FTT. t.45, v.1, 2003, s.68.

[8] *I.P.Raevskiy, V.V.Eremkin, V.G.Smotrakov, E.S.Gagarina, M.A.Malitskaya*. FTT, t.42, v.1, 2000, s.154.

[9] *E.V.Colla, T.Yu.Koroleva, N.M.Okuneva and S.B.Vakhrushev.* Phys.Rev.Lett. v.74, n.9, 1995, p.1681.

[10] *M.D.Qlinchuk, E.A.Eliseev, V.A.Stefanovich, B.Xilger.* FTT. t.43, v.7, 2001, s.1247.

[11] *A.U.Sheleq, I.A.Afonskaya, K.V.Podkovskaya, N.F.Kurilovich, L.E.Soshnikov.* FTT. t.37, v.5, 1995, s.1492.

[12] *M.E.Kassem, M.El-Muraiklu, L.Al-Houty, A.A. Mohamed*. Phase Trans., v.38, 1992, p.229.

[13] *A.Gonzalo, L.Alonzo*. J.Phys.Chem., v.25, N3, 1964, p.303.

[14] *R.M.Sardarli, O.A.Samedov, İ.Sh.Sadigov, A.I. Nadjafov, F.T.Salmanov.* FTT, t.47, v.9, 2005, s.1665.

F.T. Salmanov

VANADİUM ATOMLARI İLƏ AŞQARLANMIŞ $TlInS_2$ KRİSTALLARININ RELAKSOR XASSƏLƏRİNƏ γ-ŞUALARIN TƏSİRİ

γ-şualarının $TlInS_2$<V> birləşməsinin relaksor xassələrinə təsiri öyrənilmişdir. Müəyyən olunmuşdur ki, Foqel-Fulçer temperaturu T_f temperaturun azalması istiqamətilə, Berns temperaturu T_d isə – temperaturun artması istiqamətində sürüşür. Nəticədə relaksor halının mövcud olma temperatur oblastı ~ 40K genişlənir.

Ф.Т. Салманов

ВЛИЯНИЕ γ-ОБЛУЧЕНИЯ НА РЕЛАКСОРНЫЕ СВОЙСТВА ЛЕГИРОВАННЫХ ВАНАДИУМ КРИСТАЛЛОВ $TlInS_2$

Изучено влияние γ-облучения на релаксорные свойства соединения $TlInS_2$<V>. Установлено, что в этом соединении температура Фогеля-Фулчера T_f смещается в сторону низких температур, а температура Бернса T_d – в сторону высоких температур. В результате температурный интервал существования релаксорного состояния расширяется на ~40K.

Received: 29.03.06

$(Bi_2Te_3)_{1-x}(TlInTe_2)_x$ BƏRK MƏHLULLARININ BƏZİ İSTİLİKFİZİKİ XASSƏLƏRİ

M.M. SEYİDOV, Ç.İ. ƏBİLOV, Y.N. BABAYEV
Naxçıvan Dövlət Universiteti
Az7000 Azərbaycan Respublikası Naxçıvan şəh., Universitet şəhərciyi

$(Bi_2Te_3)_{1-x}(TlInTe_2)_x$ bərk məhlul ərintilərində termo-e.h.q. əmsalının ümumi istilikkeçirməsinin, və kristallik qəfəs istilik-müqavimətinin temperatur asılılıqları tədqiq edilmişdir. Onlarda elektron və fononların səpilmə mexanizminin mürəkkəb olduğu aşkar edilmişdir. Bu, bir tərəfdən kristallik qəfəsin əlavə istilik müqavimətinin yaranması, digər tərəfdən isə istilikkeçirmənin bipolyar hissəsinin güclü təsiri ilə əlaqədardır. Müəyyən edilmişdir ki, $(Bi_2Te_3)_{0,99}(TlInTe_2)_{0,01}$ tərkibində səpilmənin təbiəti qeyri-mütəhərrikdir.

Bismut seskvitelluridi qiymətli termoelektrik materialı olduğundan, onun əsasında yeni tərkeibli bərk məhlulların alınması və xassələrinin tədqiqi, onların elektron texnikası qurğularında tətbiq olunması mümkünlüyünü aşkar edə bilər. Ədəbiyyatda Bi_2Te_3 əsasında alınan və xassələri tədqiq edilən çoxlu sayda bərk məhlullar mövcuddur [1-3], lakin $(Bi_2Te_3)_{1-x}(A^{III}B^{III}C_2)_x$ tipli bərk məhlullar (burada, A^{III} və B^{III} qallium yarımqrupu elementləri, C isə halkogenlərdir) tərəfimizdən ilk dəfə olaraq alınıb. Bu məqalədə $(Bi_2Te_3)_{1-x}(TlInTe_2)_x$ bərk məhlullarının (burada x=0,01·və 0,03) kinetik əmsallarının temperatur asılılıqlarının öyrənilməsinin nəticələri açıqlanır. Göstərilən bərk məhlullar Bi_2Te_3 ilə $TlInTe_2$ birləşməsi arasındakı fiziki-kimyəvi qarşılıqlı təsirin təbiəti araşdırılarkən aşkar edilmişdir [4]. Tədqiq edilən bərk məhlulların istilikfiziki xassələri [5]-də verilən metodlara əsasən paralellopiped şəkilli polikristallik nümunələrdə ölçülmüşdür. Ərintilər ampula üsulu ilə bir zonalı sobada ~1100K temperaturunda Bi_2Te_3 və $TlInTe_2$ komponentlərindən tədrici soyudulma texnologiyası ilə sintez edilmişdir. Tarazlıq halına nail olmaq üçün ərintilər ~773K temperaturunda 280 saat müddətində termiki emala məruz edilmişdir.

Şəkil 1-də $(Bi_2Te_3)_{1-x}(TlInTe_2)_x$ bərk məhlul ərintilərinin termo-e.h.q. əmsalının temperatur asılılığı göstərilmişdir. Tədqiq edilən nümunələrdə termo-e.h.q. əmsalının dəyişməsi mürəkkəb zona qurulmasına malik olan yarımkeçiricilərdə olduğu kimidir. Nəzərə alınsa ki, Bi_2Te_3 birləşməsi belə yarımkeçiricilərdəndir [6], o zaman $\alpha \sim f(T)$ asılılığını qanunauyğun saymaq olar. Bütün temperatur intervalında bərk məhlulun hər iki tərkibində p-tip keçiricilik müşahidə edilir.

$(Bi_2Te_3)_{1-x}(TlInTe_2)_x$ bərk məhlul ərintilərinin ümumi istilikkeçiriciliyinin temperatur asılılıqları 2-ci şəkildə əks olunub. Nümunələrin tərkiblərinin yaxın olmasına baxmayaraq, onlarda $æ_{üm}$-nin temperatur asılılıqları bənzər deyil. $(Bi_2Te_3)_{0,97}(TlInTe_2)_{0,03}$ tərkibində bütövlükdə, $(Bi_2Te_3)_{0,99}(TlInTe_2)_{0,01}$ tərkibində isə ~500K temperaturuna qədər ümumi istilikkeçirmə mənfi üstlü qanuna əsasən dəyişir. Lakin ~500K-dən başlayaraq $(Bi_2Te_3)_{0,99}(TlInTe_2)_{0,01}$ tərkibinin istilikkeçiriciliyi artmağa başlayır. Belə dəyişmənin aydınlaşdırmaq məqsədilə ərintilərdə elektron və fonon istilikkeçiriciliyinin qiymətləri hesablanmış, onların $æ_{üm.}$-yə olan təsirinin dərəcəsi müəyyənləşdirilmişdir. Bu məqsədlə fonon istilikkeçirməsindən qəfəs istilik müqavimətinə keçirilərək istiliyin daşınma mexanizmi qismən aydınlaşdırılmışdır. Şəkil 3-də $(Bi_2Te_3)_{1-x}(TlInTe_2)_x$ bərk məhlul nümunələrinin qəfəs istilik müqavimətinin (W_q) temperaturdan asılılığı göstərilmişdir. Göründüyü kimi, $(Bi_2Te_3)_{0,99}(TlInTe_2)_{0,01}$ tərkibində ~400K-nə qədər, $(Bi_2Te_3)_{0,97}(TlInTe_2)_{0,03}$ tərkibində isə bütün temperatur intervalında istiliyin daşınması üçfononlu mexanizm üzrə baş verir. Bu zaman istilik müqavimətinin dəyişməsi fonon istilik müqavimətinin nəzəri qiymətinin (W_q^0) temperaturla dəyişməsinə uyğun gəlir.

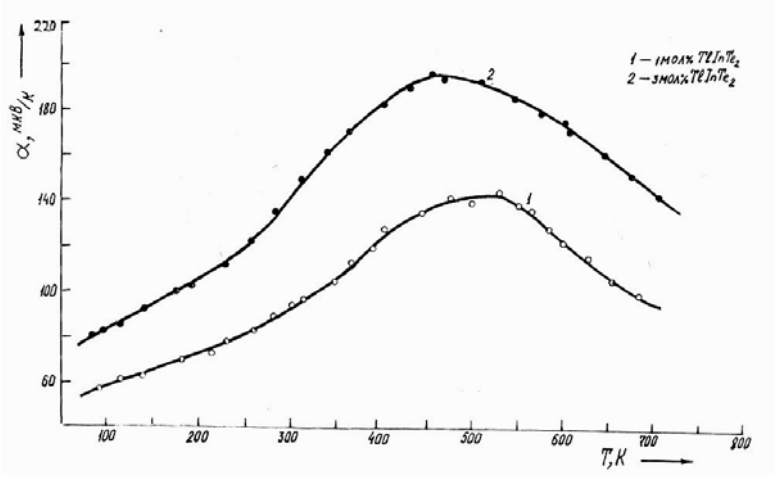

Şəkil 1. $(Bi_2Te_3)_{1-x}(TlInTe_2)_x$ bərk məhlul ərintilərinin termo-e.h.q. əmsalının temperatur asılılığı.

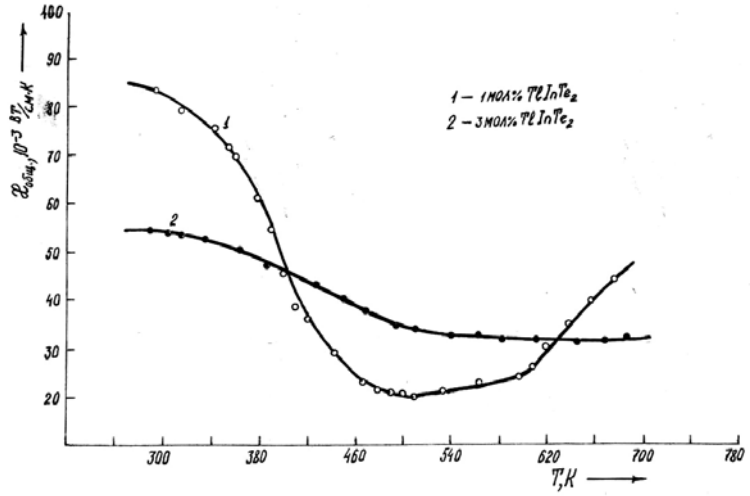

Şəkil 2. $(Bi_2Te_3)_{1-x}(TlInTe_2)_x$ bərk məhlul ərintilərinin ümumi istilik-keçirməsinin temperatur asılılığı.

Lakin ~400K-dən başlayaraq ~700K temperaturuna qədər $(Bi_2Te_3)_{0,99}(TlInTe_2)_{0,01}$ tərkibində (~500K-də bir qədər zəifləməklə) əlavə istilik müqaviməti (ΔW_q) yaranır. Görünür, 400K-dən yüksək temperaturlarda üçfononlu istilik daşınmasına səpilmənin optiki-akustik mexanizmi əlavə olunur. Miqdarca bu mexanizmin dəyərini $\Delta W = W_{təcrübə} - W_{üçfonon}$ kimi qiymətləndirmək olar. ~500-550K temperatur intervalındca kristallik qəfəs müqavimətinin zəifləməsi müşahidə olunur. Hesablamalar göstərmişdir ki, ~400-500K temperatur intervalında $(Bi_2Te_3)_{0,99}(TlInTe_2)_{0,01}$ tərkibinin istilikkeçirməsi $T^{0,75}$ qanunu üzrə dəyişir. Bu amil elektron-fonon qarşılıqlı təsirinə bir işarədir, yəni burada qəfəs istilikkeçirməsi fononların elektronlardan səpilməsi ilə məhdudlaşır. Məlumdur ki, yüksək temperaturlarda fononların istilik müqapvimətinin artması bipolyar istilikkeçirməsinin meydana gəlməsi hesabına ola bilər [7].

Bu məsələyə aydınlıq gətirmək üçün məlum sadə düsturdan $æ_{b-p} = 2L_0\sigma T\left(\frac{\Delta E}{kT}+1\right)^2$ istifadə edərək $(Bi_2Te_3)_{0,99}(TlInTe_2)_{0,01}$ tərkibi üçün bu kəmiyyətin qiymətləri hesablanmışdır.

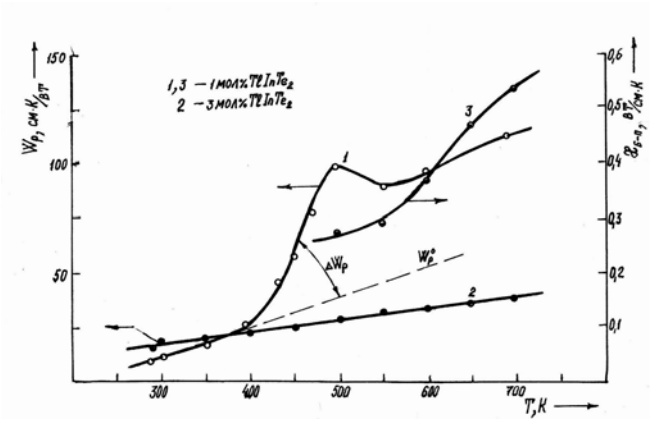

Şəkil 3. $(Bi_2Te_3)_{1-x}(TlInTe_2)_x$ bərk məhlul ərintilərinin kristallik qəfəs istilikmüqavimətinin temperatur asılılığı və $(Bi_2Te_3)_{0,99}(TlInTe_2)_{0,01}$ tərkibli ərintidə bipolyar istilikkeçirmənin temperaturla dəyişməsi.

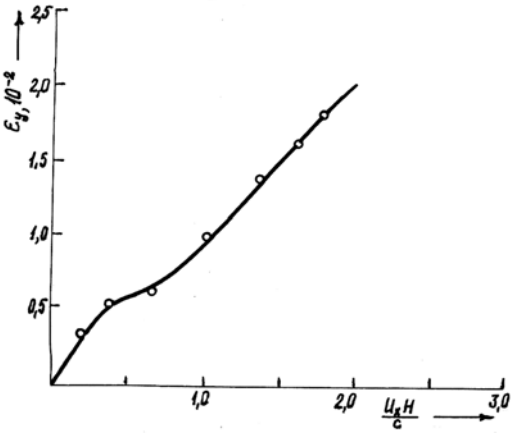

Şəkil 4. $(Bi_2Te_3)_{0,99}(TlInTe_2)_{0,01}$ tərkibli ərintidə Nernst-Ettinqsqauzen əmsalının U_HH/c kəmiyyətindən asılılığı.

Formulaya daxil olan qadağan zonasının eninin qiyməti göstərilən tərkibin xüsusi elektrikkeçiriciliyinin temperatur asılılığından təyin edilmişdir və o ~0,3 eV dəyərindədir. Şəkil 3-dəki 3 saylı əyri $(Bi_2Te_3)_{0,99}(TlInTe_2)_{0,01}$ tərkibində bipolyar istilikkeçiriciliyinin temperaturdan asılılığını göstərir. Göründüyü kimi, ~480-500K temperaturundan başlayaraq $æ_{b-p}$-nin artması müşahidə olunur. Bu səbəbdən belə bir nəticəyə gəlmək olar ki, yüksək temperaturlarda kristallik qəfəs müqavimətinin və bütövlükdə istilikkeçirmənin artması bipolyar istilikkeçiriciliyinin hesabına olur.

$(Bi_2Te_3)_{0,99}(TlInTe_2)_{0,01}$ tərkibində termo- və qalvanomaqnit xassələrinin ölçülməsi nəticəsində, elektron və fononların səpilmə mexanizminin təbiəti aydınlaşdırılmışdır. [8] ədəbiyyatında göstərilir ki, səpilmənin təbiətinin mütəhərrik və ya qeyri-mütəhərrik olması dərəcəsini ölçüsüz Nernst-Ettinqsqauzen (ε_y) və Riqa-Ledyuk (SH) əmsallarının maqnit sahəsinin gərginliyi və yaxud U_HH/c kəmiyyətinin (burada U_H – yükdaşıyıcılarının Holl yürüklüyü, H-maqnit sahəsi gərginliyi, c-isə işıq sürətidir) asılılıqlarından müəyyənləşdirmək olar. [9] işinə əsasən səpilmə mütəhərrik təbiətlidirsə onda $\varepsilon_y \sim U_HH/c$ asılığı əyrisi $U_HH/c=1$ dəyərində maksimum qiymətə malik olur. Əgər

səpilmə qeyri-mütəhərrikdirsə o zaman $U_H H/c \approx 1$ vəziyyəti alınır. Şəkil 4-də $(Bi_2Te_3)_{0,99}(TlInTe_2)_{0,01}$ tərkibi üçün Nernst-Ettinqsqauzen əmsalının $U_H H/c$ kəmiyyətindən asılılığı göstərilmişdir. Göründüyü kimi, asılılıqda ε_y əmsalı $U_H H/c$ oxu boyunca vahiddən böyük qiymətlərə malik olur. Bu amil səpilmənin qeyri-mütəhərrik olduğunu göstərir.

[1] *B.M.Qolsman, V.A.Kudinov, İ.A.Smirnov*. Poluprovodnikoviye termoelektricheskiye materiali na osnove Bi_2Te_3. M., Nauka, 1972, 320s.

[2] *N.X.Abrikosov, V.F.Bankina, L.V.Poreskaya, E.V.Skudnova, S.N.Chiyevskaya*. Poluprovodnikoviye xalkoqenidı i splavı na ix osnove. M., Nauka, 1975, 220s.

[3] *V.V.Leonov, E.N.Chunaryev.* İssledovaniye svoystv splavov sistemi Bi_2Te_3-Sb_2Te_3-GeTe-PbTe. İzv. RAN Neorqan. materiali, 1980, t.16, №12, s.2133-2135.

[4] *M.M.Seyidov.* Bi_2Te_3-$TlInTe_2$ sisteminin hal diaqramı. 19-cu «Kimya-2005» Beynəlxalq kimya konfransının materialları. Türkiyə, İzmir şəh. 2005, Egey Universitetinin tipoqraf. s.736.

[5] *A.S.Oxotin, N.S.Puşkarskiy, R.P.Borovikova, V.A.Simonov.* Metodi izmereniya xarakteristik termoelektricheskix materialov i preobrazovateley. M., Nauka, 1974, 167s.

[6] *C. Champness, L. Kipling.* Conad J. Phys. 1966, v.44, N10, p.769.

[7] *V.S. Oskotskiy, I.A.Smirnov*. Defektı v kristallax i teploprovodnost. M., Nauka, 1972, 160s.

[8] *S.A.Aliev, Dj.A.Baqirov, E.R.İskenderov, E.İ.Zulfiqarov, S.İ.Safarova.* O neupruqom xaraktere rasseyaniya elektronov v $Pb_{1-x}Sn_xTe$. Izv.RAN Neorqan. Materiali, 1933, t.29, №4, s.499-502.

[9] *S.A.Aliyev, U.X. Suyunov, D.Q.Arasli, M.İ.Aliyev.* Neupruqost rasseyaniya elektronov v Ag_2Te. Fizika i texnika poluprovodnikov. 1973, t.7, №6, s.1086-1091.

M.M. Seidov, Ch.I. Abilov, Y.N. Babaev

THE SOME THERMOPHYSICAL PROPERTIES OF SOLID SOLUTIONS $(Bi_2Te_3)_{1-X}(TlInTe_2)_X$

Temperature dependences of coefficients of termo-e.m.f, general heat conductivity and phonon heat resistance of alloys of solid solutions $(Bi_2Te_3)_{1-x}(TlInTe_2)_x$ are investigated. It is revealed complexity of the mechanism of electron and phonon scattering in them, caused as with the advent of additional thermal resistance of a crystalline lattice as the influence of the appreciable contribution of bipolar heat conductivity component. The inelastic character of scattering in compound $(Bi_2Te_3)_{0,99}(TlInTe_2)_{0,01}$.

М.М. Сеидов, Ч.И. Абилов, Я.Н. Бабаев

НЕКОТОРЫЕ ТЕПЛОФИЗИЧЕСКИЕ СВОЙСТВА ТВЕРДЫХ РАСТВОРОВ $(Bi_2Te_3)_{1-X}(TlInTe_2)_X$

Исследованы температурные зависимости коэффициентов термо-э.д.с., общей теплопроводности и решеточного теплосопротивления сплавов твердых растворов $(Bi_2Te_3)_{1-x}(TlInTe_2)_x$. Выявлена сложность механизма рассеяния электронов и фононов в них, обусловленного как появлением добавочного теплового сопротивления кристаллической решетки, так и влиянием ощутимого вклада биполярной составляющей теплопроводности. Установлен неупругий характер рассеяния в составе $(Bi_2Te_3)_{0,99}(TlInTe_2)_{0,01}$.

Received: 04.01.06

THE MASS DISTRIBUTION AND PROBLEM OF SUBSTANCE STRUCTURE

A.A. ABBASZADE*, Kh.A. GADGIYEVA*, E.Z. BABAYEV**
*Azerbaijan National Air-Cosmic Agency**
*Firm "Risk"***

The mass distribution principle, as the directional one for the studying of the substance structure and time-space has been suggested. The physical meaning of the confirmations about the existence of zero mass for the substance particles has been considered. The meaning about of the non-existence of zero masses for all substance states has been said.

The metaphysical conceptions in physics are the sources of the development and stagnation. If we come back to the old times, we will see that physical thought was operated by the different ideas and categories in the relation to home attributes and this or that quality, which was considered as the main one, took place on each progress step. The experimental physics doesn't love this theme, and especially metaphysics (physic philosophy), which on its opinion doesn't bring any definite practical profit, and demand the enormous efforts. Doubly theoretical physics is related to it with big interest. However, this interest often transfers into frank disliking, because of the filling of fatal despair. From this moment the errors from the one conception to another one and vice versa are begun on eternally locked circle.

In the given paper we attempted to short the boundaries for such errors, though we know, that relations, given to the consideration, won't have the significant influence on practicing physics, at least in such form, we mean that these formulas aren't working. Moreover, we note, that we have the doubt that given approach is the disputable.

Whet is the "first": substance or the space? This eternal question is enough sore point for the physics and philosophy in all times, and nowadays it is also actual one. There are always two points of view about the relation of space and time to the substance in history of physics-philosophy. The first from them we can call the substantial conception. In it the space and time were treated as independent essences, existing with the substance and independently from it. Demokrit and Newton were agreed with this conception. Accordingly, the relation between the space, time and substance was introduced as the relation between three types of independent substations. This was led to the conclusion about the independence of properties of space and time on the character of the material processes, flowing in them. Second conception can be called the relational one. Its followers understand the space and time not as the independent essences, but as the systems of the relations, created by the interacted material objects. Outside this interaction system the space and time were presented as common forms of coordination of material objects and their states. Correspondingly, the dependence of the properties of the space and time on the interaction character of material systems was allowed. The relational approach is character for the conception of space and time of Aristotel, Leybniza, Halilei and Puankare.

On the assumption of the relativism positions, i.e. accepting the primary substance as the reasons and the source of space and time, accepting the mass as universal and invariant substance metrics [1,2], we conclude: outside the substance the space-time and metrics aren't defined. As it is seen from the expression: $M \neq R \bullet T = 0$ is the de-escalation, the space and time are empty outside the substance, where M is substance mass, the equality to zero we accept for the substance absent, R substance metrics, T is time. The substance mass distribution dictates and creates the metrics of the space and space itself: $\Delta R = \Delta M \bullet^{-1} \Delta T$ - substance distribution in time creates the space.

Process: $\Delta T = \Delta M \bullet^{-1} \Delta R$ of this redistribution gives the physical meaning to the time conception and creates the last.

If we imagine the space substance as homogenous and isotropic ones, i.e. absolutely homogeneous in all directions and to put the observer into it, then he can't define the extension and time motion and each time moment won't differ from the previous one. But if the shift in substance distribution to the side of nonhomogeneous takes place in the one of these time moments in the result of medium fluctuation, i.e. the mass distribution appears and consequently, time moments will be different, thus if substance redistribution (mass distribution) designates as ΔM, then:

$$R = \frac{M}{\Delta M} \tag{1}$$

$$T = \frac{\Delta M}{M} \tag{2}$$

The expressions (1) and (2) are substation relations,

If $\Delta M = 0$ then, $$R = \lim_{\Delta M \to 0} \frac{M}{\Delta M} = \infty \tag{3}$$

and $$T = \lim_{\Delta M \to 0} \frac{\Delta M}{M} = 0 \tag{4}$$

The formulas (3) and (4) are conditions of absolutely homogeneous (isotropic) substance of the space (there is no planets, Galaxies and other bodies in Universe).

For the modern picture of Universe at the condition, that it is locked system:

If $\Delta M \neq 0$ and always $\Delta M < M$, i.e. $0 < \Delta M < M$, then:

$$R = \frac{M}{\Delta M} > 1 \quad (5) \quad \text{and} \quad T = \frac{\Delta M}{M} < 1 \tag{6}$$

The formulas (5) and (6) are the conditions of stationary state of Universe in present (there are planets, black holes, stars and Galaxies).

In the case, if Universe is the open system, then at the condition: $\Delta M \geq M$,

$$R = \frac{M}{\Delta M} \leq 1 \quad (7) \quad \text{and} \quad T = \frac{\Delta M}{M} \geq 1 \tag{8}$$

The expressions (7) and (8) are accessible and can be considered as condition point of Universe divarication.

In the case, if we take the local region of modern Universe and consider it as open system (in the relation to Universe), then if $\Delta m = m$ (i.e. either pressing of the substance

into the point (into object) or the explosion takes place), where m is substance mass of local region, and Δm is substance mass distribution of local region. Then

$$r=\frac{m}{\Delta m}=1 \quad (9) \quad \text{and} \quad t=\frac{\Delta m}{m}=1. \quad (10)$$

Here r and t are metrics and time of local region.

The conditions (9) and (10) are conditions of the creation of massive object or its existence.

$$\text{If } \Delta m>m; \quad \text{then} \quad R=\lim_{\Delta m\to\infty}\frac{m}{\Delta m}=0 \quad (11)$$

and

$$T=\lim_{\Delta m\to\infty}\frac{\Delta m}{m}=\infty \quad (12)$$

The expressions (9), (10), (11) and (12) are conditions of region divarication (for example, explosion of supernova (star)). For example, for the condition of black hole: $T=\infty$, $R=0$, that doesn't disagree to the conclusions of common theory of relativity in approximation.

The substance discontinuity is the one from the evident properties of it. Nowadays, the science operates by two types of substance: substances and fields, to which the vacuum can be summed in the capacity of the third one on our opinion. The discontinuity properties have been established for the thirst two substance types (supposing the universality of this substance quality), that allow to consider it profitable for the vacuum also.

In the end of 19 century M. Plank [3] introduced the so-called Plank mass $m_P\approx 1{,}2\cdot 10^{19}$ GeV/s^2. Though, nowadays Plank mass is considered as fundamental physic value, characterizing the energetic scale of the superunity theory of all interactions, including the gravitational and is accepted as transfer mass, after which substance transfers in field state.

We propose, that for each type of the substance there is its own transfer mass m_P, after which the one substance type transfers into another one.

For the relativist body the conception of gravitational mass isn't useable. There is no point to talk about gravitational photon mass, if for the vertically fallen photon this value is less in two times, than for the flying horizontally one. The mass of the system of two photons, the E energy of which is $2E$, if they fly in opposite directions and it is equal to zero if they fly in one direction. It is strange, that in spite of the fact, that mass nonadditivity doesn't lead to disagreements; we had the situation, when the system from two photons looses such qualitative characteristic as mass one at the peer angles between two flying photons, at the one direction. We suppose, that the confirmation: $m=0$ is physically empty and has formal character.

Analyzing the above mentioned, as the confirmation of official science [4], let's give the following discussions. Each massive object, whichever less mass it has, will have the gravitational field. However, the modern conception about graviton, as about elementary particle leads us to the conclusion, that this field of the quite essential type, the quantum of which doesn't have common physical properties. Let's suggest, that quantum of gravitational field would have the characteristics of common physical mass, then we close to the opinion of some physics, according to which, if graviton would have the mass, then it would create the gravitational field.

From it it's followed, that either graviton doesn't have the mass, or there is mass without gravitation (we understand the mass only as the quantity of some substance in the given case), but having other physical properties.

This transfer mass doesn't have by own gravitational field, but has other (another) physical properties, probably by the primary field from which the other fields and substance types are created at the change of m_n value.

The set of authors say the thought, that the substance of the gravitation field is the vacuum substance [5]. Such approach makes the graviton the vacuum quantum and takes the excess difficulty of the question. In the capacity of the example, it is possible to suppose, that the main criterion of the difference, for example, quantum of electromagnetic field from the gravitational quantum is the qualitative characteristic on mass.

Topological physics bases on the conception of substance reflection in space and then the geometric characteristics become the basis ones for the flux of the laws and regularities. We have another question, how this or that image forms. In order to answer on this question the applied formulas with taking under the consideration of above mentioned expressions (1) and (2) are needed.

[1] *L.B. Okun.* O pisme R.I. Khrapko Chto est massa? Uspekhi fizicheskix nauk, T.170, №12, 2000 g.

[2] *A.A. Abbaszade, G.Z. Babaev, X.A. Gadgieva*. Edinaya mera prosessov v prirode. Dokladi NAN Azerbaijana, T.LIX, №1-2, 2003 g.

[3] *A. Eynshteyn.* Sobranie nauchnix trudov, t.2, M.Nauka, 1975, 849s.

[4] *M. Plank.* İzbrannie trudi. M. Nauka, 1975,-s.232

[5] *J.T. Akhmedli, I.I. Feldman.* Prostranstvo-Vremya. Azerneshr, 1991g, 248 s.

A.A. Abbaszadə, X.A. Hacıyeva, E.Z. Babayev

KÜTLƏ PAYLANMASI VƏ MATERİYANIN QURULUŞUNUN PROBLEMLƏRİ

Bu məqalədə materiyanın strukturunu öyrənmək məqsədi ilə kütlənin paylanması prinsipi təklif olunmuşdur. Materiyanın metrikası nəzərdən keçirilmiş və onun zərrəciklərinin kütləsinin sıfra bərabər qiymət almasının fiziki mənası araşdırılmışdır.

А.А. Аббасзаде, Х.А. Гаджиева, Э.З. Бабаев

РАЗНОМАССНОСТЬ И ПРОБЛЕМА СТРУКТУРЫ МАТЕРИИ

Предложен принцип разномассности, как направляющий для изучения структуры материи и пространства-времени. Рассмотрен физический смысл утверждений о наличии нулевой массы для частиц материи. Высказано мнение о несуществовании нулевых масс для всех состояний материи.

Received: 05.01.06

EXACT EXPRESSION FOR THE THERMODYNAMICAL POTENTIAL OF A PARABOLIC QUANTUM WIRE

R.G. AGHAYEVA
Institute of Physics of the National Academy of Sciences of Azerbaijan
AZ1143, Baku, H. Javid ave., 33

The exact formula is obtained for the thermodynamical potential of a parabolic quantum wire directed perpendicular to the impressed magnetic field.

The purpose of the present paper is to receive the exact formula for the thermodynamical potential of a parabolic quantum wire (QW) which axis direct perpendicular to the impressed magnetic field. Gazeau et. all [1] considered the analogous problem for QW directed parallel to magnetic field.

All the calculations in this paper are made in the basis of coherent state [2], as the coherent-state method is the most simple and convenient way of solving the problem. The derivation of the thermodynamical potential (Ω) is based on residue series in the complex plane, like that in [1]. The expression for Ω, derived in this paper, will be used in future for calculation the exact formulae of different physical values (for example, the thermoelectromotive force and the magnetic moment).

Let us consider a quantum wire (QW) in uniform stationary magnetic field. We choose the vector potential in the form $\vec{A} = (0, xH, 0)$ which corresponds to the magnetic field H, parallel to the z axis. The QW is directed along the y axis and characterized by parabolic confinements in the plane (x, z).

The Hamiltonian of the problem under consideration is

$$\aleph = \frac{1}{2m}\left[p_x^2 + \left(p_y + m\omega_c x\right)^2 + p_z^2\right] + \frac{1}{2}m\omega_0^2\left(x^2 + z^2\right) \quad (1)$$

where x is the usual canonical coordinate, p_x is its conjugate momentum, $\omega_c = eH/mc$ is the cyclotron frequency, c is the velocity of light in vacuum, m is electron mass, e is the absolute value of its charge and ω_0 characterizes the parabolic potential of the QW for electron in conduction band.

Since $\aleph$ is independent of y it is possible to replace $p_y \to p_y$ everywhere. The Hamiltonian (1) can be now written as

$$\aleph = \aleph_1 + \aleph_2 + \aleph_3 \quad (2)$$

where

$$\aleph_1 = \frac{1}{2m}\left[p_x^2 + m^2\omega^2\left(x - x_0\right)^2\right] \quad (3)$$

$$x_0 = -\left(\frac{\omega_c}{\omega}\right)^2 \frac{cp_y}{eH} \quad (4)$$

$$\omega^2 = \omega_c^2 + \omega_0^2 \quad (5)$$

$$\aleph_2 = \frac{1}{2m}\left(p_z^2 + m^2\omega_0^2 z^2\right) \quad (6)$$

$$\aleph_3 = \left(\frac{\omega_0}{\omega}\right)^2 \frac{p_y^2}{2m} \quad (7)$$

$\aleph_1$ and $\aleph_2$ are two independent harmonic oscillator Hamiltonians. It is known [2], [3] that the Hamiltonian and wave function for harmonic oscillator in the coherent- state (CS) representation can be written in the form:

$$\aleph_1 = \hbar\omega\left[A_\alpha^+ A_\alpha^- + \frac{1}{2}\right] \quad (8)$$

$$A_\alpha^- = \frac{1}{\sqrt{2\hbar}} e^{i\omega t}\left[\sqrt{m\omega}\left(x - x_0\right) + \frac{ip_x}{\sqrt{m\omega}}\right] \quad (9)$$

$$|\alpha\rangle = \left(\frac{m\omega}{\pi\hbar}\right)^{1/4} \exp\left[-\left(\sqrt{\frac{m\omega}{2\hbar}}\left(x - x_0\right) - \alpha e^{-i\omega t}\right)^2 + \frac{\left(\alpha e^{-i\omega t}\right)^2}{2} - \frac{|\alpha|^2}{2}\right] \quad (10)$$

$$\aleph_2 = \hbar\omega_0\left(A_\gamma^+ A_\gamma^- + \frac{1}{2}\right) \quad (11)$$

$$A_\gamma^- = \frac{1}{\sqrt{2\hbar}} e^{i\omega_0 t}\left(\sqrt{m\omega_0}\, z + \frac{ip_z}{\sqrt{m\omega_0}}\right) \quad (12)$$

$$|\gamma\rangle = \left(\frac{m\omega_0}{\pi\hbar}\right)^{1/4} \exp\left[-\left(\sqrt{\frac{m\omega_0}{2\hbar}}z - \gamma e^{-i\omega_0 t}\right)^2 + \frac{\left(\gamma e^{-i\omega_0 t}\right)^2}{2} - \frac{|\gamma|^2}{2}\right] \quad (13)$$

where α and γ are the arbitrary complex numbers.

It is easy to check that $|\alpha\rangle$ and $|\gamma\rangle$ satisfies all necessary requirements of the CS.

For example, in the case of $|\alpha\rangle$:

1) $|\alpha\rangle$ is eigenstate of boson annihilation operator and integral of motion A_α^-:

$$A_\alpha^-|\alpha\rangle = \alpha|\alpha\rangle \quad (14)$$

$$\left[i\hbar\frac{\partial}{\partial t} - \aleph_1, A_\alpha^\pm\right] = 0 \quad (15)$$

$$\left[A_\alpha^-, A_\alpha^+\right] = 1 \quad (16)$$

2) $|\alpha\rangle$ is known to comply with normalization condition

$$\langle\alpha|\alpha\rangle = 1 \quad (17)$$

The wavefunctions $|\alpha\rangle$ form a complete system, but they are not orthogonal.

3) $|\alpha\rangle$ can be created from the ground state $|0\rangle$ for which

$$A_\alpha^-|0\rangle = 0 \quad (18)$$

From the foregoing it transpires that one should present the solution of the wave equation of the problem (2)

$$\left(i\hbar\frac{\partial}{\partial t} - \aleph\right)\psi = 0 \quad (19)$$

in the form

$$\psi = |\alpha\ \rangle|\gamma\ \rangle|k_y\rangle \quad (20)$$

where $|k_y\rangle = e^{ik_y y}$, $\hbar k_y = p_y$.

Let us calculate the thermodynamical potential Ω for the case under consideration. In Fermi- Dirac statistics Ω is given by

$$\Omega = -\frac{1}{\beta} Tr \ln\left(1 + e^{-\beta(\aleph-\xi)}\right) \quad (21)$$

with $\beta = 1/k_B T$, T is temperature, k_B is the Boltzmann contact, ξ is the chemical potential of the conductivity electrons.

We consider the case of physical interest:

$$\aleph - \xi > 0 \quad (22)$$

Let us prove that

$$\ln\left[1 + e^{-\beta(\aleph-\xi)}\right] = \int_{-\infty}^{+\infty} \frac{e^{-(il+1)(\aleph-\xi)\beta/2}}{2(il+1)\cos h(\pi l/2)} dl \quad (23)$$

much as [1].

It is necessary for that to reduce the right hand members to the left- hand side using the contour integration.

In accordance with the Jordan lemma we take an integration path at $\aleph - \xi > 0$ lying in the lower halt- plane, where the integrand under consideration has only simple poles:

$$l = l_0^{(n)} = -i(2n+1), \quad n = 0,1,2,... \quad (24)$$

Using residue theorems we get the right hand members in the form

$$\sum_{n=0}^{\infty} (-1)^n (n+1)^{-1} e^{-\beta(n+1)(\aleph-\xi)}. \quad (25)$$

The application of the formula (1.511) from [4] to the series (25) finishes our proof.

Taking into account the expression (23) we transform formula (21) to the following form:

$$\Omega = -\frac{1}{\beta}\int_{-\infty}^{+\infty} \frac{e^{(il+1)\xi\beta/2}}{2(il+1)\cosh(\pi l/2)} \theta(l) dl \quad (26)$$

where $\theta(l)$ is the function

$$\theta(l) = Tr\ e^{-(il+1)\aleph\beta/2} \quad (27)$$

Now we shall calculate $\theta(l)$ in the basis of CS.

Substitute the expressions (2), (8), (11), (7) into equation (27). For further calculation we adopt the following relations according to equations (22)-(25) of [5]:

1) The trace of an arbitrary operator M equals

$$TrM = \frac{L_y}{2\pi}\int dk_y \frac{1}{\pi}\int d^2\gamma \frac{1}{\pi}\int d^2\alpha \langle\alpha|\langle\gamma|\langle k_y|M|\alpha\rangle|\gamma\rangle|k_y\rangle \quad (28)$$

where $\{\alpha, \gamma, k_y\}$ are the set of quantum numbers in the CS, $(1/\pi)d^2\alpha = (1/\pi)d(\mathbf{Re}\,\alpha)d(\mathbf{Im}\,\alpha)$ is the real element of the area in the complex plane and $(1/\pi)d^2\gamma = (1/\pi)d(\mathbf{Re}\,\gamma)d(\mathbf{Im}\,\gamma)$.

2) the identity valid for boson operators

$$\langle\alpha|\exp\left(\chi A^+A^-\right)|\alpha\rangle = \exp\left[-\left(1-e^{\chi}\right)|\alpha|^2\right] \tag{29}$$

3) the Poisson integral in the form

$$\int_{-\infty}^{+\infty} dk_y\, \mathbf{exp}\left(-bk_y^2\right) = \sqrt{\frac{\pi}{b}},\ \mathbf{Re}\,b > 0 \tag{30}$$

4) and

$$\int d^2\alpha e^{-C|\alpha|^2} = \frac{\pi}{C},\ \ \mathrm{Re}\,C > 0. \tag{31}$$

In our case

$$b = \frac{\hbar^2}{2m}\cdot\frac{\beta}{2}\left(\frac{\omega_0}{\omega}\right)^2(il+1) \tag{32}$$

$$C = 1 - e^{\chi} \tag{33}$$

and

$$\chi = \begin{cases} \chi_0 = -(il+1)\beta\hbar\omega_0/2 \\ \dfrac{\omega}{\omega_0}\chi_0 \end{cases}$$

at the integration over γ (34)

at the integration over α (35)

It is easy to check that $\mathbf{Re}\,b > 0$ and $\mathbf{Re}\,C > 0$ writing $l = \mathbf{Re}\,l + i\,\mathbf{Im}\,l$ and taken into account that $\mathrm{Im}\,l < 0$ for the integration path lying in the lower half – plane.

Introducing the well-known function $\mathbf{sh}\,a = \left(e^a - e^{-a}\right)/2$ we finally get

$$\theta(l) = \frac{L_y}{4\hbar}\frac{\omega}{\omega_0}\sqrt{\frac{m}{\pi\beta(il+1)}}\frac{1}{\mathrm{sh}\left(\dfrac{\chi_0}{2}\right)\mathrm{sh}\left(\dfrac{\omega}{\omega_0}\dfrac{\chi_0}{2}\right)}. \tag{36}$$

The substitution of (34) - (36) into (26) leads to the following expression for Ω:

$$\Omega = \int_{-\infty}^{+\infty}\frac{N(l)}{D(l)}dl \tag{37}$$

where

$$N(l) = -\frac{L_y}{8\hbar}\sqrt{\frac{m}{\pi\beta^3}}\frac{\omega}{\omega_0}e^{(il+1)\xi\beta/2} \tag{38}$$

$$D(l) = (il+1)^{3/2}\cosh(\pi l/2)\mathrm{sh}\left[(il+1)\beta\hbar\omega_0/2\right]\mathrm{sh}\left[(il+1)\beta\hbar\omega/2\right]. \tag{39}$$

Now we shall calculate Ω for the case $\xi < 0$. The integral over l can be evaluated by using residue theorems at the condition that the integrand function satisfies the Jordan lemma. The latter is valid if the integration path at $\xi < 0$ lies in the lower half – plane. Observe that in the lower halt – plane the integrand function has only simple poles the same as in (24).

We now determine Ω by applying the residue theorems to (37):

$$\Omega = -2\pi i\sum_{n=0}^{\infty}\left.\frac{N(l)}{\dfrac{\partial D(l)}{\partial l}}\right|_{l=l_0^{(n)}} \tag{40}$$

Substituting (38) and (39) into (40) we find

$$\Omega = \sum_{n=1}^{\infty}\Omega_n \tag{41}$$

where

$$\Omega_n = \frac{L_y}{4\hbar}\sqrt{\frac{m}{2\pi\beta^3}}\frac{\omega}{\omega_0}\frac{(-1)^n e^{n\xi\beta}}{n^{3/2}\,\mathbf{sh}\left[n\beta\hbar\omega_0/2\right]\mathbf{sh}\left[n\beta\hbar\omega/2\right]} \tag{42}$$

Obraztsov [6] deduced a formula relating the thermoelectromotive force *(Q)* in a quantizing magnetic field to the entropy *(S)* of a semiconductor:

$$Q = -\frac{S}{eN} \tag{43}$$

It is known that the average number of electrons (N) is given by

$$N = -\left(\frac{\partial\Omega}{\partial\xi}\right)_{T,V} \tag{44}$$

and

$$S = -\left(\frac{\partial\Omega}{\partial T}\right)_{\xi,V} \tag{45}$$

where V is the volume.

Calculate Q stating from (41)-(45). As result we obtain:

$$Q=\frac{k_B}{e}\frac{\sum_{n=1}^{\infty}\left\{n\beta\xi-n\frac{\hbar\omega\beta}{2}\mathbf{coth}\left(n\frac{\hbar\omega\beta}{2}\right)-n\frac{\hbar\omega_0\beta}{2}\mathbf{coth}\left(n\frac{\hbar\omega_0\beta}{2}\right)-\frac{3}{2}\right\}\Omega_n}{\sum_{n=1}^{\infty}n\Omega_n} \tag{46}$$

Put $n=1$ and $\omega_0=0$ in (46). Then we derive the well known result for the thermoelectromotive force of nondegenerate electron gas [6]:

$$Q=-\frac{k_B}{e}\left(\frac{3}{2}+\frac{\hbar\omega_C\beta}{2}\coth\frac{\hbar\omega_C\beta}{2}-\beta\xi\right) \tag{47}$$

I wish to express my sincere thanks to Prof. Hashimzadeh F.M. for helpful discussion and support.

[1] *J.P.Gazeau, P.Y.Hsiao, and A.Jellal.* Phys. Rev. B 2002, 65, p. 094427-1 – 094427-9.
[2] *I.A. Malkin and V.I. Man'ko.* Dynamic Symmetries and Coherent State of Quantum System. M., «Nauka». 1979.
[3] *R.G. Agayeva.* J. Phys. A: Math. Gen. 1980, 13, p. 1685-1699.
[4] *Gradshteyn I.S. and Ryzhik I.M.* Tables of Integrals, Sums, Series and Products. M., «Nauka». 1971.
[5] *R.G. Agayeva*. Proceeding of Third International Seminar «Group Theoretical Methods in Physics», London, «Gordon and Breach», 1984, v.2, p. 213-222.
[6] *Yu.N.Obraztsov*. FTT 1965, **7**, p. 573-581.

R.Q. Ağayeva

PARABOLİK KVANT MƏFTİLİN TERMODİNAMİK POTENSİALI ÜÇÜN DƏQİQ İFADƏ

İstiqaməti maqnit sahəsinə perpendikulyar olan parabolik kvant məftilin termodinamik potensialı üçün dəqiq ifadə alınmışdır.

Р.Г. Агаева

ТОЧНОЕ ВЫРАЖЕНИЕ ДЛЯ ТЕРМОДИНАМИЧЕСКОГО ПОТЕНЦИАЛА ПАРАБОЛИЧЕСКОЙ КВАНТОВОЙ ПРОВОЛОКИ

Получено точное выражение для термодинамического потенциала параболической квантовой проволоки, направленной перпендикулярно к приложенному магнитному полю.

Received: 16.02.06

ON PION CORRECTION TO QUARK MASS IN NEXT-LEADING ORDER OF MEAN-FIELD EXPANSION IN NJL MODEL

R.G. JAFAROV
Institute of Physics Problems, Baku State University
Z.Khalilov, str., 23, AZ 1148 Baku, Azerbaijan

The correction to quark mass are calculated in Nambu - Jona-Lasinio model with 4 – dimensional cutoff regularization and with dimensional-analytical regularization in the next-to-leading order of mean-field expansion. The analytical calculations show that the pion correction to quark mass is equal to zero. Comparing the results in both regularization one can signify that the zero value of the pion correction to quark mass is the regularization-independent fact of Nambu - Jona-Lasinio model.

1. Introduction

The chiral-symmetrical Nambu - Jona-Lasinio (NJL) model [1] with the quark content [2] is one of the most successful theoretical laboratories for investigation of the phenomenon of the spontaneous breakdown of chiral symmetry and for study of the light hadrons in the non-peturbative region [3,4]. The NJL model was intensively investigated also at finite temperature and density [5] and with various external fields [6].

The nonrenormalizability of the NJL model implies a suitable choice of regularization. The most common regularizations for NJL model traditionally entail a four-dimensional cutoff (FDC) regularization [3,7,8] or three-dimensional momentum cutoff regularization [3,4]. Other regularization schemes are also used for NJL model [9].

Scalar meson contributions in the chiral quark condensate in the framework of the dimensional-analytical regularization (DAR) have been calculated in [10,11]. These contributions for physical values of parameters were found to be significant and should be taken into account in choice of the parameters values. The improved fit of parameters has been carried out in $SU_V(2)\times SU_A(2)$ - NJL model.

In [8] systematical comparison of the dimensional-analytically regularized NJL model with the NJL model with FDC regularization has been done. Apart from the corrections to chiral condensate, the corrections to quark mass in both regularizations were also calculated. The numerical calculations at two characteristic values of condensate showed that the pion contributions to quark mass in both regularizations are equal to zero. Also it was supposed in [8] that an absence of the pion corrections to quark mass is a regularization-independent fact of NJL model.

The present work, which essentially based on results of [8], is devoted to analytical calculations of the pion correction to quark mass.

2. NJL model with dimensional-analytical regularization and with four-dimensional cutoff. Meson contributions in chiral condense

The model under consideration contains up and down quarks fields $\psi(x)$, each with n colors. The $SU_V(2)\times SU_A(2)$ - invariant Lagrangian of this model is:

$$L = \overline{\psi}\, i\partial\psi + \frac{g}{2}\left[\left(\overline{\psi}\,\psi\right)^2 + \left(\overline{\psi}\, i\gamma_5\tau^\alpha\psi\right)^2\right] \quad ,$$

where τ^α-are Pauli matrices normalized by $\mathrm{tr}(\tau^a\tau^b)=2\delta^{ab}$. For formulating of the mean-field expansion we use an iteration scheme of the solution of Schwinger-Dyson equation with the fermion bifocal source, which has been developed in [12].

The unique connected Green's function in the leading mean-field approximation is a single-particle Green's function (quark propagator):

$$S^{(0)} = (m - p)^{-1},$$

where the dynamical quark mass m is a solution of the gap equation:

$$1 = -8ign_c\int\frac{d\tilde{q}}{m^2 - q^2} \qquad (1)$$

where $d\tilde{q} \equiv d^4q/(2\pi)^4$.

The solution of the gap equation (1) in DAR and FDC regularization leads to [8]:

$$1 = k\Gamma(\xi)\left(\frac{M^2}{m^2}\right)^{1+\xi} \quad , \qquad (2)$$

$$1 = k_\Lambda\left(1 - \frac{1}{x}\log(1+x)\right). \qquad (3)$$

respectively. Here, $k_\Lambda = \frac{gn_c\Lambda^2}{2\pi^2}$, $k = \frac{gn_cm^2}{2\pi^2}$, $x = \frac{\Lambda^2}{m^2}$;. ξ and Λ are regularizations parameters in DAR and in FDC regularization correspondingly.

Meson contribution to chiral condensate can be calculated in the next-to-leading term of the mean-field expansion.

Ratio of the first iteration condensate $\chi^{(1)}$ to leading-approximation condensate $\chi^{(0)}$ in the pion channel has the form [8,10]:

$$r_\pi = -\frac{24ign_c}{1-8ign_cJ}\int d\tilde{p}d\tilde{q}\,\frac{m^2 - p^2 + 2pq}{(m^2 - p^2)^2\left[m^2 - (p-q)^2\right]}A_\pi(q), \qquad (4)$$

where $J=\int d\tilde{p}\,\frac{m^2+p^2}{(m^2-p^2)^2}$

In (4) the pseudoscalar amplitude A_π is [10]:

$$A_\pi=\frac{ig}{1+L_p} \tag{5}$$

where $L_p(p)=ig\int d\tilde{q}\,trS^{(0)}(p+q)\gamma_5 S^{(0)}(q)\gamma_5$ - pseudoscalar quark loop.

Making use of the gap equation (1) we obtain the following form for amplitude A_π in momentum space: $L_s(p)=ig\int d\tilde{q}\,trS^{(0)}(p+q)S^{(0)}(q)$

$$A_\pi=-\frac{1}{4n_c p^2 I_0(p^2)}\ , \tag{6}$$

where

$$I_0(p^2)=\int\frac{d\tilde{q}}{\left(m^2-(p+q)^2\right)(m^2-q^2)} \tag{7}$$

The calculation of the integral (7) in both regularizations (in DAR and in FDC regularization) leads to:

$$I_0^{DAR}(p^2)=\frac{i}{(4\pi)^2}\frac{\xi}{k}F\left(1+\xi,\ 1;\ 3/2;\ \frac{p^2}{4m^2}\right), \tag{8}$$

$$I_0^{FDC}(p^2)=\frac{i}{(4\pi)^2}\left[\log(1+x)-\frac{x}{1+x}F\left(1,1;3/2;\frac{p^2}{4m^2(1+x)}\right)-\right.$$
$$\left.-\frac{p^2}{6m^2(1+x)}F\left(1,1;5/2;\frac{p^2}{4m^2(1+x)}\right)+\frac{p^2}{6m^2}F\left(1,1;5/2;\frac{p^2}{4m^2}\right)\right]. \tag{9}$$

Here $F(a, b; c; z)$ is the Gauss hypergeometric function.

The pseudoscalar amplitude A_π^{pole} according to the pole (p^2=0) representations of the formulas (8) and (9) and the gap equation (2) in both regularizations (at n=3) takes the following forms:

$$(A_\pi^{pole})^{DAR}=\frac{1}{12p^2I_0^{DAR}(0)}=-\frac{2igm^2}{\xi p^2}, \tag{10}$$

$$(A_\pi^{pole})^{FDC}=\frac{1}{12p^2I_0^{FDC}(0)}=-i\frac{4\pi^2}{3\left(\log(1+x)-\frac{x}{1+x}\right)p^2}\ . \tag{11}$$

As a measure of quantum fluctuations of the chiral condensate in pion channel, it is used the first iteration condensate to the leading-approximation condensate in pole approximation of amplitude (10) in DAR [10]:

$$\tau_\pi^{DAR}=\frac{1}{8o} \tag{12}$$

Using the pole approximation of amplitude (11) in calculation of the ratio r_π^{FDC} in Euclidean momentum space in FDC regularization, we obtain for ratio of the first iteration condensate to the leading approximation condensate:

$$\tau_\pi^{FDC}=-\frac{log(1+x)}{8\left(log(1+x)-\frac{x}{1+x}\right)}. \tag{13}$$

3. Pion correction to quark mass

In [8] it has been obtained the formula for the correction to quark mass in next-to-leading approximation of the mean-field expansion. We'll use that formula having the following form:

$$\frac{\delta m_\pi}{m}\cong b_\pi^{(1)}(m^2)-a_\pi^{(1)}(m^2)\ , \tag{14}$$

where $a_\pi^{(1)}$ and $b_\pi^{(1)}$ are the first order mass functions. These functions are defined by the following equations:

$$p^2a_\pi^{(1)}(p^2)=-3\int\frac{d\tilde{q}}{m^2-(p-q)^2}A_\pi^{pole}(q) \tag{15}$$

$$b_\pi^{(1)}(p^2)=r_\pi-3\int\frac{d\tilde{q}}{m^2-(p-q)^2}A_\pi^{pole}(q)\ . \tag{16}$$

Using in (15) and (16) the leading singularity approximation for $\left(A_\pi^{pole}\right)^{DAR}$ (10) and $\left(A_\pi^{pole}\right)^{FDC}$ (11) and calculating the integrals in DAR and FDC regularization (taking also into consideration (14)) we obtain for pion corrections to quark mass the following expressions:

$$\left(\frac{\delta m_\pi}{m}\right)^{DAR}=r_\pi{}^{DAR}-\frac{3}{8\xi}\ , \tag{17}$$

$$\left(\frac{\delta m_\pi}{m}\right)^{FDC} = r_\pi{}^{FDC} + \frac{log(1+x)}{8\left(log(1+x) - \frac{x}{1+x}\right)}. \quad (18)$$

From (17) and (18) according to (12) and (13) it follows that the pion contribution to quark mass is equal to zero. It means that the zero value of the pion correction to quark mass is independent from the regularization choice in NJL model.

[1] *Y. Nambu and G. Jona-Lasinio*. Phys. Rev. 122, 1961, 345.

[2] *T. Eguchi and H. Sugawara*. Phys. Rev. D 10 (1974) 4257; K. Kikkawa. Prog. Theor. Phys. 56, 1976, 947; H. Kleinert. in: Understanding the Fundamental Constituents of Matter, Ed. A. Zichichi, Plenum Press, N.Y., 1978, p. 289.

[3] *S.P. Klevansky*. Rev. Mod. Phys. 64, 1992, 649.

[4] *T. Hatsuda and T. Kunihiro*. Phys. Reports 247, 1994, 221.

[5] *A.S.Vshivtsev, V.Ch. Zukovsky and K.G. Klimenko*: JETP 84, 1997, 1047; D. Ebert, K.G. Klimenko: hep-ph/0305149; *D. Ebert , K.G. Klimenko, M.A. Vdovichenko and A.S.Vshivtsev* : Phys. Rev, D 61, 2000, 025005

[6] *D. Ebert and M.K. Volkov*: Phys. Lett, B 272, 1991, 86; *D.M. Gitman, S.D. Odintsov, Yu.L. Shil'nov*: Phys. Rev, D 54, 1996, 2968 (hep-th/9604163);

[7] *Brevik, D.M. Gitman, S.D. Odintsov*: Grav, Cosmol, 3, 1997, 100 (hep-th/9611138).

[8] *E. Babaev*. Phys. Rev. D 62, 2000, 074020 ; G. Ripka. : Nucl. Phys. A 683, 2001, 463.

[9] *R.G. Jafarov and V.E. Rochev:* hep-ph/0406333.

[10] *S. Krewald and K. Nakayama:* Annals. of Phys. 216, 1992, 201.

[11] *R.G. Jafarov and V.E. Rochev*: Centr. Eur. J. of Phys, 2, 2004, 367 (hep-ph/0311339).

[12] *V.E. Rochev*: hep-ph/0312004.

[13] *V.E. Rochev*: J. Phys. A: Math. Gen. 30, 1997, 3671.

[14] *V.E. Rochev and P.A. Saponov*: Int. J. Mod. Phys. A13, 1998, 3649.

[15] *V.E. Rochev:* J. Phys. A: Math. Gen. 33, 2000, 7379.

R.Q. Cəfərov

NİL MODELİNDƏ ORTA SAHƏ PAYLANMASININ BAŞ HƏDDİNDƏN SONRAKI HƏDDƏ PİONUN KVARKIN KÜTLƏSİNƏ DÜZƏLİŞLƏRİNƏ DAİR

NİL modelində orta sahə paylanmasının baş həddindən sonrakı həddə dördölçülü kəsmə requlyarlaşmasında və ölçülü-analitik requlyarlaşmada kvarkın kütləsinə düzəlişlər hesablanmışdır. Analitik hesablamalar göstərir ki, kvarkın kütləsinə pionun düzəlişləri sıfıra bərabərdir. Hər iki requlyarlaşmadakı hesablaşmaların müqayisəsi göstərir ki, kvarkın kütləsinə pionun düzəlişlərinin sıfra bərabərliyi NİL modelində requlyarlaşma seçimindən asılı olmayan faktdır.

Р.Г. Джафаров

К ПОПРАВКАМ ПИОНА В МАССУ КВАРКА В СЛЕДУЮЩЕМ ЗА ГЛАВНЫМ ПОРЯДКЕ РАЗЛОЖЕНИЯ СРЕДНЕГО ПОЛЯ В МОДЕЛИ НИЛ

Вычислены поправки в массу кварка в модели НИЛ в регуляризации с четырехмерным обрезанием и в размерно-аналитической регуляризации в следующем за главным порядке разложения среднего поля. Аналитические вычисления показывают, что пионные поправки в массу кварка равны нулю. Сравнение результатов вычислений в обеих регуляризациях дает возможность утверждать, что равенство нулю пионной поправки в массу кварка является фактом модели НИЛ, независимым от выбора регуляризации.

Received: 31.01.06

THE DIFFERENTIAL METHOD FOR DETERMINATION OF BASIC OPTICAL PARAMETERS OF ATMOSPHERIC AEROSOL IN UV BAND

H.H. ASADOV, M.M. ALIYEV, E.S. ABBASZADEH
159, Azadlig ave. ANASA, Baku, AZ1106, Azerbaijan

In the article "The differential method for determination of basic optical parameters of atmospheric aerosol" the new approach to calculation of optical depth and Junge index is proposed. This approach is based on proposed differential method and previously proposed three-wavelength method of measurements in UV band.

It is well known, that the aerosol is one of main parts of the Earth's Atmosphere. The basic optical parameter of the atmospheric aerosol is optical depth of aerosol and some other parameters, including Junge index [1]. Also it is well-known, that main and widely used method for determination of aerosol optical depth is Langley method [2].

The essence of this method is that we should take logarithm from both sides of equation of extinction of optical irradiation in atmosphere and bring this equation to the linear type, where slope of which will be equal to linear sum of separate optical depths:

$$\tau_{\sum} = \tau_{aer} + \tau_{oz} + \tau_{mol} + \tau_{\mathrm{Re}\,y}, \qquad (1)$$

where $\tau_{aer}, \tau_{oz}, \tau_{mol}, \tau_{\mathrm{Re}\,y}$ are accordingly optical depths of aerosol, total ozone, gas molecules and Reyleigh scattering.

In Langley method in order to calculate τ_{aer} we should use known, computed, or measured outside of UV band parameters τ_{oz}, τ_{mol} and $\tau_{\mathrm{Re}\,y}$ for some fixed wavelengths.

Therefore problems related with direct measurements of optical depth of aerosol in UV band leads to necessity to carry out non-direct measurements and then to calculate the optical depth using parameters determined outside of UV band. Here we also should note that well – known ozonometrical method of Dobson envisages in some cases removal of aerosol error using two pair of wavelength method for linear approximation of wavelength dependence of aerosol optical depth, but this method doesn't allow us to carry out aerosol measurements removing influence of atmospheric ozone.

As a result the Dobson method cannot be considered as universal and accurate method for research of optical parameters of components of the atmosphere in UV band. Such a universal property is possessed according to our view – point by three-wavelength method of atmospheric measurements in UV band that was described in [3].

In this article we shall describe the variant of application of this method for determination of main optical parameters of aerosol. First of all we should describe the differential method that will be also used. As it is well known [1], the optical depth of aerosol $\tau_{\lambda\,aer}$ is determined by Ongstrem formula

$$\tau_{\lambda\,aer} = C\,\lambda^{-\alpha}, \qquad (2)$$

where *C*- parameter of Ongstrem; α - parameter related with Junge index *n* as follows:

$$\alpha = n - 3.$$

Taking derivative of equation (2) on λ we have following equation

$$\frac{d\tau_{\lambda\,aer}}{d\lambda} = -\alpha C_1 \lambda^{-(\alpha+1)} \qquad (3)$$

or

$$\frac{\Delta\tau_{\lambda\,aer}}{\Delta\lambda} = -\alpha C\,\lambda^{-(\alpha+1)}. \qquad (4)$$

The foregoing formula (4) is the basis of proposed differential method. The formula (4) is the transcendental equation in relation to parameter α, and this equation may be solved using graphic method.

The essence of the graphic method includes plotting of set of curves of function

$$\frac{\Delta\tau_{\lambda\,aer}}{\Delta\lambda} = f(\alpha, \lambda, \tau_0) \qquad (5)$$

for given discrete values of λ, for given continuous interval $\alpha = \alpha_{min} \div \alpha_{max}$.

The crossing points of above curves with the horizontal line $y = \frac{\Delta\tau_{\lambda\,aer}}{\Delta\lambda}$ will give us needed values of $\alpha_1, \alpha_2, \ldots, \alpha_n$.

This process of solution of equation (5) is illustrated conditionally in fig. 1.

It is obvious, that solution of equation (5) envisage presence of estimate of differential parameter $\frac{\Delta\tau_{\lambda\,aer}}{\Delta\lambda}$. In order to calculate this parameter we use abovementioned three-wavelength method.

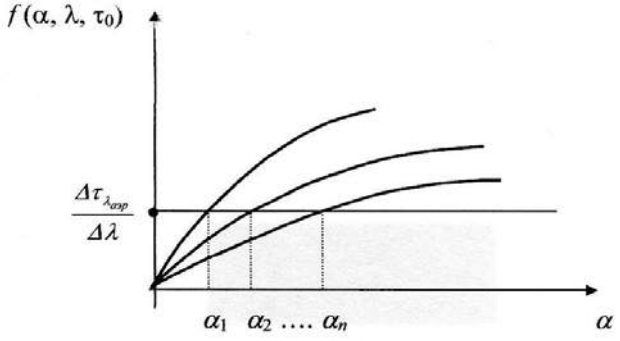

Fig. 1. Schematic illustration of proposed method.

Now we describe in brief the basics of this method and the variant of its application for considered task. According to three-wavelength method we should carry out measurements in three-wavelength λ_1, λ_2, λ_3 where $\lambda_1 < \lambda_2 < \lambda_3$. As a result we obtain parameters $I_1(\lambda_1)$; $I_2(\lambda_2)$ and $I_3(\lambda_3)$ which accord to intensities of Solar irradiation at the Earth level in appropriate wavelengths. Then we should calculate following relative parameter z

$$z = \frac{\sqrt[d]{I_1(\lambda_1)\cdot I_3(\lambda_3)}}{I_2(\lambda_2)}, \qquad (6)$$

where $d=2\pm\Delta$; Δ - parameter which is regulated by computer.

For further description of the method we use the Bouger – Beer formula, which in general may be written as

$$I = \Delta\lambda \cdot \omega \cdot S_0 \cdot 10^{-\left[\gamma \mu X + \tau_{\mathrm{Re}y} m + \tau_{aer} m_1\right]}, \qquad (7)$$

where S_0- the solar irradiation flux at the level of upper border of the atmosphere; γ - optical absorption of ozone; μ - optical mass of ozone; X - total content of ozone; τ_{Rey} - optical depth of Reyleigh scattering; m - optical mass of Reyleigh scattering; τ_{aer} - optical depth of aerosol; m_1 - optical mass of aerosol.

Taking into considerations formulas (6) and (7) we have:

$$z = \frac{\sqrt[d]{S_{01}\cdot S_{03}}}{S_{02}} \cdot 10^{-\left[\mu X\left(\frac{\gamma_{\lambda_1}+\gamma_{\lambda_3}}{d}-\gamma_{\lambda_2}\right)+m\left(\frac{\tau_{Rey\lambda_1}+\tau_{Rey\lambda_3}}{d}-\tau_{Rey\lambda_2}\right)+m_1\left(\frac{\tau_{aer\lambda_1}+\tau_{aer\lambda_3}}{d}-\tau_{aer\lambda_2}\right)\right]}. \qquad (8)$$

In order to obtain the aerosol part of formula (8) we should regulate the parameter d in such order that meets following equation

$$\mu X\left[\frac{\tau_{0\lambda_1}+\tau_{0\lambda_3}}{d}-\tau_{0\lambda_2}\right]+m\left[\frac{\tau_{Rey\lambda_1}+\tau_{Rey\lambda_3}}{d}-\tau_{Rey\lambda_2}\right]=0. \qquad (9)$$

The indication of meeting of the condition (9) is to be carried out by auto correlation analysis of parameter Z. The computer should regulate the value of d till achievement of maximal value of ratio of high frequency component of parameter Z, to the low frequency part because the aerosol has most variability among other components of atmosphere. After meeting the condition (9) the equation (8) will be transformed to following formula

$$z = \frac{\sqrt[d]{S_{01}\cdot S_{03}}}{S_{02}} \cdot 10^{-m\left(\frac{\tau_{aer\lambda_1}+\tau_{aer\lambda_3}}{d}\tau_{aer\lambda_2}\right)}. \qquad (10)$$

Then assuming linear type of dependence of function $\tau_{aer}(\lambda)$ in narrow band $\lambda_1 \div \lambda_3$ we have

$$z = \frac{\sqrt[d]{S_{01}\cdot S_{03}}}{S_{02}} \cdot 10^{-m\left(\tau^*_{aer\lambda_1\lambda_3}-\tau_{aer\lambda_2}\right)}, \qquad (11)$$

where

$$\tau^*_{aer\lambda_1\lambda_3} = \frac{\tau_{aer\lambda_1}+\tau_{aer\lambda_3}}{d}. \qquad (12)$$

From the equation (11) we obtain following formula

$$\left(\tau^*_{aer\lambda_1\lambda_3}-\tau_{aer\lambda_2}\right) = ln\frac{\sqrt[m+d]{S_{01}\cdot S_{03}}}{\sqrt[m]{z\cdot S_{02}}}. \qquad (13)$$

Taking into consideration the linear dependence of $\tau_{aer}(\lambda)$ in the narrow band $\lambda_1 \div \lambda_3$ we have

$$\frac{\Delta\tau_{aer\lambda_1,\lambda_2,\lambda_3}}{\Delta\lambda^*} = \frac{1}{\Delta\lambda^*} ln\frac{\sqrt[m+d]{S_{01}\cdot S_{03}}}{\sqrt[m]{z\cdot S_{02}}}, \qquad (14)$$

where

$$\Delta\lambda^* = \left|\frac{\lambda_1+\lambda_3}{d}-\lambda_2\right|. \qquad (15)$$

Therefore, the considered combination of proposed differential method and three-wavelength method allows us to obtain estimates of differential parameter $\frac{\Delta\tau_{\lambda aer}}{\Delta\lambda}$, which is necessary for calculation of parameter α and parameter n using formula (4).

Summarizing the foregoing we can formulate the proposed method of calculation of atmospheric aerosol optical parameters (optical depth and Junge index) as follows.

1. Carrying of three-waves measurements, in such regime, when ratio of high – frequency component of autocorrelation function of parameter Z to low frequency part reaches its maximal value.

2. Calculation of differential parameter $\frac{\Delta\tau_{\lambda aer}}{\Delta\lambda}$ on the basis of data, obtained during realization of item 1.

3. Carrying out of graphical solution of equation (5) shown in fig. 1.

In conclusion we should stress out, that the proposed differential method in comparison with the Langley method bases on results of direct measurements in UV band, which conditions high authenticity of results obtained using this method.

[1] *P. Gushchin, N.N. Vinogradova.* Total Content of Atmospheric Ozone, Leningrad, Gidrometeoizdat, 1983. (In Russian).

[2] *T.F. Eck, B.N. Holben, L.S. Reid.* J. of Geoph. Res., 1999, v.104D, N.24, p.31.

[3] *H.H. Asadov, M.M. Aliyev, A.A. Isayev*. Fizika, 2004, v.X, N.1-2, p. 52-56.

H.H. Əsədov, M.M. Əliyev, E.S. Abbaszadə

ATMOSFERDƏKİ AEROZOLUN ƏSAS OPTİK PARAMETRLƏRİNİN UB DİAPAZONDA TƏYİN EDİLMƏSİ ÜÇÜN DİFFERENSİAL METOD

Qeyd edilmişdir ki, mövcud metodlar atmosferdə aerozolun optik sıxlığını UB diapazonda dəqiq təyin etməyə imkan vermirlər. UB diapazonda atmosferdəki aerozolun optik sıxlığını təyin etmək üçün Anqstrem qanununa və əvvəllər təklif edilmiş üç dalğalı ölçmə metoduna əsaslanan differensial metod təklif edilmişdir. Metod riyazi cəhətdən əsaslandırılmış, onun tətbiqi ardıcıllığı şərh edilmişdir.

Х.Г. Асадов, М.М. Алиев, Э.С. Аббасзаде

ДИФФЕРЕНЦИАЛЬНЫЙ МЕТОД ДЛЯ ОПРЕДЕЛЕНИЯ ОСНОВНЫХ ОПТИЧЕСКИХ ПАРАМЕТРОВ АЭРОЗОЛЯ АТМОСФЕРЫ В УФ ДИАПАЗОНЕ

Отмечено, что существующие методы не позволяют точно определить оптическую плотность аэрозоля атмосферы в УФ диапазоне. Для определения оптической плотности аэрозоля атмосферы в УФ диапазоне предложен дифференциальный метод на основе закона Ангстрема и ранее предложенного трехволнового метода измерений. Дано математическое обоснование метода, пояснено последовательность его применения.

Received: 23.05.06

THE CONDITIONS OF OBTAINING OF HOMOGENEOUS MULTI-COMPONENT THERMOELECTRIC ALLOYS

F.K. ALESKEROV
Scientific-Production Association "Selen" NASA
Baku-1143, F. Agayev, 14

The review of the articles on the heterogeneity of low-temperature materials on the base of chalcogenides of bismuth and stibium, obtained by the different technological methods has been formed. The influence of the appearing samples at the doping of the heterogeneity on the properties (micro- and macro-heterogeneity), obtained by the methods of powder metallurgy and vertically directed crystallization has been established. The regions of eutectic and island structures have been found in heterogeneous alloys, created by the compounds Bi_2Te_3, Sb_2Te_3 and Sb_2Se_3.

Introduction

The treatment of high-effective thermo-electrics on the base of multi-component systems of solid solutions (Bi-Te-Se) <impurities> and (Sb-Te-Se-Bi) <impurities> leads to the creation and wide distribution of thermo-electric generators and refrigerators for the wide temperature interval. Nowadays the question is open: how we should change the compositions of solid solutions, in order to provide the high values of thermoelectric efficacy (Z) in wide temperature regions (100-700°K). Moreover, the material should have such concentration of current carriers, in order the optimal (including $Zmax$) values of thermoelectromotive force (α) and electroconductivity (δ) are supplied for the given temperature interval. That's why the task of the Z increase should be solved in the interconnection with the study of their structures and compound homogeneity. From other side, the knowing of component distribution allows to treat the technology of the obtaining of thermoelectric alloys of high quality.

First part of the given paper is dedicated to the short analysis of known experiment results on heterogeneity of alloys $A_2^{V}B_3^{IV}$, obtained by different methods of crystals of solid solutions on the base Bi_2Te_3 and Sb_2Te_3. In the second part of the paper the structures of the layers $Te^{(I)}$-$Te^{(I)}$ are given and analyzed.

Bi_2Te_3, Bi_2Te_3-Sb_2Te_3, Sb_2Te_3-Sb_2Se_3-Bi_2Te_3 are doped by impurities, created the optimal concentrations of current carriers.

First part

The heterogeneities in alloys obtained by the different methods

As the irregular distribution of the composition, so the possible creation of the strange phase at the synthesis (two-phase creations by eutectic type) influence on the properties of bismuth and stibium chalcogenides. The monograph [1], in which the characteristics are considered, influencing on the formation of micro- and macro-heterogeneous in growing sample was the one of the earliest works: the longitudinal and transversal layer heterogeneities, homogenization and introduced additions.

Many refs had been published in the further years in this direction, however, the wide review of authors [2], dedicated to the homogeneity of solid solutions $Bi_{1-x}Sn_xTe_{1-y}Se_y$ (x=0,01; y=0,06, 0,12), grown on the Chochralsky method with the replenishment of liquid phase from the floating crucible demands the special attention. The authors revealed the influence of tin atoms on the homogeneity distribution of main components: in monocrystals Bi_2Te_3 the tin increases the compound heterogeneity; the fluctuation of Sb and Te content increases on 0,3% in stibium telluride. The studying of electrophysical properties of the system $Bi_{2-y}Sn_yTe_{3-x}Se_x$ was the continuity of these investigations [3]. The methods of micro-analysis of the surface levels have been changed. Thus, the defects of crystalline structure and dislocation structure of bismuth telluride and above mentioned solid solution have been studied by the method of transmission electron microscopy. The dislocations, situated in basis plane (0001) are the dominant defect type in the given monocrystals, also the presence of the defects of the packing and very small dislocation loops is shown. As all investigated monocrystals are pronounced semiconductors, so the observable defects don't influence the significant influence on their electrophysical properties [3].

As a whole, heterogeneities and the structure unsoundness of material structures on the base of Sb_2Te_3 and Bi_2Te_3 influence on the obtaining of the optimal concentrations of the electrons and holes. Many publications are dedicated to these problems; some of them are [2,3,4-7]. At the investigation of the structure of these materials, the investigators [4-7] dispute in the relation to the presence of these or that defects. The different frequency and the composition of the initial materials, and also different conditions of alloy synthesis take place. The heterogeneities in them will be significantly differ because of the peculiarities of the growing technology of crystals by the type Sb_2Te_3, Bi_2Te_3 and their solid solutions.

The influence of the obtaining technology on the crystal heterogeneities (Bi-Te-Se) and (Sb-Bi-Te)

The micro-heterogeneities of the Bi_2Te_3-Sb_2Te_3 (x=0,3; 0,6) system have been formed in [8] after the sample synthesis from them, obtained by the methods of directed crystallization from the alloy, pressing, storage extrusion, investigated by roentgen-spectral analysis. The qualitative analysis of the distribution curves of Se and Te concentrations proves the data [1] and shows on the presence in the solid solutions, obtained by the directed crystallization and extrusion method, longitudinal layer heterogeneity. The solid solutions, prepared by the methods of powder metal-lurgy reveal the micro-heterogeneity, statistically distributed on the volume (micro-heterogeneities exceed 150 mcm). More homogeneous samples have been obtained by the directed crystallization. Such samples are called by directed

crystals (DC). The less homogeneous crystals are pressed ones (here the sizes of heterogeneities change in the dependence on the grain sizes, used in the powders). The homogeneity of the extruded samples depends on the homogeneity of the initial storages. However, the extrusion process itself significantly homogenizes the material [2].

Bi-Sb-Te homogeneity. The more high homogeneity $Bi_{0,52}Sb_{1,48}Te_3$ is caused by the less temperature interval between the lines of liquidus and solidus in the system Bi_2Te_3-Sb_2Te_3, than in system Bi_2Te_3-Bi_2Se_3 in the comparison with $Bi_2Te_{3-x}Se_x$ [2]. The concentration heterogeneity, observable in the extruded samples $Bi_{0,52}Sb_{1,48}Te_3$ doesn't have the layer character, inherent in $Bi_2Te_{3-x}Se_x$.

Eutectic on Te base in the materials of n- and p-types

The eutectic containing the pure Te has been revealed by the authors in the alloy $Bi_2Te_{3-x}Se_x$ [8]. The quantity, structure and composition of it are defined by the method of sample obtaining. At the investigation of the layer surfaces of the crystals by the composition $(Bi_{0,25}Sb_{0,75})_2$ $(Te_{0,95}Se_{0,05})_3$ the eutectic had been revealed. It was situated between basis planes of solid solutions [2]. This two-phase system consisted on the pure Te and material disseminations of the composition $(Bi,Sb)_2(TeSe)_3$, in which the ratio of the concentrations Bi and Sb is close to 34:66mol.%. The solid solution in eutectics is strongly enriched by Te. The composition of the second phase, revealed in grown crystals on Bridgmen method and doped by Te excesses $(Bi_2Te_3)_{25}$ $(Sb_2Te)_{70}$ $(Sb_2Se)_5$, is defined as 90%Te with small quantity of Bi, Sb, Se, that corresponds with data [8].

The streaks, having the eutectic structures are created in two-phase region between crystals of solid solution $(Bi, Sb)_2Te_3$. The distribution heterogeneity of excess Te at the band recrystallization of solid solution $Bi_{1,6}Sb_{0,4}Te_3$ was also mentioned in [2]. The α change on the ingot and inversion of its sign is explained by this. The authors [9] inform about segregation of the doping impurity $CdCl_2$ in upper part of the ingot (90 mol% $BiTe_3$ – 10 mol% Bi_2Se_3) and change of the composition because of the significant evaporation of Te and Se.

The monocrystals of solid solutions (Bi_2Te_3-Bi_2Se_3) and (Sb_2Te_3-Bi_2Te_3), grown by Chochralsky method, are characterized by the most homogeneity in the comparison with other materials (obtained by other known methods) [2]. The $Bi_2Te_{2,7}Se_{0,3}$ samples have the less homogeneity, if they have been obtained by the methods of directed crystallization, extrusion and powder metallurgy.

At the corresponding purity of the initial components the composition of given crystals becomes the homogeneous one. The monocrystalline sample, grown up from materials of 99,9999% purity, is the most homogeneous one. The thermo-elements, produced from such alloys and also the intercalationed crystals Bi_2Te_3 are more perfect; they are used in different scientific-technical aims [10-12].

Second part

Interlayer structure and electrophysical properties

Method of experiment

The monocrystals Bi_2Te_3, (Bi_2Te_3-Bi_2Se_3) и (Sb_2Te_3-Bi_2Te_3-Sb_2Se_3) had been obtained by Bridgmen method [13] and known method of vertically directed crystallization. In scientific investigations and industrial manufacturing the growing up the multi-component crystals by Bridgmen method has the set advantages [13]:

- repeatability and homogeneity of ingots, repeatability of the composition at the synthesis of multi-component crystals and solid solutions, the saving of the calculated components because of the system insularity, the possibility of crystal obtaining with microstructural characteristics and sizes of monocrystalline regions, which are acceptable for the studying of the properties.

Ampoules by the internal diameter 8-20mm, produced from the quartz glass, were washed firstly by nitric acid at the temperature ~350°K during 0,5 hours, further, by the distillated water many times. The degassing was carried out either in the stove, or in the flame of oxygen bumer at the continuous spooling.

The initial furnace was prepared from the components Te, Se, Bi, Sb of pure 99,9999% (treated by needed purity). The furnace components were weighted with the delicacy +-0,005g, common mass of furnaces depends on the ampoule size and was from 100 till 200g. The opened ampoule after the preliminary heating at 400-600°K was put into upper low-temperature part of heated stove, where the temperature is lower on ≈ 70°K, than liquidus temperature of furnace $T_{lic.}$, by conic part, and was lifted with the velocity 5 mm/h. At the sample obtaining by the method of directed crystallization the velocities 10, 20 and 30 mm/h were used.

The perfectness and heterogeneity of crystal structures were investigated by method of electron microscopy. The investigations were carrying out on the electron microscope JEM-35CX. The samples, cut from three parts of the crystal: initial, middle and final, had been investigated. The surface was obtained by the simple chipping on the planes before investigation (0001).

The results and their discussion

The sample heterogeneities, obtained by methods of Bridgmen and vertically directed crystallization had been analyzed. The samples, obtained by Bridgmen method were more perfect and in the middle region the regular distribution of the components took place Sb, Bi, Te, Se. The significant accumulations of the impurities were observed in the interlayer space of the samples, obtained by directed crystallization (we will call them, as it was mentioned - (DC)). The nonmonotonic change of component concentrations in crystallizing solid solutions P - ($Sb_2Te_3$70 mol% Sb_2Se_3·5 mol% - Bi_2Te·25 mol%) < impurities> has been established. The presence of two-phase region, appearing at the achievement of Te concentration and having the layered structure has been revealed by us. The streaks, having two-phase eutectic structures are clearly seen in two-phase region in the beginning of the ingot of samples by p-type with the additions of Te superstoichiometry (no more, than 3% weigh.). This is proved by electron-microscopic photos (fig.1). The analysis shows, that these planes are eutectic ones Sb_2Se_3-Se (having the composition on state diagram $SbSe_3$ 50 mol % - Se 50 mol %); they are situated on basis plane (0001) and very negatively influence on thermoelectromotive force. Thus, in the beginning of the ingot the thermoelectromotive force has the value $\alpha = +(130 \div 160)\frac{mcV}{C^\circ}$, and in final has the value

$\alpha = +(230-240)\frac{mcV}{C^\circ}$. The middle part is more homogeneous one; the thermoelectromotive force oscillates in limits (195-205) $\frac{mcV}{C^\circ}$ at the value $\delta = (1300-1100)\,\mathrm{Om^{-1}cm^{-1}}$. The electron-microscopic photo (fig.2) of this compound by p-type of the surface of basis plane shows the significant quantity of lamination steep $Te^{(I)}$-$Te^{(I)}$ and its micro-crystal structure. Such dispersion along the length of this plane (~10-12mm) practically doesn't influence on thermoelectric parameters. The analogical micro-dispersion structures are observed in Bi_2Te_3 <Cu, In> and doped solid solution (Bi_2Te_3·95 mol % - Bi_2Se_3·5 mol %) <$CdCl_2$,Cu, In>.

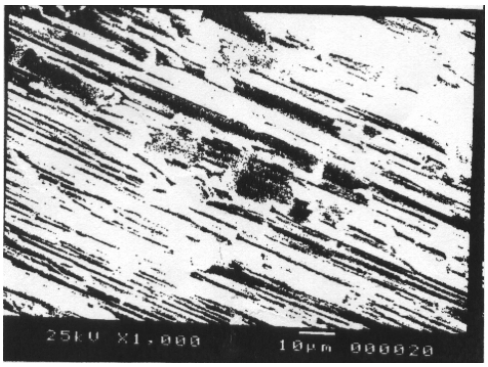

Fig.1. The electron-macroscopic photo of two-phase eutectic Sb_2Se_3-Se.

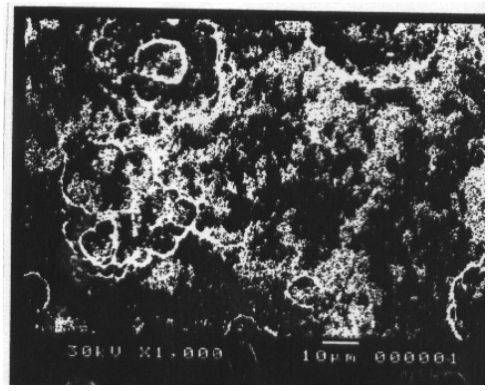

Fig.2. The electron-macroscopic photo of crystal of the system ($Sb2Te_3$·75 mol % - Bi_2Te·25 mol %)<3·0 weight Te>.

The electron-microscopic image of pure Bi_2Te_3 < In, Cu is given on the fig.3, and the island distribution of the impurity in the solid solution by n-type (doped by Cu and In) is shown on the fig.4. Such islands, situated on the surface of the plane (0001) along the layers $Te^{(I)}$-$Te^{(I)}$ in the middle part of ingots doesn't negatively influence on the electrophysical parameters (DC). At this it is seemed, that electric resistance of the islands changes the optimization conditions of parameters of such multi-layered structures in the comparison with earlier considered cases of the layers, having the normal conductivity (δ). The complex impurities (B, Cu, $CdCl_2$, Te, Sb, $SbCl_3$) at well their quantitative ratio, one play the donor roles, other have acceptor functions, allowing to obtain the needed concentrations of current carriers (including α and δ).

Fig.3. The electron-macroscopic photo Bi_2Te_3, doped by complex impurity In(0,05 weight%) и Cu(0,05 weight%).

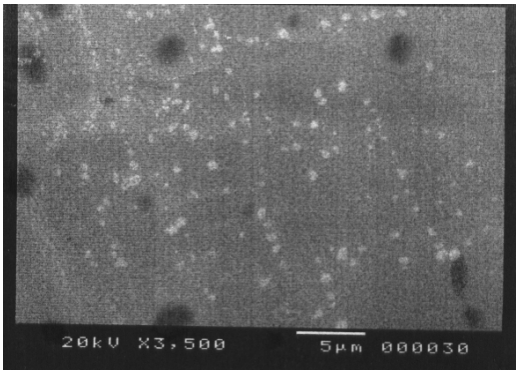

Fig.4. The islands steps of Cu on basis plane (0001) of bismuth telluride.

The investigations of the heterogeneities and elements distributions on the length and cross-section of given chalcogenides (DC) Sb and Bi (doped by impurities) were carried out by us mainly for the definition of the interconnection of conditions of obtaining and homogeneity. Here, in small degree the influence of this or that impurity heterogeneity on their thermoelectric parameters is reflected. The unit point of view on model of the introduction mechanism is absent and the complex character of introduction of impurity atoms in crystalline lattice on the base of which it could be possible to describe qualitatively the observable experimental facts. The formation of island structures in thin films and island layers $Te^{(I)}$-$Te^{(I)}$ of the crystals by type Bi_2Te_3 and Sb_2Te_3 causes the special interest of many investigators. The theory, developed in [14] can be accepted by us in the following explanations of island structures, obtained by us in the interlayers. Such the kinetics of phase impurity exfoliation in adsorbent layer on the mechanism of increased diffusion in segregation process of impurities from sample width had been investigated by authors. It is shown, that in the case of gravitation between the impurities they reveal the tendency to the formation in adsorbent layer of surface structure [14]. The main characteristics of these structures change with time by nonmonotonic way.

Thus, in our case in "closed" interlayer space $Te^{(I)}$-$Te^{(I)}$ the accumulation of the impurities is bigger, than in other defect centers (vacancies from Te, in layers $Te^{(I)}$-Bi and $Te^{(I)}$-Sb, grain limits, on external surface) takes place. In real

crystals (especially in layered materials by type of bismuth and stibium chalcogenide), consisting Se, tin, Cu, Ni, Fe, B, the distribution on the ingot (on the length and cross-section) is quite irregular. The one of the reason of this space heterogeneity can be segregation processes, caused by chemical interaction of impurities with atoms and matrix (Bi_2Te_3-Sb_2Se_3-Sb_2Te_3) – Te, Se, Bi and Sb.

The eutectic phases Sb_2Se_3-Se (fig.1) and island layers from Cu and In (fig.3 and 4) are observed in the investigated by us electron-microscopic photos (fig.1-4). Rather on the fig.3,4 in basis plane (0001) Bi_2Te_3 the created islands are the Cu layers. It is known, that Cu because of small ion radius "settles" in interlayer space $Te^{(I)}$-$Te^{(I)}$ more, than in layers $Te^{(I)}$-Bi и $Te^{(I)}$-Sb, creating the many layers and finally the islands (fig.4).

The similar phenomena are observed at the formation of film coverings created from the gas phase on massive substrates. For example, in [14] the results of direct observation of growing kinetics of island film Cu on the carbonic are analyzed. The growing of the islands is considered by them as multistage process, including in itself: diffusion of atoms on the substrate (in layered structure Bi_2Te_3 – in Van der Waals crack) $Te^{(I)}$-$Te^{(I)}$, the transfer through potential barrier on island bounder, diffusion on island surface and joyance to the elementary capture centers on the surface (the quintets $Te^{(I)}$-$Te^{(I)}$ are the surfaces in the considered variant Bi_2Te_3).

In conclusion let's consider the possible creations of eutectic alloys in the systems Bi_2Te_3, Sb_2Se_3, Sb_2Te_3 and in their solid solutions. The task is the creation of eutectics between the layers. Such layer had been revealed by us on eutectic base Sb_2Se_3-Se in basis plane (fig.1) of the system (Sb_2Te_3-Sb_2Se_3-Bi_2Te_3). This eutectic at the composition 50 at.% of Se melts at the temperature 820°K. In the conditions of high pressures its melting point can be closer to the melting point of solid solution (till 910°K) and this can be the one from the possible reasons of the simultaneous growth (DC) of solid solution and eutectic (having very low thermo-electric parameters).

In this connection the thought about the undesirability of the use of complex solid solutions, the one of the component of which can be stibium selenide.

Conclusion

From all possible heterogeneities two heterogeneity in solid solutions on the base of Bi and Sb chalcogenides have been revealed. The one heterogeneity, connected with the creation of eutectic streak from Sb_2Se_3-Se negatively influences on thermoelectric parameters of the alloy on the beginning stages of growing (DC). The other heterogeneity connects with the creation of island layers in basis plane (0001) of layered crystal by type Bi_2Te_3. The growing perspective of such multi-layered structures on the base of the multi-component alloys doesn't cause the doubts.

[1] *B.M. Goltsman, V.A. Kudinov, I.A Smirnov.* Monografiya - Poluprovodnikovie termoelektricheskie materiali na osnove Bi_2Te_3. M.: Nauka, 1972, 320 s.

[2] *I.V.Gasenkova, V.A.Chubarenko, E.A.Tyavlovskaya, T.E.Svechnikova*. J. Poverkhnost. Rentgenovskie, sinxrotronnie i neytralnie issledovaniya, 2003, № 3, s.32-41.

[3] *I.V. Gasenkova, T.E. Svechnikova*. Neorganicheskie materiali, 2004, t.40, № 6, s.663-668.

[4] *N. Frangis, S. Kuypers, C. Manolikas et al*., J. Solid State Chem, 1989, v. 69, N 8, p.817-819.

[5] *N. Frangis, C. Manolikas, S. Amelinckx*. Phys. Status. Solidi. A. 1991, v.125, p.97-106.

[6] *N. Frangis, Kuypers, C. Manolikas et al.* J. Solid. State Chem. 1990, v.84, p.314-334.

[7] *D. Maier, D. Eyidi, O. Eibl*. Stoichiometric Varlations and Strain Fields in $(Bi, Sb)_2(Se, Te)_3$ Peltier Material. Proc. of the Sixth Eur. Workshop on Thermoelectrics. Freiburg im Breisgan, 2001, p.32-35.

[8] *K.G. Gartsman, T.T. Dedergaev, A.S. Barat*. J. Neorganicheskie materiali. 1977, t.13, № 7, s.1210.

[9] *Heon Phil Ha, Dow Bin Hyun. Young Whan Cho, Jac Dong Shim*. Proc. XIV Int. Conf. on Thermoelectrics. 1995. St. Petersburg.: A.F. Ioffe Physical-Technical Institute, 1995, p.104.

[10] *J. Bludska, S. Karamazov, J. Navratil, I. Jakubec, J. Horak,* Copper intercalation into Bi_2Te_3 single crystals, Solid State Ionics 171 (2004) 251-259.

[11] *Osami Vamashita and Shoichi Tomiyoshi*, High performance n-type bismuth telluride with highly stable thermoelectric figure of merit, Journal of Applied Physics, v.95, N 11, 2004.

[12] *D.A.Pshenay-Severin, Yu.I.Ravich, M.V.Vedernikov.* J. Fizika i texnika poluprovodnikov, Rossiya, 2000, t.34, t.10, s.1265-1269.

[13] *V.I. Shtanov.* J. Kristallografiya, 2004, t.49, № 2, s.343-349.

[14] *L.I. Stefanovich, E.P. Feldman, V.M. Yurchenko*. J.Metallofizika. Noveyshie texnologii, 2002, t.24, № 8, ss.1103-1122.

F.K. Ələsgərov

BİRCİNSLİ ÇOX KOMPONENTLİ TERMOELEKTRİK MATERİALLARIN ALINMASININ TEXNOLOJİ ŞƏRTLƏRİ

Bismut və antimonun xalkogenidlərinin əsasında yaradılmış metodlarda qeyribircinsli termoelektrik materiallarının elmi ədəbiyyatda verilən məlumat göstərilir. Şaquli yönəlmiş kristallizasiya və toz metallurji metodu ilə alınmış nümunələrinin xassələrinə təsir edən legirə qeyribircinslilik müəyyən edilmişdir. Bi_2Te_3, Sb_2Te_3 və Sb_2Se_3 qeyribircinsli ərintilərdə eftektik və adalı strukturlar tapılmışdır.

THE CONDITIONS OF OBTAINING OF HOMOGENEOUS MULTI-COMPONENT THERMOELECTRIC ALLOYS

Ф.К. Алескеров

УСЛОВИЯ ПОЛУЧЕНИЯ ОДНОРОДНЫХ МНОГОКОМПОНЕНТНЫХ ТЕРМОЭЛЕКТРИЧЕСКИХ СПЛАВОВ

Установлено влияние возникающих при легировании макро- и микронеоднородностей на свойства образцов, полученных методами порошковой металлургии и вертикальной направленной кристаллизацией. Из двух исследованных неоднородностей одна связана с возникновением слоя эвтектики Sb_2Se_3-Se в системе (Sb_2Te_3-Sb_2Se_3-Bi_2Te_3), другая связана с неоднородным распределением островковых примесей в базисной плоскости $Te^{(I)}$-$Te^{(I)}$ слоистого кристалла Bi_2Te_3.

Received: 15.12.05

MATRIX COMPOSITE SENSOR FOR MEASUREMENT MERE STREAM

A.A. BAYRAMOV, N.A. SAFAROV
Institute of Physics, Azerbaijan National Academy of Sciences
Azerbaijan, Baku, Az-1143, H. Javid pr., 33

For detection and research obvious and latent heat stream in mere has been developed the extended high-resistance sensor made on special matrix technology. Detector measures both temperature of surrounding sea water, and direction of a stream. Signals from the sensor, amplified of the operational amplifier, by dint of the interface input into a computer for the further processing results of measurement and archiving of the data. The software package of processing and archiving of results of measurement is created.

1. Introduction

Detection and research obvious and latent heat stream in mere is an actual problem for studying the physical processes proceeding at oceans and the seas. It is the important problem for study and prediction of climate fluctuation for the Earth, for the solution ecological and many other things of problems of a national economy [1,2,3].

Stream at ocean can be watched on indirect indicators - to variation of temperatures or transferred stream by ice, to suspended matters, a phytoplankton (so-called tracers), fixed by means of various sensors of remote sensing in visible and thermal infrared ranges, or the sensor units directly contacting to an aquatic environment. Passive tracers, such as a chlorophyll or temperature, visualize stream in a field of temperature or colour of a sea on space films.

Possibilities of measuring by radar filming performances of stream at ocean or sea were explored repeatedly. However, systems used now are not suitable for such investigations as do not ensure the vector measuring and do not allow receiving the space field pattern of rate.

On radar snapshots the surface developments established by stream are recorded. In areas of interacting of stream there can be fronts, bands of tide rings and choppy seas; these phenomena are detected as a series of ghost lines or spots.

Borders of stream and the structures coupled to stream (fronts, meanders, spurts, mushroom structures and vortexes) are well visible in a field of temperature on snapshots in a thermal infrared range.

Fronts and the frontal areas are the most interesting phenomena at ocean. In the frontal areas intensive dynamic processes, specially there where there are aqueous masses the greatest differences of the physicochemical properties.

In the World ocean major diversity of vortexes and vortex motions is watched. Commonly ooze the frontal vortexes, the vortexes of midocean arising owing to baroclinic instability; the topographic vortexes coupled to a flow of aqueous masses, and synoptic vortexes, generated atmospheric processes, for example, typhoons.

So-called mushroom stream are the vortex formations (or structures) also, its were discovered in the beginning 80th as a result of the analysis of space snapshots. Mushroom stream is a combination of a narrow jet flow and a couple of vortexes of an opposite sign - dipoles because of what this vortex structure likes a mushroom in a slit.

Thus, widescale researches only near-surface stream in oceans and seas are carried out by methods of remote sensing and aerospace filming.

The ultrasonic sounding method is one of widely used methods of learning of surface and subsurface stream [4]. In particular, at usage of this method, the cross flows of the heterogeneous stream bears to fluctuations of an acoustic signal transiting through it. These fluctuations are changed at a frequency change of a signal in connection with a dimensional change of a Frenel zone. Accordingly, these fluctuations of signals on two different frequencies are coherent in a low-frequency spectral range and incoherent in a high-frequency diapason. Thus discontinuity of ocean will be small on matching with a difference in across-sectional dimension of a Frenel zone for various frequencies. Function of a coherence of signals on various frequencies depends on a spatial distribution of a stream. Therefore multifrequent sounding of stream reconstructs of the profile space of a stream. However with increasing of a logging depth the ultrasonic method results to greater errors.

Most precise measurements of a temperature field and a profile of a stream can be carried out only contact methods when the sensor is in an aquatic environment.

2. Experiments

There are two main problems at development of the sensor contacting to an aquatic environment:

1) If electrodes of the sensors measuring a heat stream are isolated from water, pressure of water renders destroying influence on the sensor measuring a heat stream.
2) If electrodes of the sensor adjoin to water, the water environment shunts electrodes and brings distortions in physical value of electric parameters of the sensor.

In paper results of development and research of the sensor on the basis of composite materials are given. The sensor is intended for measuring simultaneously temperature fields and the space a profile of the obvious and latent heat stream of an aquatic environment (in three coordinates). Measuring can be carried out both in near-surface areas, and on various depths in an aquatic environment. Usage for this purpose of composite materials allows us extend a research range.

Development of new polymeric composite materials, prediction and improving of their characteristics depends from binding which one is the major component of composite materials. In this connection recently the investigations in the field of a polymeric materials technology in particular conducting polymeric composite materials [5], were increasing.

The purpose of work is development of the sensor for simultaneous measuring a temperature field and the space a profile of the obvious and latent heat stream of an aquatic environment.

The material of the matrix (the belt shape) sensor unit-exemplar consists of three components:

1) Polymeric component of an exemplar, for collimating to an exemplar of pliability, a technological Q-factor and provision high resistive of the sensor unit;

1) A piezoelectric filling compound in the form of slurry in the sensor unit (comminuted and mixed in a polymer), for amplification of accumulation of charges on surfaces of a matrix and direction finding of a motion of an aquatic environment;

2) thermo-filling - a semiconductor filling compound in the form of magnetic character slurry for provision thermosensitivity of an exemplar.

As a polymer it is possible to take polytetrafluoroethylene (teflon-4) or polyethylene. On insulating properties teflon-4 belongs to best of known dielectrics. In table 1 basic characteristics of teflon-4 and polyethylene are given.

Table 1

	Resistivity, ρ, Ohm·м	Dielectric factor at f=1MHz and t^o=20°C	Dielectric loss tgδ at f=1 MHz and t^o=20°C	Temperature stability, °C	Ultimate tension, MPa	Relative elongation, %	Density, kg/m^3
Teflon -4	10^{15}÷10^{16}	1,9÷2,2	(2÷2,5)·10^{-4}	-260 ÷ +250	15÷30	250÷300	2300
Polyethylene	10^{13}÷10^{15}	2,1÷2,4	(3-5) ·10^{-4}	-70 ÷ + 90	10÷15	300÷750	910÷970

Teflon-4 is more chemical persistent than noble metals that allows to use it at manufacture of the isolation working in corrosive environments. Teflon-4 is not combustible, is not hydroscopic, is not wetted with water and other fluids. Polyethylene is more technological, relative a low-cost and more polarizable material. As the piezoelectric filling compound we used PKR-8, PKR-3 or CTS-300 because a coefficient d_{33} is high. The piezoelectric modulus d_{33} characterizes a density of charge formed on plates of an exemplar at action mechanic exertion in a direction, previous polarization. For example, CTS-300 has a density of charge d_{33} = 280pC/N, ε =100, $t_к$ = 330°C. For getting the sensor unit semiconductor heat-sensitive and piezoelectric materials immix on special technique with powdered polystyrene before achievement of homogeneous mixture. Current-output electrodes in the form of an elastic strip are superimposed in a uniform work cycle. The got exemplar is enveloped by a clean polymeric material for removal shunting in an aquatic environment (Fig.1).

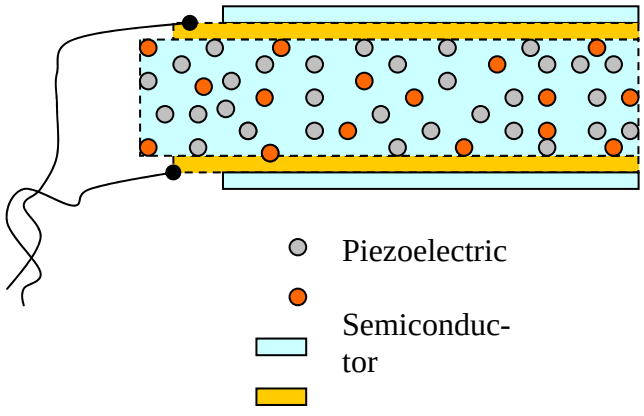

Fig. 1. Cross-section of a matrix sensor.

On fig 2 the operating principle of the matrix (belt) sensor unit is displayed in one plain. Under action of a stream the matrix detector is bended on angle Δφ from a planar state. Depending on direction of the stream $\Delta\varphi > 0$ or $\Delta\varphi < 0$, and dependence as on amplitude $I = f(\Delta\varphi)$, and in a direction *sign (I) = sign* (Δφ) occurs. Therefore at measuring output current I depending on a time t, $I = F(t)$, we get the diagram displayed on Fig.3. The direction of current variation I displays a streamline of current of an aquatic environment (on Fig.6 its are visible in the form of sharp plus (up) or subzero (down) spikes). A degree of current I increase is proportional to temperature T of an aquatic environment. Calibrating a matrix sensor in standard basins with known streams and temperatures it is possible to plot graphics $I = f(\Delta\varphi)$ in absolute units.

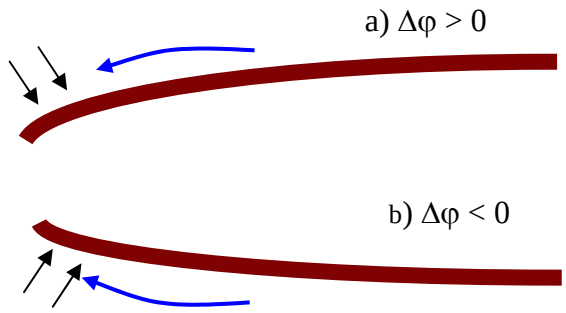

Fig 2. Operating principle of a matrix sensor in one plain.

For measuring the space of a profile of a stream in three plains (coordinates) the modulus from three matrix sensors had in three directions is agglomerated.

At occurrence of a stream in an aquatic environment the elastic strip of the sensor unit bends in the same direction and electrodes are polarized (a direction of polarization depends on a direction of a bend). The occurred charges are read out from electrodes, amplified by charge-sensitivity, converted by an Analog-Digital Converter and move on an input of a computer. The special program in a computer analyses the signals entered from the modulus of sensor units, defines temperature of an aquatic environment and a profile of a stream of current and records in a data bank. In the subsequent these data are used for construction of a temperature field and a stream of current in an aquatic environment.

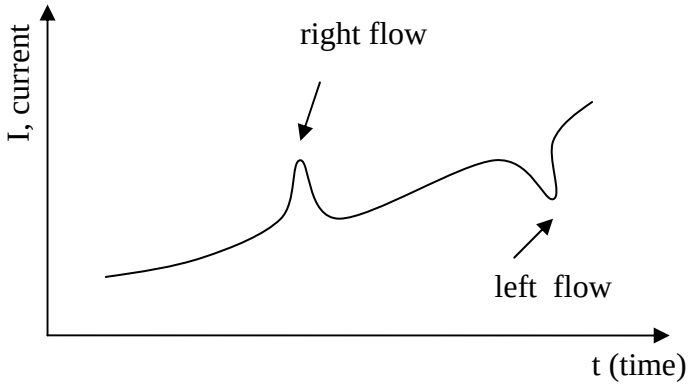

Fig.3. Variation of output current *I* from a time *t*.

The function chart of a measuring system is given on fig.4.

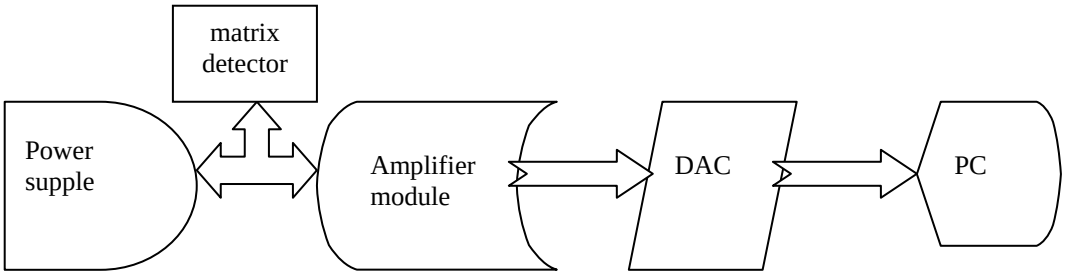

Fig.4 The function chart of a measuring system: DAC – Digital Analog Converter, PC - Personal Computer.

3. Conclusion

Detection and research obvious and latent heat stream in mere is an actual problem for studying the physical processes proceeding at oceans and the seas. There are two problems for researchers:

1) If electrodes of the sensors measuring a heat stream are isolated from water, pressure of water renders destroying influence on the sensor measuring a heat stream.

2) If electrodes of the sensor adjoin to water, the water environment shunts electrodes and brings distortions in physical value of electric parameters of the sensor.

With the purpose of the decision of these problems, has been developed the extended high-resistance sensor made on special matrix technology and measuring both temperature of surrounding sea water, and direction of a stream. Signals from the sensor, amplified of the operational amplifier, by dint of the interface input into a computer for the further processing results of measurement and archiving of the data. The software package of processing and archiving of results of measurement is created.

[1] *L. Gill.* Dynamics of an aerosphere and ocean. M.: Mir, 1991.
[2] *J. Laythill*. Waves in fluids. M.: Mir, 1981.
[3] *Le P. Blon, L. Maysek*. Surges in ocean. M.: Mir, 1977.
[4] *I.B. Esipov, K.A. Naugolnih, I.M. Fuks, M.V. Charnoski*. Sounding of a profile of stream at ocean with usage of fluctuations of a multifrequent acoustic signal. Proc. Nij. Nov. Acoustic Sciences Session. NNSU, 2002, p.11.
[5] *V.E. Gul, L.V. Shenfil*. Electroconductive polymeric composition. M.: Chemistry, 1984, p.240.

A.A. Bayramov, N.A. Səfərov

SU SELİNİN ÖLÇÜLMƏSİ ÜÇÜN MATRİSA TİPLİ KOMPOZİT DETEKTOR

Su mühitində görünən və görünməyən suyun axmasının aşkar və tədqiq edilməsi üçün xüsusi matrisa texnologiyasından istifadə olunmuş yüksək müqavimətli elastik sensor işlənilib hazırlanmışdır. Detektor eyni zamanda ətraf dəniz suyunun temperaturunu və axımın istiqamətini ölçməyə qadirdir. Sensordan gələn siqnal gücləndirilir, sonrakı emal və arxivdə saxlanılmaq üçün interfeys vasitəsi ilə kompüterə daxil olunur. Ölçü nəticələrinin emalı və yaddaşda saxlamaq üçün proqram paketi işlənib hazırlanmışdır.

А.А. Байрамов, Н.А. Сафаров

МАТРИЧНЫЙ КОМПОЗИТНЫЙ ДАТЧИК ДЛЯ ИЗМЕРЕНИЯ ВОДНОГО ПОТОКА

По специальной матричной технологии разработан и изготовлен высокоомный, эластичный детектор для определения видимых и неявных течений в водной среде. Детектор одновременно измеряет температуру и направление течения воды. Сигналы от детектора усиливаются операционным усилителем, посредством интерфейса передаются в компьютер для дальнейшей обработки результатов измерений и архивации данных. Создан пакет программного обеспечения для обработки и создания банка данных.

Received:18.01.06

CENTRIFUGAL DISTURBANCE IN SPECTRUM TRANS-CONFORMER OF THE MOLECULE OF ETHYL ALCOHOL

Ch.O. KADJAR, S.A. MUSAYEV, A.A. ABDULLAYEV, S.B. KAZIMOVA

Institute of Physics of National Academy of Sciences,
H.Javid av., 33, Baku AZ-1143 Azerbaijan

In this paper the rotary, quart, sixth and oct- centrifugal constants of A-reduction of Hamiltonian of *trans*-conformer of ethyl alcohol molecule in three axial representations have been established. The introduction in opposite spectroscopic task anew identified 33 rotary transitions, situated in range of 24,0-498,0 GGs frequencies with high $J(J=34)$ allow to decrease in three times mean-square inclination of above mentioned constants and because of this their combinations have been calculated more precisely.

The investigation of micro-waved rotary spectrum of ethanol molecule CH_3CH_2OH had been begun with identification of *Q*-branches of its *trans*-conformer [1]. Further, its isotope replaced analogues had been investigated in our country by Imanov, Kadjar, Abdurakhmanov, Ragimov and other [2-5], abroad – by Miliggen-Efinger [6], Kulot [7], Kakar [8], Lovas [9] and by others. Further, many serious works were dedicated to the investigation and identification of submillimeter rotary transitions trans- and gosh-conformers of this molecule [9-14,16-18]. Firstly on the base of the result analysis, obtained in these refs in 1975 in Sagittarius constellation (Sgr B2) the three rotary transitions have been revealed: $6_{06} - 5_{15}$ 82265,46 MHz, $4_{14} - 3_{03}$ 90117,51 MHz, $5_{15} - 4_{04}$ 104808,58 MHz [10]. After it, in constellation Hot Cores G34,3+0,15 the rotary transitions of this molecule had been revealed in big quantity [11, 12].

Table 1

The frequencies (MHz) of rotary transitions of molecule trans-ethanol

Transitions							ν_{exp}	$\Delta\nu$	Centrifugal deposit		
									Quart-	Sixth-	Oct-
1							2	3	4	5	6
4	0	4	-	3	0	3	69521,200	-0,017	-1,952	0,085	0,086
6	4	2	-	7	3	5	60136,578	0,102	-27,418	0,088	-0,013
7	5	3	-	8	4	4	94895,800	-8,249	-60,011	8,526	8,185
8	4	4	-	9	3	7	24789,250	-0,081	-8,794	0,086	-0,026
8	5	3	-	9	4	6	77235,048	-0,056	-57,330	0,289	-0,064
10	10	0	-	10	9	1	495876,700	0,113	-808,916	12,079	-2,559
10	10	1	-	10	9	2	495876,700	0,113	-808,916	12,079	-2,559
10	3	8	-	11	0	11	70336,001	-0,133	14,710	-0,069	0,009
11	3	9	-	12	0	12	61775,903	-0,022	14,521	-0,122	0,015
12	6	7	-	13	5	8	58889,529	0,008	-60,885	0,680	-0,383
14	3	12	-	13	4	9	62593,411	-0,079	-75,856	-0,082	0,069
16	4	12	-	15	5	11	50099,200	0,001	-118,431	0,044	0,291
16	4	13	-	17	1	16	64654,377	-0,050	140,553	-0,658	-0,017
17	4	14	-	18	1	17	52020,420	-0,172	138,707	-0,859	-0,016
18	1	17	-	17	2	16	297087,881	-0,099	-224,093	-0,220	-0,019
18	3	16	-	19	0	19	38769,436	0,096	-105,286	-1,538	0,054
19	4	16	-	20	1	19	31772,729	-0,143	108,427	-1,426	-0,030
23	6	18	-	22	7	15	68134,250	-0,054	-322,684	0,212	3,768
23	5	19	-	24	2	22	43838,449	-0,212	543,686	-4,017	-0,986
24	5	20	-	25	2	23	28697,089	-0,191	519,330	-4,562	-1,144
25	4	21	-	24	5	20	250150,722	-0,062	-1077,06	3,425	1,092
26	7	19	-	25	8	18	68657,454	0,021	-442,587	0,351	9,593
26	2	24	-	27	1	27	52171,970	0,015	-832,258	-8,196	-1,219
28	1	27	-	28	0	28	293453,889	-0,035	-656,144	-6,642	-0,832
28	2	26	-	28	1	27	253327,468	-0,010	-835,831	-6,377	-0,995
28	2	27	-	27	3	24	58778,250	-0,141	1154,863	3,762	0,876
29	2	27	-	28	3	26	492412,557	-0,036	-844,304	-2,411	-0,193
30	1	30	-	29	0	29	493256,377	-0,055	-579,460	-0,812	0,649
30	0	30	-	29	1	29	493238,503	-0,046	-580,100	-0,810	0,647
31	6	25	-	31	5	26	244342,608	0,208	853,466	-15,218	-7,420
32	3	29	-	32	2	30	249604,873	0,139	-1518,16	-6,441	-1,480
33	2	32	-	33	1	33	350959,413	-0,028	-1028,97	-13,215	-2,811
34	1	33	-	34	0	34	362257,701	0,021	-1124,83	-14,910	-3,472

Here $\Delta\nu = \nu_{exp} - \nu_{calc.}$.

Table 2

The rotary and centrifugal constants of CH_3CH_2OH molecule in three axial representations

Parameter	Representation		
	I^r	II^r	III^r
X (MHz)	9350,676(1)	8135,488(1)	34891,765(4)
Y (MHz)	8135,234(1)	34891,788(3)	9350,927(1)
Z (MHz)	34891,783(4)	9350,410(3)	8134,994(1)
Δ_J (κHz)	8,530(5)	118,83(6)	122,32(6)
Δ_{JK} (κHz)	-28,63(3)	-359,78(19)	-370,25(19)
Δ_K (κHz)	252,87(11)	252,98(12)	253,01(12)
δ_J (κHz)	1,738(1)	-56,86(3)	55,12(3)
δ_K (κHz)	6,63(9)	120,30(5)	-132,03(5)
H_J (Hz)	-0,011(9)	12,2(8)	12,4(8)
H_{JK} (Hz)	0,90(21)	-68,6(38)	-70,7(39)
H_{KJ} (Hz)	-9,38(79)	97,4(49)	103,2(52)
H_K (Hz)	35,76(147)	-41(1)	-44,8(21)
h_J (Hz)	-0,002(2)	-6,1(3)	6,16(39)
h_{JK} (Hz)	0,11(22)	27,3(14)	-29,4(15)
h_K (Hz)	58,8(65)	-20,2(8)	22,8(9)
L_J (MHz)	0,003(5)	-27,6(33)	-28,1(33)
L_{JJK} (MHz)	0,30(25)	128(22)	134(23)
L_{JK} (MHz)	-44,8(83)	-161(43)	-175(46)
L_{KKJ}(MHz)	47(23)	61(33)	71(37)
L_K(MHz)	-69(16)	-0,7(93)	-2(10)
L_{LJ}(MHz)	-0,0007(13)	13,8(16)	-14(1)
l_{JK}(MHz)	-0,09(15)	-49,2(93)	54(10)
l_{LKJ}(MHz)	15,3(71)	29(11)	-35(13)
l_K (MHz)	-582(145)	-0,3(46)	1,1(55)

Table 3

The defined combinations of spectroscopic parameters of CH_3CH_2OH molecule in three axial representations

Parameter	Presentation		
	I^r	II^r	III^r
A (MHz)	34891,8002	34891,7936	34891,7940
B (MHz)	9350,6482	9350,6480	9350,6480
C (MHz)	8135,2397	8135,2391	8135,2392
T_{aa} (kHz)	-232,7683	-232,5662	-232,5811
T_{bb} (kHz)	-12,0070	-12,0320	-12,0660
T_{cc} (κHz)	-5,0533	-5,1073	-5,0838
T_1 (κHz)	3,0493	3,2764	3,2828
T_2 (κHz)	-3,5553	-3,4630	-3,4510
Φ_{aaa} (Hz)	27,2705	24,4982	24,7425
Φ_{bbb} (Hz)	-0,0167	-0,0004	0,0942
Φ_{ccc} (Hz)	-0,0062	0,0910	0,0177
Φ_1 (Hz)	-19,4751	-25,5021	-25,4089
Φ_2 (Hz)	-4,6031	-5,4553	-5,4198
Φ_3 (Hz)	0,0211	0,0986	0,1075
Φ_4 (Hz)	0,0025	0,0820	0,1140
θ_1 (MHz)	-67,0808	-55,3147	-56,3899
θ_2 (MHz)	0,0023	0,0026	0,0003
θ_3 (MHz)	0,0054	0,0062	0,0059
θ_4 (MHz)	-67,6859	-63,8631	-64,1170
θ_5 (MHz)	-0,0034	0,0145	0,0023
θ_6 (MHz)	-0,0175	-0,0556	-0,0609
θ_7 (MHz)	-756,0766	-707,7655	-711,4906
θ_8 (MHz)	1,8591	4,0902	-7,4367
θ_9 (MHz)	-4,4117	10,6619	5,8051

In Lovas's paper [9], the analytic review of all earlier obtained investigation results of molecule trans-ethanol and calculations of centimeter and millimeter spectrums of this molecule, representing the astrophysical interest are given. Further, Pearson and others identified 450 transitions with high $J \geq 33$ [13], situated mainly in submillimeter region of wave lengths.

In Musayev's paper [14] 56 rotary transitions of this molecule, situated in 25,0-496,0 GHz range of wave length. The introduction in opposite spectroscopic task the new identified frequencies allow firstly to define the oct-spectroscopic constants, and also to define the rotary, quart and sixth spectroscopic constants of this molecule. Besides, in this paper the defined combinations of rotary and centrifugal constants (with the introduction of oct- terms) [15] in three axial representations [16,17] are calculated.

At the solution of opposite spectroscopic task the Vatson Hamiltonian of A-reduction was used [19-21]. Because of the strong centrifugal ethanol spectrum distortion further in solution of opposite spectroscopic task the oct- terms of centrifugal distortion had been introduced, that gave the possibility to identify 33 transitions, relating to millimeter and submillimeter region of wave lengths.

626 rotary transitions, 92 of which rotary transitions, identified in ref [9], 450 rotary transitions, identified in ref [13], 51 millimeter and submillimeter transitions, identified in ref [14] and 33 rotary transitions, identified by us, 20 from which relate to millimeter and 13 relate to submillimeter range of wave lengths, have been introduced into opposite spectroscopic problem. The rotary and centrifugal constants till decimal terms of rotary Hamiltonian in three axial representations are obtained.

The introduction in opposite spectroscopic task of anew identified 33 rotary transitions, situated in range of 24,0-498,0 GHz frequency with high $J(J=34)$ allow to decrease in three times the mean-square inclination of above-mentioned constants and because of it their defined combinations had been calculated more precisely.

The frequencies of rotary transitions, identified by us, and also the centrifugal deposits of separately quart, sixth and oct- terms of these transitions are given in the table 1. The rotary and centrifugal constants of CH_3CH_2OH molecule in three axial representations are given in table 2. The defined combinations of spectroscopic constants of molecule *trans*-conformer of ethyl alcohol, defined on the base of the constants given on the base of table 2, are given in the table 3.

The rotary and centrifugal constants, obtained at the solution of the opposite spectroscopic task and their correlation matrix in representation II^r are given in the table 4.

[1] *L.M. Imanov, Ch.O. Kadzhar.* "Q-Vetv vrashatelnoqo mikrovolnovogo spektra molekuli CH_3CH_2OH. Izv. AN Azerb. SSR, seriya FTMN 2, 51. (1961).

[2] *L.M. Imanov and Ch.O. Kadzhar.* "Superhigh – Frequency Spectrum and Dipole Moment of the Ethyl alcohol Molecule. Opt. Spectrosc. 14, 156. (1963).

[3] *L.M. Imanov, Ch.O. Kadzhar, and I.D. Isaev.* "Microwave Rotational Spectrum of the CH_3CH_2OH and CH_3CHDOH Molecules. Opt. Spectrosc. 18, 194, 1965.

[4] *L.M. Imanov, A.A. Abduraxmanov, R.A. Ragimova.* Mikrovolnoviy spektr i effektivniye postoyanniye molekuli CD_3CH_2OH. Optika i spektroskopiya, t. 19, №2, 306.,1965.

[5] *Ch.O. Kadzhar, I.D. Isaev, and L.M. Imanov.* "Radio-Spectroscopis Structure Determination of the Ethanol Molecule. J. Struct. Chem. 9, 375. (1968).

[6] Michelsen-Efinger P.J., Le, Jour, DE Phys. Spectre de rotation en microondes de la molecule d'alcool etylique *CH_3CH_2OH*. v, 30, avr 11, p. 336. (1969).

[7] *A.P. Culot.* Contribution a l'etude de la molecule d'alcool ethylique en spectroscopic hertzienne. Ann, Soc, Scient, Brux., v, 83, N 1, p. 65. (1969).

[8] *R.K. Kakar, P.J. Seibit.* Microwave Rotational Spectrum of *gauche*-Ethyl Alcohol. J.Chem. Phys, v, 57, N 9, p, 4060. (1972).

[9] *F.J. Lovas.* Microwave Spectra of Molecules of Astrophysical Interest, XXI, Ethanol *(C_2H_5OH)* and Propionitril *(C_2H_5NH)*. J. Chem, Phys., v.11, N2, p.251-300. (1982).

[10] *B. Zuckerman, B. Turner, D.Jonson, F. Clarc, F.Lovas, N. Fourikis, P. Palmer, Morris., A. Lilley, I. Ball, C.Gottlieb, M. Litvak, H. Penfield.* Detection of Interstellar *Trans*-Ethyl Alcohol. Astrophys, J., v, 196, N1, p, 99-102. (1975).

[11] *T.J. Millar, H.Olafsson, A. Hjalmarson, P.D.Brown.* "The detection of Ethanol in W51M," Astron, Astrophys, 205, L5. (1988).

[12] *T.J. Millar, G.H. Macdonald, and R.J. Habing,* "The detection of hot ethanol in G34,3+0,15," Mon. Not. R.Astron, Soc, 25, 273. (1995).

[13] *J.C. Pearson, K.V.L.N. Sastry, M. Winnewisser, E.Herbst, F.C.D. Lusia.* The Millimeter- and Submillimeter-Wave Spectrum of *transe*-Ethyl Alcohol. J. Mol. Spectrosc., v. 24, N1, p.246-261. (1995).

[14] *S.A. Musaev.* Sentrobejnoe vozmushenie trans-konformera molekuli etanola (oktichnie termi). Dokl, NAN Azerbaijana, , t, 57, № 4-6, s, 111. (2001).

[15] *Rao Ch,V,S.* Centrifugal-Distortion Coefficients of Asymmetric-Top Molecules, Reduction of the Octic Terms of, Rotational Hamiltonian. J, Mol, Spectrosc, v102, N1, p, 79. (1983).

[16] *S.A. Musaev.* Dissertasiya d.f.m.nauk. Sentrobejnoe vozmushenie i vnutrennee vrashenie v molekulax etilovogo i izopropilovogo spirtov .BAKU – 2003.

[17] *O.I.Baskakov, Ch.O. Kadjar, S.A. Musaev, D.A. Rzaev, E.Yu. Salaev.* Submillimetroviy spektr molekuli *trans*-etanola, Trudi VII Vsesoyuznogo simpoziuma po molekulyarnoy spektroskopii visokogo i sverxvi-sokogo razresheniya. Tomsk, chast 3, s, 84. (1986).

[18] *J.C. Pearson, K.V.L.N. Sastry, E. Herbst, and Frank C. De Lusia.* The Millimeter- and Submillimeter-Wave Spectrum of *gauche*-Ethyl Alcohol. J. Mol. Spectrosc., v. 175, N 1, p. 246. (1996).

[19] *J.K.G. Watson.* Determination of Centrifugal Distortion of Asymmetric-Top Molecules. J.Chem. Phys., v. 46, N 5, p.1935-1949. (1967).

[20] *J.K.G.Watson.* Determination of centrifugal-Distortion Coefficietts of Asymmetric-Top Molecules. III. Sextic Coefficients. J. Mol.,Spectrosc.,v.48, N10, p.4517-4524. 1968.

[21] *J.K.G. Watson*. Mass Derivatives of Molecular Parameters and Distortions in $r^{(2)}_m$ Structures J. Mol. Spectrosc., v.207, N 1, p.16-24. (2001).

Ç.O. Qacar, S.A. Musayev, A.A. Abdullayev, S.B. Kazımova

ETİL SPİRTİ MOLEKULUNUN TRANS - KONFORMERİNİN SPEKTRİNDƏ MƏRKƏZƏQAÇMA HƏYƏCANLANMASI

Etil spirti molekulunun trans – konformerinin fırlanma homiltoniyanın kvartik, sekstik və oktik spektral sabitləri təyin olunmuşdur. Bu molekulun misalında, ilk dəfə olaraq, reduksiya olunmuş fırlanma homiltaniyanın $J=34$ qiymətlərində oktik spektral sabitlərinin təyin olunan kombinasiyası hesablanmışdır.

Ч.О. Каджар, С.А. Мусаев, А.А. Абдуллаев, С.Б. Кязимова

ЦЕНТРОБЕЖНОЕ ВОЗМУЩЕНИЕ В СПЕКТРЕ ТРАНС-КОНФОРМЕРА МОЛЕКУЛЫ ЭТИЛОВОГО СПИРТА

В этой работе уточнены вращательные, квартичные, секстичные и октичные центробежные постоянные гамильтониана А – редукции транс-конформера молекулы этилового спирта в трех осевых представлениях. Включение в обратную спектроскопическую задачу заново идентифицированные 33 вращательных перехода, попадающих в диапазон частот 24,0-498,0 ГГц с высокими *J (J=34)*, позволило в среднем в 3 раза уменьшить среднеквадратичное отклонение вышеуказанных постоянных и, благодаря этому, более точно вычислить их определяемые комбинации.

Received: 23.12.05

THE CONSTRUCTION PECULIARITIES OF LAYERED ORGANIC-INORGANIC SUPRASTRUCTURAL ANSAMBLE

S.Sh. GAKHRAMANOV
SPS "Selen" of National Academy of AR,
F. Agayev, 14, Baku, Azerbaijan

The modern positions on the directed designing of supramolecular systems have been considered on the bases:
- Layered misfit compounds,
- clathrates and silicates with frame structures,
- layered hydroxides,
- layered structures with variable size of structural planes,
- layered compounds with variable size of structural cavities with "guests" of different size in "master" lattice,
- matrix crystals.

It is shown that the sizes and forms of matrix molecules and "guest" (cluster) molecules play the important role in the organization of the regularities of suprastructure layered misfit compounds, clathrate compounds and silicates with frame structures, different intercalated layered compounds and hydroxides.

It is established, that nonvalency chalcogen-chalcogen interactions play the special role in the creation of the supramolecular chalcogenide clusters.

Introduction

The supramolecular physico-chemistry is the scientific direction in the center of attraction of which are the creation processes from the separate molecules of complex systems, connected in a single whole by the means of the intermolecular interactions. These interactions keep the fragments together – the electrostatic forces, hydrogen connection, Van der Waals forces in a whole are significantly weaker, than covalent connections in the molecule itself. For the increase of the durability of connections, the big enough joining "blocks" are used in them. The developed system of the connections because of the big surface of the contact is created. The ability to the molecular recognition is the main property of self-organizing supramolecular objects. The component recognition supposes the "complementary", - the mutual accordance of ensemble participants (substrate and receptor) as the geometric, so on the level of the creation of intermolecular connections [1]. The author of the given paper [1] pointed the different scientific disciplines as the objects of supramolecular chemistry, especially emphasized the set of the objects of inorganic and organic chemistry.

In the paper [1] it is emphasized, that intercalates, clathrates and structures of the type "master-guest" exist only in solid state. These structures aren't discrete supramolecules, and are referred to the solid supramolecular ensembles. The ensembles of the "guests" in "longitudinal" structures of the "master" and discrete supramolecules are emphasized. The "longitudinal structures are the one-, two- or three-dimensional continuous or the half-continuous crystal creations with ion or covalent connection character. Nowadays, the circle of these objects (and common definitions and conceptions to them) is drawn approximately. However, the some classification of objects of supramolecular inorganic chemistry is present. The intercalates with "guests" of different size in "master" degree, clathrates, silicates with frame structures, complex phosphates of molybdenum and vanadium are referred to them [2]. Here [2] the discussion of the objects of inorganic supramolecular chemistry is limited by the compounds by the type "guest-master". They give the possibility of the studying of the ensembles, in which the "guest" molecules create the strong connections with longitudinal structures. These structures influence on the geometrical and typological correspondence of the components (complementary), and also on the peculiarities of their self-organizing. The studying of the given objects and also multiphase and other complex layered objects can give the information about the new mechanisms of their creation.

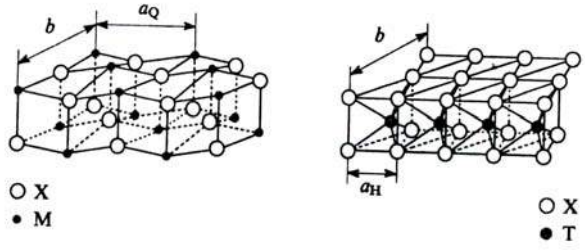

Fig.1. The substructures MX (Q-layer) and TX_2 (H-layer) with disproportionate lattice parameters (a_q and a_H) [6].

The principle of geometric and typological complementary can be broken at the creation of the inorganic supramolecular ensembles. In the paper [2] the (as the systems "guest-master") layered intercalates (for example, in layered dichalcogenide matrix, graphite, clays) are especially emphasized. In them the layers in "master" lattice are connected because of Van der Waalse interactions; the layers are shifted at the "guest" coming, and the change of interlayer distance is the sign of the intercalate creation [3]. The value of this change depends on the "guest" sizes and can be in 3-5 times greater, than the initial crystallographical parameter of "master" lattice. However, the limit intercalate stoichiometry is caused not only by the ration of "guest" sizes and holes in "master" lattice. This intercalate stoichiometry $AaMX_2$ (*A*-metal, MX_2 layered dichalcogenide matrix) is defined by the conditions of the filling of conduction band by the A donor electrons (i.e. by electron stabilization of whole $AaMX_2$ structure), that is shown in papers [4-5]. The geometrical facts go on the second plane – it is proved by small sizes of *M* atoms in $AaMX_2$ systems, the absence of the changes of

interlayer distances, small limit value *a* and dependence of the value *a* on valence *A* and *M* states (see fig.1 and 2).

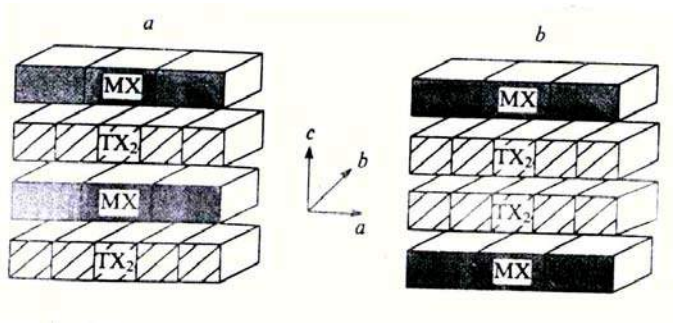

Fig.2. The scheme image of monolayer (*a*) and bilayer (*δ*) misfit structures [6].

So-called "matrix crystals" – supramolecular ensembles – synthetic opal with holes of the definite sizes, created the regular cubic sublattice are known. The quasi-lattice with enormously big parameters is formed at the filling of the holes (for example by the selenium – "guest"). The geometric disproportion of sublattices is compensated by the deformation of one from them ("guest").

Another example of the disproportion of "guest" and "master is the variety of intercalates in layered dichalcogenide matrix – misfit compounds. They can be referred to the objects of supramolecular chemistry. These compounds present themselves the suprastructures, consisting from the structural elements, disproportionate in one crystallographical direction. It is need also to consider the peculiarities of structure self-organization of misfit layered compounds – synthetic chalcogenides with general formula $(MX)_{1+x}$ $(TX_2)_m$ *(M-Sn, Pb, Bi, Sb, Ln; T-Ti, V, Nb, Ta, Cr; X-S, Se; x=0,08-0,28; m=1=1,2)* (fig.2).

The properties of misfit compounds should be defined significantly by the power competition, responsible for the saving of the hardness of disproportionate substructures (layered dichalcogenide matrix TX_2, from the one side and cubic structure of MK-c "guest" – from the another one, and strengths, connecting them in united suprastructure. At the same ratios of the given strengths the additive scheme of compound property estimation doesn't work. The disproportion leads to the defect creation, and also to the fragmentation of one of sublattices, influencing on compound properties [6].

The further consideration of the given problem is connected with nano-chemistry objects.

The nano-chemistry shows, that classic equations of chemistry kinetics aren't applicable at particle nano-sizes. The excess energy of surface atoms, the part of which is big in the relation to the inside atoms, significantly influences on the temperature of phase transfers in nano-particles. If their sizes are comparable for example with delocalization radius of charge carriers, the nonlinear electric phenomena appear. The appearance of new original methods of nano-particle creation is connected with this.

The region of nano-chemistry, which has the aim to create the closed or half-closed nano-and micro-reactors, is wide. For example, the polymers are created, in which the monodisperse empty spheres occupy 75% of volume. The diameter of these spheres can be regulated, beginning from the nano-sizes (10 nm), finishing by (1000 nm). The molecular constructions are created (by type "vaz"), able to "catch" of "guest" molecules and release them. The molecular traps - karseplexes are synthesized. All these structures are related to the class of molecular containers, which are able to catch the given molecules and release them at the change of conditions [7-9] (fig.3).

The nano-chemistry creates the own objects – nano-particles, nano-reactors, nano-containers from the one side, and from the other one – uses the advantages of nano-particles, their special and flexibly variable properties for the own needs. Thus, two key conceptions are already defined – nano-particle and nano-reactor. The nano-particle characterizes the size parameter. The nano-reactor defines the nano-particle function. For example, *Fe* cluster almost totally loses its special properties and approximates to the metallic iron at the atom number in cluster n=15. At n>15 it stays as the cluster in size meaning, but it loses qualities of "nano-reactor", in which the qualities become the size function.

The nano-holes in different porous materials can be calculated by nano-reactors till the state, when their structure and properties of reacting system depend on the size of holes. When these dependences disappear, the nano-holes become only nano-sized, in which caught particles behave as they would be in unlimited volume [7]. However, very often the separation of conceptions nano-particle and nano-reactor is impossible. Nevertheless, these conceptions are needed for the recognition of two sides of sized effect – as the pure scaled space and as the physico-chemical phenomena, when properties "guest-atoms" depend on the size (very important sides in nano-chemistry).

And now few words about nano-reactors. The "empty" tube silicon fibers – one-dimensional nano-reactors have been created. The quazi-two-dimensional nano-reactors – hard graphite-like planes, connected by flexible-chain bridges from carbonic chains have been synthesized. The distances between graphite-like planes in such reactors can be varied [10]. The opposite and continuous pressing – the widening of interplane space is achieved because of the stimulating of conformational transfers in полиметиленовых chains – from rolled in nod of conformation (planes are maximally approached) till longitudinal chain (planes are maximally shifted).

The descriptions of principally new organization of chemical substance on the level, when at the creation of different materials from the components the leading meaning has not their reacting ability, and correspondence of sizes and forms of molecules – "guests" – to the frame holes, constructed by other molecules, - "masters" (or to hole of another, more big molecule – master) are paid attention. Such principle of compound creation allows us to join the coordinationally-saturated molecules, not including into chemical interaction with each other, in submolecules, and submolecular crystalline phases, thermodynamically more stable, than impurity of initial components [11]. The clarity in above mentioned phenomena is put by interactions, with the creation of izostructural cluster compounds. The main conceptions of clathrate chemistry gave the beginning the real searches of submolecular creations. The investigations of clathrate compounds [12-14] helped to understand, why at total absence of valence chemical connections between molecules of initial components they are able to join in thermodynamically stable phase.

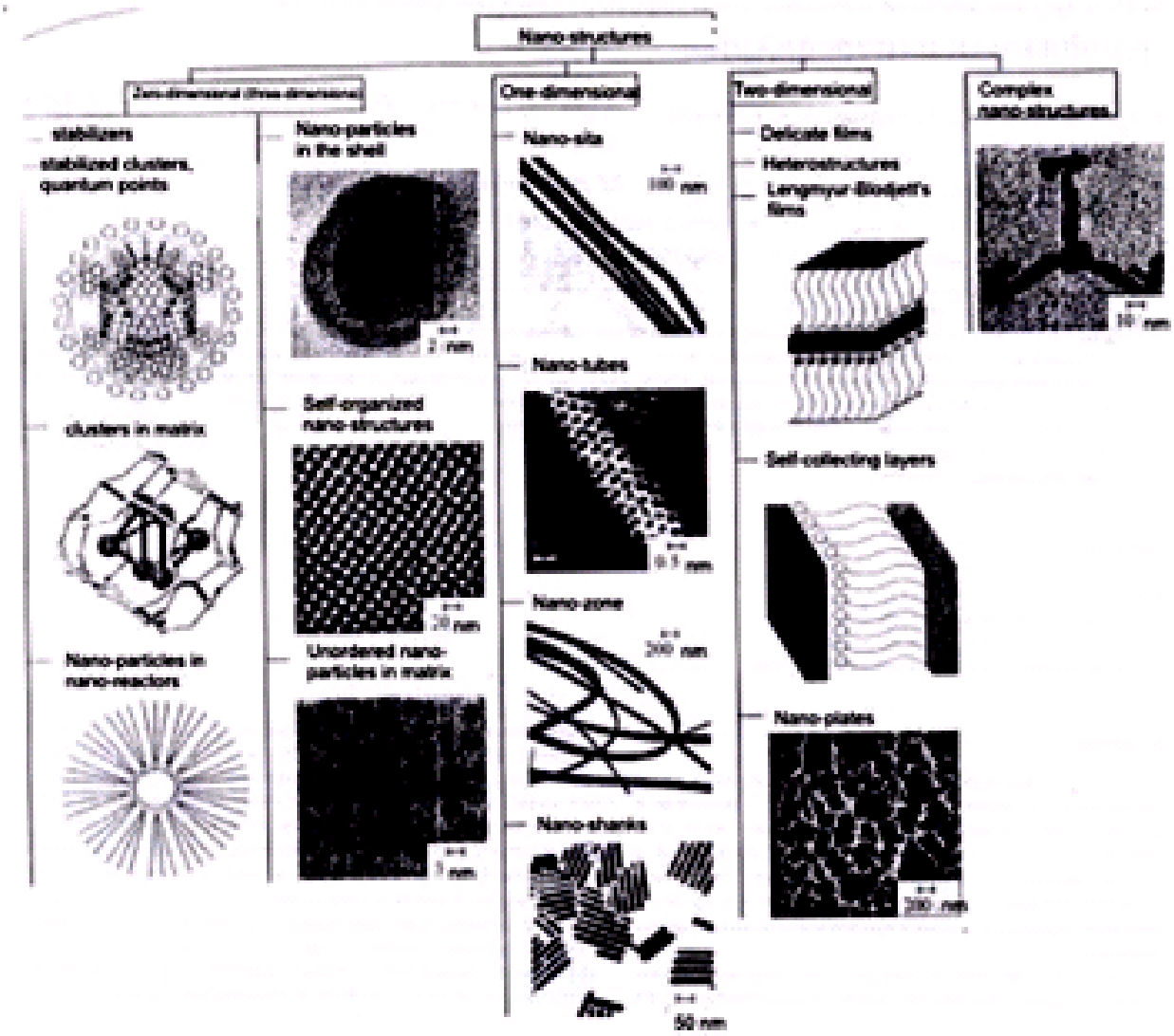

Fig.3. The nano-structure classification [19].

D.Len [1] emphasized the important role of invalency interactions in formation of similar compounds; the new conception "supramolecular chemistry", which he has defined as "chemistry outside the molecule", "chemistry of molecular ensembles and intermolecular connections" has been introduced by him.

The opening of clathrato-creating complexes of metals had been enriched the science of materials by many new objects. The revealing of supermolecular compounds allows to reveal one more thermodynamically profit mechanism of germ creation of new phase.

Thus, the necessity of the consideration of organization of chemical substance in the correspondence with sizes and forms of "guest" and "master" molecules of matrix has been became [15-19]. This is demonstrated on the fig.3.

The world of layered structures is rich; the methods of their creation and use are diverged. The community of layered systems is revealed in inorganic and organic world – in world of all nature systems. All this says about the unity of the mechanism of cleavage nature creation. Let's consider the one more example of the creation of layered structures.

Layered structures with variable size of structural holes

Such structures can be used in the capacity of two-dimensional nano-reactors. In these compounds the layers are connected between each other by Van der Waalse forces. Moreover, it is easy to change the size pf interlayer space. The layered structure increases the diffusion of diverge compounds in interlayer space and thus, eases the chemical modification of layered compounds.

In this relation the works, dedicated to the synthesis of nano-composites with the use of layered matrixes are interest. The compounds with negatively charged layers and cations in interlayer space – allumosilicates are widely used. However, such materials have the set of disadvantages, prohibited to the studying of formation mechanism of nano-structures in layered matrix.

Thus, the goal of the present paper is the review, analysis and revealing of common regularities in layered structures with elements "guests" in organic and inorganic suprastructures such as: clathrate compounds, eutectics,

misfit compounds and other layered systems with intercalates of different sizes in master lattice.

Layered double hydroxides

The layered double hydroxides (LDH) of the composition $M^{2+}_{1-x} M^{3+}_{x} (OH)_2 [X^{n-}_{x/n} \cdot mH_2O]$ (*X*-anion) are the more widely-spread two-dimensional nano-reactors. The compounds with M^{2+}=Mg^{2+}, Zn^{2+}, Fe^{2+}, Co^{2+}, Ni^{2+}, Cu^{2+}, Cd^{2+}, Sn^{2+} and M^{3+}=Al^{3+}, Fe^{3+}, Cr^{3+}, Mn^{3+}, Ga^{3+}, In^{3+}, Bi^{3+} are present. As a rule, the radiuses of cations M^{2+} and M^{3+}, participating in formation of layered structure, shouldn't differ more, than in 1,5 times. Practically any anion or anion complex can be in the capacity of the anion X^n. LDH structure presents itself the system of positively charged hydroxide layers $[M^{2+}_{1-xd} M^{3+}_{x} (OH)_2]^x$ and anions, situating in interlayer space [20]. Structure of layered double hydroxides is presented on the fig.4.

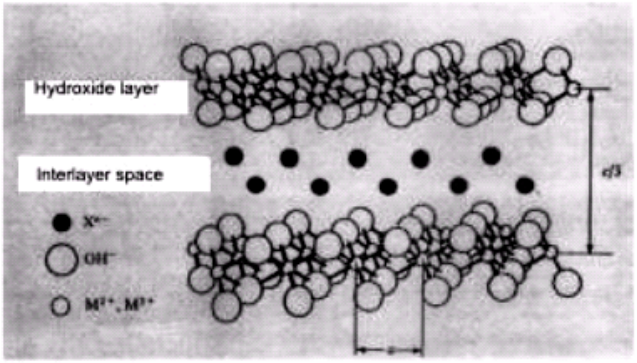

Fig.4. The scheme image of the structure of layered double hydroxides [7].

Besides anions in interlayer space the labile aqua molecules are present often. Given structure is stable because of the electrostatic interaction between positively charged hydroxide layers and interlayer anions, bringing the negative charge [20].

The anion situation in interlayer space can be diverged. As a rule, anions are situated in interlayer space thus, that in order to minimize its size.

LDH have the set of unique properties, important for the directed synthesis of nano-materials. The one of such properties is the stability of layered structure LDH in wide range of change of the sizes of cations and anions. Thus, samples LDH *Mg-Al* have been obtained, containing the different anions with sizes from 0,3 till 5 nm in interlayer space.

Thermal decomposition of LDH carries out with saving of layered structure that allows us to carry out the chemical reactions with the participation of anions of interlayer space at the high temperatures without the matrix decomposition [20]. Many functional properties of materials on the base of LDH connect with especial properties of intercalated anions in them.

The given properties open the wide possibilities for the chemical design of nano-composite materials on the base of layered double hydroxides.

The existence of hard hydroxide layers in LDH structure, limiting the interlayer space, creates the conditions for the synthesis of nano-systems, similar with conditions of their synthesis in nano-reactors. In [20] the composite obtaining, consisting from the nano-particles of *CdS* in interlayer space of LDH, is described. At thermolysis of *Cu*-consisting LDH at 400°C the creation of spherical particles of cuprum, by the size 2-5 nm (in interlayer space of matrix) and 5-8 nm (on surface) take place. At thermolysis of *Ni*-consisting LDH the spherical particles of *Ni* by diameter ~5 nm with very narrow particle distribution on sizes are formed. The increase of thermolysis temperature till 800°C leads to the increase of particle sizes till 15 nm with simultaneous distribution widening. And at thermolysis of *Co*-consisting LDH at 400-800°C the large (~100 nm) metal particles in form of discs, the size and morphology of which practically don't depend on thermolysis temperature, are created.

Thus, the use of nano-reactors opens the possibility for the design of functional nano-materials with given physicochemical parameters. Moreover, the solid-state matrix allows to avoid the aggregation of nanopartricles and defend them from external influences. The semiconductor layered materials by type: *GaSe*, Bi_2Te_3, SB_2Te_3, *InSe* and others can be such solid-state matrixes. Thus, the given examples prove the advisability of use of layered structures in the capacity of two-dimensional nano-reactors.

The consideration of design principles of supramolecular compounds with the use of organic cucurbituril

Such work was made by authors of papers [9,21-22] on organic macro-cycle cavidants – cucurbit[*n*]uril, $[C_6H_6N_4O_2]_n$ (*n*=5-10). The existence of hydrophobic intermolecular hole equally with polarized carbonyl groups of portals of cucurbiturils causes the high specificity of the creation of compounds by the type "guest-master", is shown by them. The possibility of cucurbiturils to be in the capacity of the synthetic containers, in which the biomolecular reactions between specially chosen "guests" carry out with high regio- and stereoselectivity, has been considered [9].

The introduction of gas molecules, metal ions, organic molecules into hole leads to the creation of stable compounds, having the unusual structure and interest properties. In review of paper [9] the synthesis and structure of supramolecular materials, obtained with the use of macro-cycle cavidants, having the trivial name as cucurbiturils, are considered.

The compounds of cucurbit[6]uril by type "guest-master"

The cucurbituril of $C_{36}H_{36}N_{24}O_{12}$ composition (cucurbit[6]uril (5)), constructed from six glycoluril fragments, connected by methylene groups has been studied more well.

The existence of enough hard intramolecular hole causes the possibility of cucurbit[6]uril (5) the introduction of small guest molecules.

The creation of the compounds has been proved by crystallographicly, and also by different physicochemical methods [9]. The cucurbit[6]uril (5) creates the stable compounds of the introduction with amines and diamines, alkyl and benzylammonium ions, dye molecules.

The supramolecular compounds of cucurbit[6]uril with cluster aquacomplexes of metals

The use of volume fragments, not having its geometry, able to create the developed system of intermolecular connections because of the big contact surface, is the important condition of directed constructing of nano-sized complexes or supramolecular compounds. The cluster aquacomplexes of molybdenum and tungsten are suitable enough large molecular constructing blocks for the creation of supramolecular compounds with cucurbit[6]uril (5) [9].

The given compounds have chain structure, in which the supramolecules of structure type "barrel" with two coverings are connected between each other because of the short (in the comparison with sum of Van der Waalse radiuses, which is equal to 3,9Å of nonvalency interactions Se…..Se (3,59-3,72Å). The hole cucurbit[6]uril in the compound $\{[W_3Se_4(H_2O)_6Cl_3I_2(P_yHCC_{36}H_{36}N_{24}O_{12})\}Cl_3 \cdot 18H_2O$ has the pyridine cation.

The interactions of chalcogen-chalcogen between neighbour clusters, which are character for three-nucleus of chalcogenide clusters of transfer metals [9].

Chalcogen-chalcogen interaction between neighbour cluster fragments M_3Y_4 of supramolecular compounds is similar to interactions between chalcogen atom layers in layered dichalcogenide transfer metals $MY_2(Y=S,Se)$ [23].

The comparison of the structures of chain supramolecular compounds $\{[Wo_3Se_4(H_2O)_8Cl]_2(C_{36}H_{36}N_{24}O_{12})\}Cl_6 \cdot 16H_2O$ and $\{[Wo_6HgSe_8(H_2O)_{14}Cl_4](C_{36}H_{36}N_{24}O_{12})\}Cl_4 \cdot 14H_2O$ [3] shows that they relate to each other as matrix and intercalate from the construction point of view: mercury atom is introduced between chalcogenide clusters M_3Y_4 practically don't change the main parameters of supramolecules. Thus, as the authors of paper [9] conclude, the chemistry of supramolecular compounds of chalcogenide clusters is connected with chemistry of layered compounds more close, than it would be expected. In both cases the nonvalency interactions chalcogen-chalcogen play the important role in the structure creation.

Conclusion

The considered review and analysis of cucurbiturils clathrates, layered dichalcogenides allow us to consider the organic and inorganic systems in the capacity of the molecular constructing fragments for the directed construction of nano-sized ordered layered supramolecular compounds. In hole of one frame the introduction of different "guests" and also clusters leads to the interaction between them and it becomes the motive force of creation of supramolecular compound. It is established, that in chemistry the nonvalency interaction chalcogenide-chalcogenide play important role in structure creation.

The peculiarities of synthesis of functional nano-composites on the base zero-, one- and two-dimensional solid-state nano-reactors, connected with formation of holes (zeolites, pores of mezoporous matrixes) or with interlayer holes of layered compounds. With the help of the intercalation method of dichalcogenides and metals, it is easy to create the layered crystals, using the longitudinal structural blocks TX_2 and introduced reagents in solution at T=300°K.

[1] *Dzh.M. Len.* Supramolekulyarnaya ximiya. Kontseptsii i perspektivi. Nauka, Novosibirsk, 1998.

[2] *Muller, H.Router., S. Dillinger.* Angew Chem., Int. Engl., 34, 2328 (1995).

[3] *R. Scholhorn.* In. Inclusion Compounds, Vol.1. (ed. J.L Atwoood) Academic Press. London, 1984. p.249.

[4] *V.S. Pervov, V.V. Volkov, A.T. Falkingof, E.V. Makhonina, N.V. Elizarova*. J.Neorqanicheskie materiali, 132, 675 (1996).

[5] *V.S. Pervov, C.V. Makhonina V.V. Volkov*, Mol. Cryst Lug.Cryst., 341, 935, (2000).

[6] *V.S. Pervov, Dzh.V. Dobrokhotova, E.V. Makhonina, V.V.Volkov, V.M. Novotortsev*. J.Neorganicheskie materiali, 2002, t.38, №3, s.347-350.

[7] *Yu.D. Tretyakov, A.V. Lukashin, A.A. Yeliseev*, Sintez funktsionalnix nanokompozitov na osnove tverdofaznikh nanoreaktorov, J.Uspekhi ximii, 73 (9) 2004, s.975-998.

[8] *V. Kawazoe*. Clusters and Nanomaterials: Theory and Experiment, Springer Verlag, Berlin, 2001.

[9] *O.A. Gerasenko, D.G. Samsonenko, V.P. Fedin.* Supramolekulyarnaya ximiya kukurbiturilov, J.Uspekhi ximii, 71 (9) 2002, s.840-863.

[10] *A.L. Bulachenko*, Nanoximiya – pryamoy put k visokim texnologiyam novogo veka., J.Uspekhi ximii, 75 (5), 2003, s.419-437.

[11] *M.P Anisimov*, Nukleatsiya: teoriya i eksperiment, J.Uspekhi ximii 72 (7) 2003, s.666-703.

[12] *K.A. Kovnir, A.V. Shevelkov*. Poluprovodnikovie klatrati, sintez i stroenie i svoystva. J.Uspekhi ximii 73(9) 2004, s.999-1017.

[13] *G.S. Nolas, G.A. Slack, S.B. Schjuman.* In Recent Trends in Thermoelectric Materials Research (Ed. T.M. Tritt) Academic Press, San Diego, 2001.

[14] *A.V Shevelkov*, Sozdanie materialov na osnove supramolekulyarnikh klatratov, J.Vesnik Moskovskogo universiteta, ser 2, tom 44, №3, 2003, s.163-171.

[15] *I.D. Mikheykin, M.Yu.Kuznetsov, E.V. Makhonina, V.S. Pervov*. Defekti v neorganicheskikh suprastrukturakh s nesorazmernimi elementami. Staticheskaya model Frenkelya-Kontorovoy dlya konechnikh sistem. Dokladi Akademii nauk, 2001, tom 376, №6, s.785-788.

[16] *J. Rouxel, A. Meerchaut, G.A. Wiegers.* Chaloogenide Misfit Layer Compounds H.J. Alloys Compd 1995, v.229., p 144-157.

[17] *J. Barin, O. Knacke, O. Kubashewsky.* Thermodynamic Properties of Inorganic Substances Berlin 1977.

[18] *V.S. Pervov, E.V.Makhonina,* Sloistie misfitnie soedineniya, J. Uspekhi khimii 69(6) 2000, s.528-538.

[19] *A.S. Golub, Ya.V. Zubavichus, Yu.A. Slokhotov, Yu.N. Novikov*, Monosloevie dispersii dikhalkogenidov perekhodnikh metallov v sinteze interkalirovannikh soedineniy, J.Uspekhi khimii 72(2)2003,s.138-158.

[20] *F.C. Hawthorn, S.V. Krivovichev, P.C. Burns,* Rev, Mineral., Geochem., 40, 1 (2000).

[21] *G.M. Mamardashvili, N.Dzh. Mamardashvili, O.I. Koyfman*. Supramolekulyarnie kompleksi porfirinov, J.Uspekhi khimii 74 (8) 2005, s.839-843.

[22] *G.A. Karakhanov, A.L. Maksimov, E.A. Runova*. Sozdanie supramolekulyarnikh metallokompleksnikh kataliticheskikh sistem dlya organicheskogo i neftekhimicheskogo sinteza, J.Uspekhi khimii 74 (1) 2005, s.104-107

[23] *M.N. Sokolov., AV. Virovets, D.N. Dybtsev.* Angew Chem., Int Ed., 39 1659 (2000).

S.Ş. Qəhrəmanov

LAYLI QEYRİ-ORQANİK VƏ ORQANİK SUPRASTRUKTUR ANSAMBLLARININ QURULUŞUNUN XÜSUSİYYƏTLƏRİ

Aşağıdakı supramolekulyar sistemlərinin istiqamətləndirilmiş quruluşunun müasir əsasnaməsi verilir:

-Laylı misfit birləşmələrin, klatratlarının karkas strukturlu silikatların, laylı hidrooksidlərin, laylı struktur ölçüsü dəyişən struktur müstəvilərinin, laylı birləşmələrin ölçüsü dəyişən struktur aralıqların müxtəlif ölçülü "qonaqlarının", "qəbul edən qəfəsdə", matrisli kristallar.

Göstərilir ki, suprastruktur laylı misfit birləşmələrinin, klatratların, karkas strukturlu silikatların, müxtəlif interkalyasiya olunmuş laylı birləşmələrinin, hidrooksidlərin qanunauyğun təşkil olunmasında əsas rolu matris molekulların və "qonaqlar" molekullarının (klasterlərin) ölçüləri və formatları təşkil edir.

Təyin olunur ki, halkogenid supromolekulyar klasterlərin əmələ gəlməsində əsas rolu halkogen-halkogen qeyri-valent əlaqələndirmələr oynayır.

С.Ш. Кахраманов

ОСОБЕННОСТИ КОНСТРУИРОВАНИЯ СЛОИСТЫХ ОРГАНО-НЕОРГАНИЧЕСКИХ СУПРАСТРУКТУРНЫХ АНСАМБЛЕЙ

Рассмотрены современные положения по направленному конструированию супрамолекулярных систем на основе:

- слоистых мисфитных соединений,
- клатратов и силикатов с каркасными структурами,
- слоистых гидрооксидов,
- слоистых структур с переменным размером структурных плоскостей,
- слоистых соединений с переменным размером структурных полостей с "гостями" различного размера в решетке "хозяина",
- матричных кристаллов.

Показано, что в организации закономерностей супраструктурных слоистых мисфитных соединений, клатратов и силикатов с каркасными структурами, различных интеркалированных слоистых соединений, гидрооксидов главную роль играют размеры и формы молекул матриц и молекул (кластеров) "гостей".

Установлено, что в образовании супрамолекулярных халькогенидных кластеров особую роль играют невалентные взаимодействия халькоген-халькоген.

Received: 22.12.05

VAHİD TEXNOLOJİ ŞƏRAİTDƏ ALINMIŞ *p*, *n*-TİP KEÇİRİCİLİYƏ MALİK $Pb_{1-x}Mn_xTe(Se)$ EPİTAKSİAL TƏBƏQƏLƏRİ

H.R. NURİYEV, R.M. SADIQOV, S.S. FƏRZƏLİYEV, M.B. HACIYEV

AMEA Fizika İnstitutu,

Azərbaycan, Bakı, Az-1143, H. Cavid pr., 33

Təqdim olunan işdə molekulyar dəstədən kondensasiya metodu ilə BaF_2 (111) altlıqları üzərində $Pb_{1-x}Mn_xTe(Se)$ (x=0,01) epitaksial təbəqələrinin böyümə xüsusiyyətləri tədqiq olunmuşdur. Əlavə Te(Se) mənbəyinin temperaturunu tənzimləməklə vahid texnoloji şəraitdə tələb olunan elektrofiziki parametrli ($\mu_{n,p}$(77K)=(2,5÷3)·10^4 sm^2/V·s; (n,p_{77K})=5·10^{16}÷1·10^{17} sm^{-3}), yüksək kristal mükəmməlliyə ($W_{½}$=90÷100") və *p*, *n*-tip keçiriciliyə malik $Pb_{1-x}Mn_xTe(Se)$ (x=0,01) epitaksial təbəqələrinin alınma texnologiyası işlənib hazırlanmışdır. Müəyyən edilmişdir ki, keçiriciliyin inversiyası əlavə Te(Se) mənbəyinin temperaturunun 420 K-dən yuxarı qiymətlərində baş verir.

Spektrin infraqırmızı diapazonunun intensiv öyrənilməsi, darzolaqlı yarımkeçirici materiallar əsasında optoelektron cihazların hazırlanmasını vacib bir məsələ kimi qarşıya qoyur. Bu materiallar içərisində $A^{IV}B^{VI}$ tipli birləşmələr və onların əsasındakı bərk məhlullar xüsusi yer tutur [1].

$A^{IV}B^{VI}$ tipli yarımkeçiricilər qrupuna daxil olan $Pb_{1-x}Mn_xTe(Se)$ bərk məhlulları spektrin 3÷5 mkm dalğa uzunluğunda işləyən cihazların hazırlanmasında istifadə olunmaq üçün böyük perspektivə malikdir. Belə ki, bu bərk məhlullarda Mn ionlarının olması onlarda yarımmaqnit yarımkeçiricilərə məxsus yeni xassələrin mövcudluğunu üzə çıxarır və onların əsasında texnikada geniş tətbiq olunan, maqnitlə idarə olunan diodların hazırlanmasına böyük imkanlar yaradır [2].

1980-ci ildən başlayaraq yarımmaqnit xassəli belə bərk məhlulların massiv monokristalları alınmış və onların fiziki xassələri geniş tədqiq olunmuşdur [3-5]. Göstərilən bərk məhlulların epitaksial təbəqələrinin alınması və onların əsasında yuxarıda adı çəkilən diodların hazırlanması böyük əhəmiyyət kəsb edir. Bu isə $Pb_{1-x}Mn_xTe(Se)$ bərk məhlullarının yüksək kristal mükəmməlliyə, *p*, *n*-tip keçiriciliyə və tələb olunan elektrofiziki parametrlərə malik epitaksial təbəqələrinin alınması məsələsini qarşıya qoyur.

Təqdim olunan işdə 10^{-4} Pa vakuumda molekulyar dəstədən kondensasiya metodu ilə BaF_2 (111) altlıqları üzərində $Pb_{1-x}Mn_xTe(Se)$ (x=0,01) epitaksial təbəqələrinin böyümə xüsusiyyətləri tədqiq olunmuşdur. Altlıq qismində BaF_2 mionokristallarının təzə doğranmış (111) layları, mənbə kimi isə sintez olunmuş $Pb_{1-x}Mn_xTe(Se)$ (x=0,01) bərk məhlulları istifadə olunmuşdur. Alınmış təbəqələrin kristal mukəmməlliyi elektronoqrafiya, elektronmikroskopiya, rentgendifraktometriya metodları ilə tədqiq edilmişdir. Göstərilmişdir ki, daha yüksək kristal mükəmməlliyə və elektrofiziki parametrlərə malik epitaksial təbəqələri kompensəedici əlavə Te(Se) mənbəyindən istifadə etməklə almaq olar. Aparılmış tədqiqatlar nəticəsində məlum olmuşdur ki, altlığın temperaturunun T_{alt}=663÷673 K, kondensasyia sürətinin υ_K=8÷10Å/s qiymətlərində qalınlığı 0,5÷1 mkm və kristal mükəmməlliyi $W_{½}$=90÷100" olan *n*-tip keçiriciliyə malik epitaksial təbəqələr almaq mümkündür (Şək. 1.*a, b*).

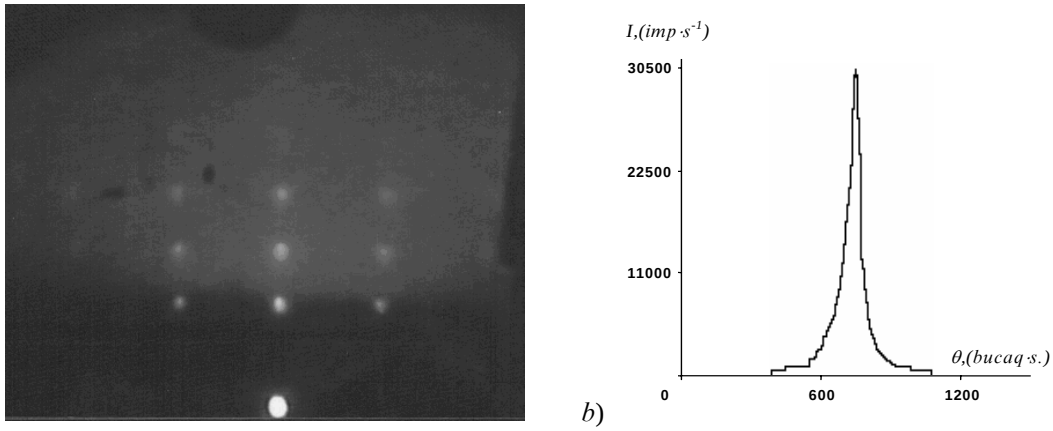

Şək.1. $Pb_{1-x}Mn_xSe$ (x=0,01) epitaksial təbəqəsinin elektronoqramı (*a*), rentgendifraksiya əyrisi (*b*).

Elektronmikroskopiya tədqiqatları göstərir ki, alınmış epitaksial təbəqələrin səthində qara ləkələr müşahidə olunur (Şək.2.a). Ədəbiyyatdan məlum olduğu kimi bu ləkələr, tərkibdə olan artıq qurğuşun atomlarının oksidləşməsi nəticəsində əmələ gəlir [6-7]. Alınmış epitaksial təbəqələrdə yükdaşıyıcıların yürüklüyünün qiyməti aşağı olur. Göstərilən qara ləkələri aradan götürmək və uyğun olaraq epitaksial təbəqələrdə yükdaşıyıcıların yürüklüyünü artırmaq üçün böyümə prosesində kompensəedici əlavə Te(Se) mənbəyindən istifadə edilmişdir. Bununla da qara ləkələri yox etmək, uyğun olaraq alınmış təbəqələrin kristal mükəmməlliyini və yükdaşıyıcıların yürüklüyünü artırmaq mümkün olmuşdur.

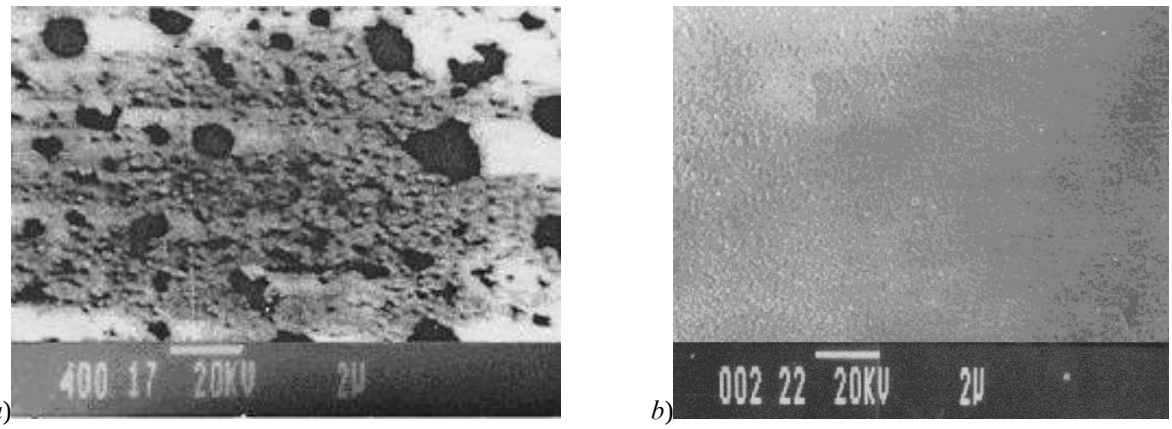

a) *b*)

Şək.2. $Pb_{1-x}Mn_xTe$ (x=0,01) epitaksial təbəqəsinin səthinin eletronmikroskopiya şəkilləri: *a*–Te mənbəyindən istifadə etmədikdə; *b*–Te mənbəiyndən istifadə etdikdə.

Epitaksial təbəqələrin böyümə müddətində əlavə Te(Se) mənbəyinin temperaturu 370÷460 K intervalında dəyişir. Kompensəedici Te(Se) mənbəyinin temperaturunun 430 K-dək artması ilə bu ləkələr tamamilə aradan götürülür və alınmış epitaksial təbəqələr parlaq, hamar səthə malik olur (Şək. 2.*b*). Əlavə Te(Se) mənbəyinin temperaturunun 420 K-dən sonrakı artımı nəticəsində təbəqələrdə keçiricilik tipinin inversiyası baş verir, *n*-tip keçiricilik *p*-tiplə əvəz olunur (Şək.3.). Bu fakt böyümə prosesində tez uçan komponentlərin boş qalan yerlərinin $A^{IV}B^{VI}$ birləşmələri üçün akseptor rolunu oynayan Te(Se) atomları ilə doldurulması ilə izah olunur. Alınmış təbəqələrdə yükdaşıyıcıların yürüklüyü $\mu_{n,p}(77K)=(2,5\div3)\cdot10^4$ sm²/V·s, konsentrasiyası isə $(n,p_{77K})=5\cdot10^{16}\div1\cdot10^{17}$ sm^{-3} qiymətini alır. Beləliklə, vakuumu pozmadan vahid texnoloji şəraitdə, *n*, *p*-tip keçiriciliyə və yüksək kristal mükəmməlliyə malik $Pb_{1-x}Mn_xTe(Se)$ (*x*=0,01) epitaksial təbəqələri alınmışdır. Yüksək kristal mükəmməlliyə, *n*, *p*-tip keçiriciliyə malik $Pb_{1-x}Mn_xTe(Se)$ (x=0,01) epitaksial təbəqələrinin vahid texnoloji şəraitdə alınması onların əsasında yaradılmış *p*–*n* keçidlərin, aktiv elementlərin həssaslığını aşağı sala biləcək proseslərin təsirinin qarşısını alır və yüksək fotoelektrik parametrlərə malik, spektrin infraqırmızı oblastında işləyən fotoqəbuledicilərdə istifadə olunmasına geniş imkanlar yaradır.

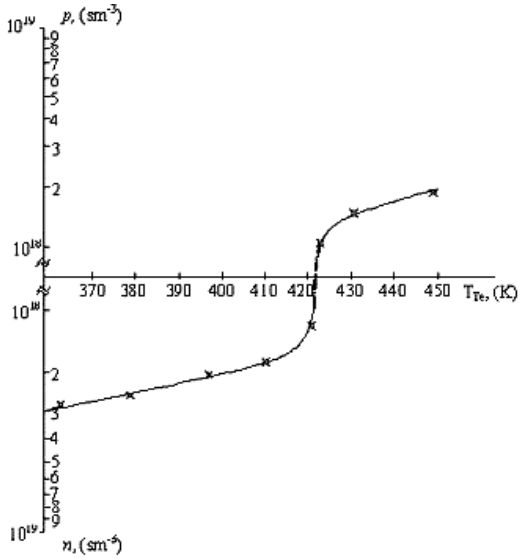

Şək.3. $Pb_{1-x}Mn_xTe(Se)$ (x=0,01) epitaksial təbəqələrində yükdaşıyıcıların konsentrasiyasının kompensəedici əlavə Te(Se) mənbəyinin temperaturundan asılılığı.

[1] *A.V.Matveenko, Yu.V.Medvedev, N.N.Berçenko.* Zarubejnanaya elektronnaya texnika, 11,1982, 54.(Rus dilində).

[2] *E.İ.Roqaçeva, A.S.Soloqubenko i dr.*. Neorqaniçeskiye materialı, 34, 1998, 669. (Rus dilində).

[3] *D.Q. Andrianov, N.M. Pavlov, A.S. Savelğev, V.İ.Fistul, Q.İ.Üiskarişvili*, FTP, 14, 1980,1202. (Rus dilində).

[4] *V.Q.Quk, E.V.Osipova, T.İ.Papuşina.* Neorqaniçeskiye materialı, 28, 1992, 340. (Rus dilində).

[5] B.*A.Akimov, A.V.Nikoriç, L.İ.Ryabova* i dr., FTP, 23, 1989, 1019. (Rus dilində).

[6] *İ.R.Nuriyev, A.M.Nazarov, S.S.Farzaliyev, N.V.Faradcev, R.M.Sadıqov,* "Xəbərlər", Baku, 5, 2002, 123. (Rus dilində).

[7] *İ.R.Nuriyev, S.S.Farzaliyev, R.M.Sadıqov*, "Poverxnost", Rentqenovskiye, sinxrotronnıye i neytronnıye issledovaniya, Moskva, 2, 2004. 110. (Rus dilində).

I.R. Nurıyev, R.M. Sadıgov, S.S. Farzalıyev, M.B. Hadjıyev

$Pb_{1-x}Mn_xTe(Se)$ EPITAXIAL FILMS WITH p, n-TYPE CONDUCTIVITY RECEIVED IN A UNIFORM WORK CYCLELE

In this work peculiarities of the growth of $Pb_{1-x}Mn_xTe(Se)$ epitaxial films, grown on BaF_2 (111) substrate by the molecular beam condensation method are investigated. By regulation of the temperature of additional source of Te(Se) in a single technological cycle the technology for obtaining structural-perfect films of $Pb_{1-x}Mn_xTe$ (Se) (*x*=0,01) with various *n* and *p*-type conductivity and fixed parameters

($\mu_{n,p}$(77K)=(2,5÷3)·10^4 cm^2/V·s; (n,p_{77K})=5·10^{16}÷1·10^{17} cm^{-3}) has been developed. Is established, at the temperatures of additional source Te(Se) higher than 420 K an inversion of conductivity takes place.

И.Р. Нуриев, Р.М. Садыгов, С.С. Фарзалиев, М.Б. Гаджиев

ЭПИТАКСИАЛЬНЫЕ ПЛЕНКИ $Pb_{1-x}Mn_xTe(Se)$ p, n-ТИПА ПРОВОДИМОСТИ, ПОЛУЧЕННЫЕ В ЕДИНОМ ТЕХНОЛОГИЧЕСКОМ ЦИКЛЕ

В настоящей работе исследуются особенности роста эпитаксиальных пленок $Pb_{1-x}Mn_xTe(Se)$ (x=0,01), выращенных на подложках BaF_2 (111) методом конденсации молекулярных пучков. Регулированием температуры дополнительного источника паров Te(Se) в едином технологическом цикле разработана технология получения пленок $Pb_{1-x}Mn_xTe(Se)$ (x=0,01) *p* и *n*-типов проводимости с заданными электрофизическими параметрами ($\mu_{n,p}$(77К)=(2,5÷3)·10^4 $см^2$/В·с; (n,p_{77K})=5·10^{16}÷1·10^{17} $см^{-3}$) и высоким кристаллическим совершенством ($W_{½}$=90÷100"). Установлено, что при температуре дополнительного источника паров Te(Se) выше 420К происходит инверсия проводимости.

Received:17.01.06

THE HALFTONING OF ELECTROSTATIC LATENT IMAGE OF Se ELECTROPHOTOGRAPHIC LAYERS BY THE SCANNING OF THE FOCUSED LASER BEAM

N.I. IBRAGIMOV, V.G. AGAYEV
Institute of Physics of NAS of Azerbaijan
Baku, Az-1143, H. Javid av., 33

It is established, that scanning (step 200mcm) of selenium EPh layers by the focused (∅ 100mcm) laser beam with λ=0,354 and 0,514 mcm and radiation density W=10÷10^3 Vt/cm^2 provides the halftoning of the latent electrostatic image because of: Se evaporation till the substrate (W 10^3 Vt/cm^2); melting of the amorphous layer and shunting sublayer of trigonal Se (W=25÷10^2 Vt/cm^2); change of photoelectric properties of amorphous Se under the beam influence (W 10 Vt/cm^2).

The electric field of the latent image is created by the charges, situated on the external surface of the electrographical (EPh) layer and charges of the opposite sign, induced in the conducting layer substrate. The field, created by these charges, corresponds to the condenser field, the distances between the facings of which is equal to the width of the photosemiconductor, coated on the layer. The configuration of electric field under the latent electrostatic image plays the important role at its appearance. As rule, the big electric contrast on image bou7ndaries is caused by the dispersion field (fig.1). The field lines of latent image should be behind the boundaries of photosemiconductor layer, in other case the toner (developer) particles, charged negatively, won't gravitate to the layer. The field lines lock mainly through EPh layer inside the total locked image regions. That's why the toner particles are evaporated on the edges of total regions. This is the meaning of the "edge effect", that's why the dispersion field plays so important role near the edges of latent image.

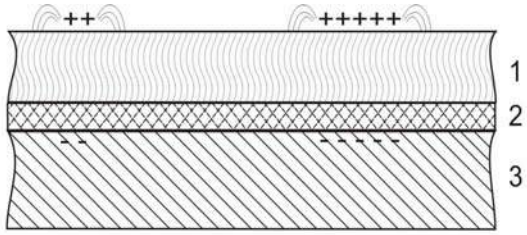

Fig.1. The configuration of electrostatic field of latent image under the exhibited EPh layer on the narrow and wide regions of original nigrescence.
1 – layer of amorphous Se;
2 – shunting sublayer of trigonal Se;
3 – conducting substrate.

By the methods of conformal transformations it was showed, that the biggest resistance of dispersion field took place near the edge of condenser facing $E_{max} = E/\sqrt{2(1+\cos\varphi)}$, where φ is the conversion coefficient [1]. Even near the obtuse facing edge (φ 174°) that corresponds to the edge of latent image, the field resistance is higher on the order, than in the distant regions from the edge. The last plays the important role in the creation of the "edge effect". Thus the "edge effect" is caused by the nonhomogeneous of electric field of the latent image and dispersion field is significantly bigger near the element edges, than in central region.

The existence of the "edge effect" makes the obtaining of the image from the original, having the big parts of total nigrescence and moreover the gray-level, impossible. In this case only narrow regions of the image (texts and schemes) are well revealed.

There are three methods of the elimination of "edge effect": the method of revealing electrode, the method of the halftoning of electrostatic image and method, based on the use of the metallized carrier [2-4]. The first and third methods lead to the complication of the apparatus, that's why the halftoning of the electrostatic image is considered the perfect one. It includes the image transformation with the continuous optical density of the nigrescence in the system of the points or the lines, the one of which is the independent image region in the correspondence of the electric field resistance.

The halftoning can be carried out by mechanical, optical and electrical method. For the mechanical halftoning the strokes (grooves) by the depth and width 100 mcm, are coated on the polished surface of the substrate by the steel needle. At the coating on such substrate of the photosemiconductor, all irregularities are revealed on the EPh layer surface with all consequences. However, such raster is ineffective, i.e. the its meaning is the different width of EPh layer, the enough width of which is difficult to carry out.

The optical halftoning of latent image is the precip of the electrified (in corona discharge) EPh layer through optically total raster. The original image is exposed on the layer after raster precip. As the optical raster can be prepared photographically with big permissive ability, the raster grid won't be almost seen on the revealed image. However, the method of optical halftoning is low-yield, i.e. the raster is the temporary on the EPh layer surface.

The electric halftoning leads to the electrization of EPh layer (by corona discharge) through grid-screen, situated near the layer surface. Moreover, the irregular charge distribution appears the biggest densities of which take place in grid intervals, i.e. the temporary raster forms.

There are methods of physical halftoning [5,6], based on the creation of constant raster by the change of physical properties of definite regions of Eph layer. Thus, the separate rotational regions with low resistance are formed by ion doping way in high-ohmic photosemiconductor. The complexity of the method is the difficultness of the creation of narrow ion beams.

In the present paper the method of halftoning of latent image in EPh layer with the help of the focused (∅ 100 mcm) laser beam with photon energy ΔE_g (the width of forbidden band of photosemiconductor) is considered. EPh layer was established on the holder with microsupply, which provided its rotational-progressive (spiral) transference with step 200 mcm. The focused laser beam is directed on the layer surface (λ=0,354 and 0,514 mcm) and thus the scanning was carried out. The time of beam activity was given by the rotation speed of EPh layer and varied in enough wide limits, that allows to change the radiation density W from 10 till 103 Vt/cm^2 (without taking under the consideration of the reflection).

As it is known [7], at the Se coating on the oxidized aluminum substrate, the so-called shunting sublayer from trigonal Se (1mcm), which provides the photosensitivity of EPh layer in the red spectrum region forms under this substrate. In the coating process the layer of amorphous Se, by the width in several decades of microns is already formed under it. Thus, selenium EPh layer presents by itself the sandwich: the conducting substrate (with oxide layer), shunting sublayer from trigonal Se and thin layer of amorphous Se (fig.1.). For the raster creation, such multilayered structure is treated by the shoot by the laser beam.

The scanning results are the following ones. At W 10^3 Vt/cm^2 the output (evaporation) of Se till the substrate with the creation of delicate lines with crater-similar edges by the width 130 mcm was observed (fig.2.a). This circumstance leads to the formation of the structure of EPh layer, at which the regions with and without photosemiconductor layer by the width 200 and 130 mcm are regularly rotated correspondingly, i.e. the constant raster is created.

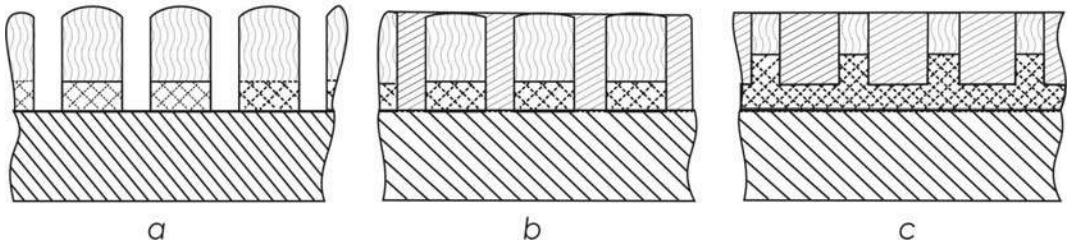

Fig.2. The scanning of selenium EPh layer by focused laser beam (λ=0,354 and 0,514 mcm) with the different radiation density W:
a – $W \gtrsim 10^3$ Vt/cm^2, Se evaporation till the substrate;
b – $W \approx 25 \div 10^2$ Vt/cm^2, the melting of shunting sublayer of trigonal Se till the substrate;
c – $W \lesssim 10$ Vt/cm^2, the increase of the width of shunting layer of trigonal Se in the result of the crystallization of the amorphous main layer.

At W $25 \div 10^2$ Vt/cm^2 the melting of Se layer under the beam till the substrate takes place, i.e. the sublayer of shunting trigonal Se is melting. Because of the speed cooling the shunting sublayer on these regions can't be in time in order to form, that decreases the photosensitivity. And the melting process of the upper amorphous layer itself, naturally changes the electric properties (it doesn't mean in what direction) and creates the character roughness (the shine is cone away). The regular rotation of the melted and initial regions by the beam creates the constant raster (fig.2b).

At W 10 Vt/cm^2 the crystallization of amorphous layer is observed. The crystallization takes place not immediately, and it has the cryptic period. It's important, that after influence by the laser beam, the photoelectric characteristics of these regions are significantly changed: the conductivity of amorphous Se increases, the time of dark slump of potential strongly decreases (EPh layer hasn't the charge). The regular rotation of such regions creates the constant raster. (fig.2.c).

The attempt of raster creation by beam scanning of the infrared laser (λ =1,06 and 10,6 mcm) of significant power wasn't successful (W 10^4 Vt/cm^2) – Se is limpid in this spectrum region. The irregular evaporation of Se because of the local substrate heating was observed.

[1] *V.A. Govorkov*. Elektricheskie i magnitnie polya. M., «Energiya», 1968, s.232.
[2] *R. Shaffert*. Elektrofotografiya. M., «Mir», 1968, s.72.
[3] *A.E. Medvedev*. Elektrofotograficheskiy sposob polucheniya rastrirovannogo izobrajeniya. AS SSSR № 390497, 1973.
[4] *M. Shloyzenger, X. Tsshayle*. Ustroystvo dlya opticheskogo naneseniya rastra na elektrofotograficheskiy tsilindr. AS SSSR № 458804, 1975.
[5] Patent Velikobritanii № 1503260, 1978.
[6] Patent Yaponii № 55-35701, 1980.
[7] *N.I. Ibragimov, M.I. Shneidman, V.G. Agayev, Z.M. Abutalibova*. Electrophotographic characteristics of Layers of amorphous Selenium on substrates with different thicknesses of oxide barrier film. Thin Sol. Films, 1991, v.196, p.L1.

N.İ. İbrahimov, V.H. Ağayev

SELEN ELEKTROFOTOQRAFİK LAYLARINDA GİZLİ ELEKTROSTATİK TƏSVİRİN RASTRLANMASI

Müəyyən olunmuşdur ki, selen EF laylarının λ=0,354 və 0,514 mkm, şüalanma sıxlığı W=10÷10^3 W/sm^2 olan fokuslanmış (∅ 100 mkm) lazer şüası ilə skanirə edilməsi (addım 200 mkm): selenin altlığacan buxarlanması (W 10^3 W/sm^2); amorf təbəqənin və şuntlayıcı triqonal selen alttəbəqəsinin əriməsi (W 25 ÷ 10^2 W/sm^2); şüanın (W 10 W/sm^2) təsiri altında amorf selenin (kristallaşma) fotoelektrik xassələrinin dəyişməsi hesabına gizli elektrostatik təsvirin rastrlanmasını təmin edir.

Н.И. Ибрагимов, В.Г. Агаев

РАСТРИРОВАНИЕ СКРЫТОГО ЭЛЕКТРОСТАТИЧЕСКОГО ИЗОБРАЖЕНИЯ СЕЛЕНОВЫХ ЭЛЕКТРОФОТОГРАФИЧЕСКИХ СЛОЁВ СКАНИРОВАНИЕМ СФОКУСИРОВАННЫМ ЛУЧОМ ЛАЗЕРА

Установлено, что сканирование (шаг 200 мкм) селеновых ЭФ слоёв сфокусированным (∅ 100 мкм) лазерным лучом с λ = 0,354 и 0,514 мкм и плотностью излучения W = 10 ÷ 10^3 Вт/см^2 обеспечивает растрирование скрытого электростатического изображения за счёт выпаривания селена до подложки (W 10^3 Вт/см^2), оплавления аморфного слоя и шунтирующего подслоя тригонального селена (W 25 ÷ 10^2 Вт/см^2), а также за счет изменения фотоэлектрических свойств аморфного селена под воздействием луча (W 10 Вт/см^2).

Received: 22.12.05

THE INFLUENCE OF OLIGONAPHTHOQUINONE ON SOME SUPERCONDUCTING PROPERTIES OF ERBIUM CERAMICS $ErBa_2Cu_3O_{7-8}$

Yu.A.VIDADI, F.V. ALIYEVA, M.A. NIZAMETDINOVA
Institute of Physics, Azerbaijan National Academy of Sciences
Azerbaijan, Baku, Az-1143, H. Javid av., 33

For samples of ceramics $ErBa_2Cu_3O_{7-\delta}$ processed in the melt of oligonaphthoquinone the increase of temperature of superconductive transition at 1.5 K and the increase of critical current on 30% at constant speed of attenuation in superconductive ring is registered

The information about influence of organic compound on the properties of high-temperature superconductors in literature are very few, the studying of this question has the scientific and practical meaning. The big interest presents the studying of the influence of oligonaphthoquinone on the properties of high-temperature superconducting ceramics $ErBa_2Cu_3O_{7-8}$. As it is known, the powders of high-temperature super semiconductors are mainly the powders with bad pressing. These powders are obtained by the methods of ceramic technology and they are the polydisperse ones with particle sizes 10-50 mcm. The universal means of the powder pressing improvement is their plasticization by organic additions. Besides it, the interaction of organic addition with structural superconductor elements can give the additional information about electron processes in the system. The obtaining of superconducting ceramics was carried out with the use of Er_2O_3 , CuO, BaO. The synthesis procedure was carried out on the following technological schemes, given on the fig.1.

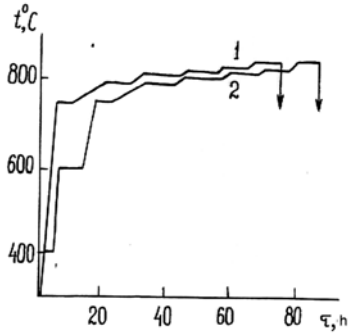

Fig.1. The temperature-time graphic of the samples.

1. The mixture of the powders of initial compound components, well deteriorated and mixed in needed proportion, is annealed on the air at the temperature 800°C during 12 hours. After cooling till room temperature the future superconductor is pressed and formed the needed form. Further it is annealed during 6 hours in oxygen atmosphere and slowly cooled.

2. The scheme of glass-ceramic obtaining, including the low-temperature annealing at 400-500 (with aim of increase of germ number in glass) and at 600-700°C (with aim of finishing of glass crystallization till the synthesis beginning of superconducting phase). The synthesis atmosphere is oxygen. The obtained results show, that the carrying out of the thermoworkings in oxygen atmosphere in temperature interval 800-850°C leads to the saving of the significant quantity of residual glass in the sample and to the slow development of synthesis process of superconducting phase.

The microstructure investigation showed, that in the dependence on the initial state the ceramic has the fine-dyspersated structure and often has large contributions of amorphic phase. In the result the samples with density $4.5 g/cm^3$ has been obtained. By the roentgen-graphical investigation and measurement of magnetic susceptibility on the alternating current it was established, that samples of $ErBa_2Cu_3O_{7-8}$ composition have 85% of superconducting phase, width and beginning of superconducting transition 2K and 92K, correspondingly.

From the tablets of superconducting ceramics by diameter 14mm and width 2 mm, the core by diameter 4 mm was cut. The residuary ring core after cutting was used for the measurement of the critical current on the known method. The temperature of superconducting transfer of initial and treated samples was measured with the help of the registration of real part of magnetic susceptibility χ in alternating magnetic field with the frequency 40 Hz.

The oligonaphthoquinone was heated till the melt obtaining. After it, the samples were put into melt and were held near the hour with the following drying on the air at the room temperature. Thus, the pore infill of the sample by the thin layer of the oligonaphthoquinone took place. In this case many granules and amount of intergranule intervals are covered by thin layer of oligomer. The sample treatment in the melt leads to the linear increase of critic parameters of superconducting ceramics. The increase of the temperature T_c on 1,5K of superconducting transition and increase critic current on 30% at the constant speed of current damping in the ring has been fixed.

The flushing of the oligomer from the sample in the melt, by the way of its holding in pure chloroform leads to the almost total reconstruction of previous values of critic parameters and T_c, which is temperature of superconducting transition decreases on the value ΔT_c=1.5K, that is seen from the fig.2.

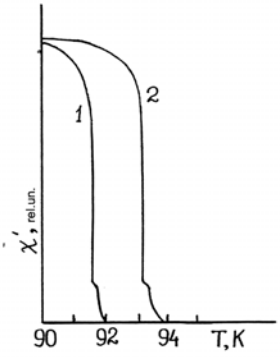

Fig.2. The temperature dependence of real part of magnetic susceptibility.

If till the treatment the full current, captured by superconductor ring was 2,8Å, then after oligonaphthoquinone adsorption it increases till 3.35Å. The dependencies of damping speed of superconducting current in the ring till and before its treatment by oligonaphthoquinone are given on the fig.3.

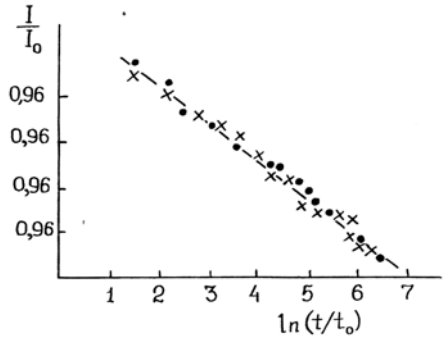

Fig.3. The damping of superconducting current in the ring:
• - till treatment by the oligonaphthoquinone
× – after the treatment by oligonaphthoquinone.

It is seen, that firstly, experiment points in logariphmic scale during 600 seconds, with satisfactory delicacy in logariphmic coordinated lay on the direct line. This allows to estimate the activation energy of pinning whirlwinds, which till our case was 0.22eV. Secondly, the experiment points, obtained till and before ring treatment in oligonaphthoquinone melt, are well laid on the one line, that evidences about the independence of relaxation velocity of superconducting current on the treatment in the ring.

The total understanding of this phenomena is still absent. In the case of the high-temperature superconducting ceramics, presenting by itself the system of superconducting grains, connected by the system of Josefson contacts, influence mechanism can be more significantly complex.

The increase of critic current in ceramics connects with the improvement of the properties of intergranule contacts, i.e. the oligonaphthoquinone probably, either creates the additional current conducting bridges, or improves the currentconducting properties already existed contacts. At the same time the increase of the temperature of the superconducting transfer, probably is connected with influence of oligonaphthoquinone adsorption on the ceramic grains. That's why it can be proposed, that reason of revealed phenomenon in given paper connected with oligonaphthoquinone adsorption from the melt on the surface of superconducting sample has the more complex character.

[1] *B.M. Hoffman et al.* J.Amer.Chem.Soc., 1967, v.89, N1, p. 27-30.
[2] *M.A. Bezborodov*. Glass-ceramics materials, Minsk, Nauka i Texnika, 1982, c.255.
[3] *A. Takeoka, M. Hasunuma et.al.* Jap.J. Appl. Phys., 1988, v.27, N 12, p.2260-2264.
[4] *N.C. Belousov, L.L. Makarshin, B.H. Parmon.* SFXG, 1991

Yu. A. Vidadi, F. V. Əliyeva, M.Ə. Nizamətdinova

OLİQONAFTOXİNONUN $ErBa_2Cu_3O_{7-8}$ KERAMİKASININ BƏZİ İFRATKEÇİRİCİ XASSƏLƏRİNƏ TƏSİRİ

Rentgenoqrafik tədqiqatlar və maqnit qavrayıcılığının ölçülməsi vasitəsiylə göstərilmişdir ki, $ErBa_2Cu_3O_{7-8}$ keramikasının oliqonaftoxinon ərintisində emalı ifratkeçirici keçidin böhranı temperaturunu 1.5K yüksəlməsinə və böhran cərəyanının 30% artmasına gətirir.

Ю. А. Видади, Ф. В. Алиева, М.А. Низаметдинова

ВЛИЯНИЕ ОЛИГОНАФТОХИНОНА НА НЕКОТОРЫЕ СВЕРХПРОВОДЯЩИЕ СВОЙСТВА ЭРБИЕВОЙ $ErBa_2Cu_3O_{7-8}$ КЕРАМИКИ

Получены сверхпроводящие керамики $ErBa_2Cu_3O_{7-8}$ с использованием окислов Er_2O_3, CuO, BaO. Рентгенографическим исследованием и измерением магнитной восприимчивости установлено, что образцы содержат 85% сверхпроводящей фазы с температурой сверхпроводящего перехода 92К. Показано, что обработка эрбиевых керамик в олигонафтохинонном расплаве приводит к увеличению критической температуры сверхпроводящего перехода на 1.5К и критического тока на 30%.

Received: 16.02.06

THE INFLUENCE OF THE RADIATION BY ELECTRONS ON ELECTROPHYSICAL AND OPTICAL PROPERTIES OF THIN MONOCRYSTAL FILMS $Pb_{1-X}Mn_XTe$

Sh.M. ABBASOV, G.T. AGAVERDIYEVA, T.I. KERIMOVA
The Institute of Radiational Problem of NAS of Azerbaijan Republic

I.R. NURIYEV, R.M. SADIKHOV
Institute of Physics, Azerbaijan National Academy of Sciences
Azerbaijan, Baku, Az-1143, H. Javid pr., 33

In the given paper the influence of electron radiation on electrophysical and optical properties of $Pb_{1-x}Mn_xTe$ (x=0.04) epitaxial films, obtained by condensation method of molecular beams on BaF_2 substrates (III).

It is established, that the samples become more photo-sensitive after radiation.

These materials present the big scientific interest and attract the investigators' attention because of the wide use of narrow-band semiconductors $A^{IV}B^{VI}$ in optoelectronic devices. They are used at the production of different devices of infrared technique [1]. The set of the methods for the obtaining of homogeneous epitaxial films of perfect structure of these materials with given thickness, composition and concentration of charge carrier has been treated [2].

The insignificant quantity of refs, dedicated to obtaining, investigation and application of epitaxial films $PbS_{1-x}Se_x$ $PbSe_{1-x}Te_x$ takes place. However, we don't have the works, which are dedicated to the influence of the radiation by electrons on electro-physic properties of thin films $Pb_{1-x}Mn_xTe$.

The crystal structure and physical properties of the films mainly are defined by substrate's parameters. It is desirable the maximal coincidence of lattice parameters, coefficients of thermal expansion of substrate and evaporated film. The use of monocrystal planes of the given compounds or solid solutions in the capacity of substrates allow to achieve the total coincidence of all parameters. From the other side, the epitaxial films and structures obtained on isolated dielectric substrates present big practical interest.

In the given paper the growth peculiarities of epitaxial films $Pb_{1-x}Mn_xTe$ (x=0.04), grown on new-chipped border of BaF_2 (111) and on polished planes (100) by method of condensation of molecular beams, are considered. The choice of BaF_2 in the capacity of the substrate is caused by the fact, that it has cubic structure of CaF_2 type with parameter of elementary cell 6,·19Å, it is gauzy in spectral range 3÷12 mcm, it is dielectric and has well mechanic density and chemically inert.

The epitaxial films $Pb_{1-x}Mn_xTe$ on BaF_2 substrates, obtained by the method of molecular-beam epitaxy [3,4] are also investigated. The film width was near 0.5÷1mcm.

The measurements were treated on the structures, created by two silver contacts, obtained by the evaporation in vacuum. The width of actuation length was 0.5-1.5cm at the gap value from 16 till 64 mcm. The variable air-gap and ohmic structure conductivities can be measured on the standard scheme.

The epitaxial films are grown by the methods of condensation of molecular beams in the vacuum 10^4 Pa. The source of molecular beams were alloys $Pb_{1-x}Mn_xTe$ (x=0,04), before synthesized by corresponding chemical composition.

The additional compensating source of the steams Te in growth process was used with the aim of the obtaining of the films with more perfect structure and needed values of electro-physic parameters. The investigations show, that epitaxial growth takes place at substrate temperature T_n=473÷523K. The films with more perfect structure ($W_{1/2}$=90÷100), width 0,5÷1 mcm are obtained at the condensation velocities 8÷9Å/sec and T_n=613÷653 K.

The initial samples were obtained at the room temperature on linear accelerator of electrons ELA-6 (E=5MeV, $d\Phi/dt$~10^{12}cm^2·sec^{-1}, $\Phi \le 7\cdot10^{17}$cm^{-2}). The temperature dependencies of specific resistance of each sample ρ were measured before and after radiation (fig.1).

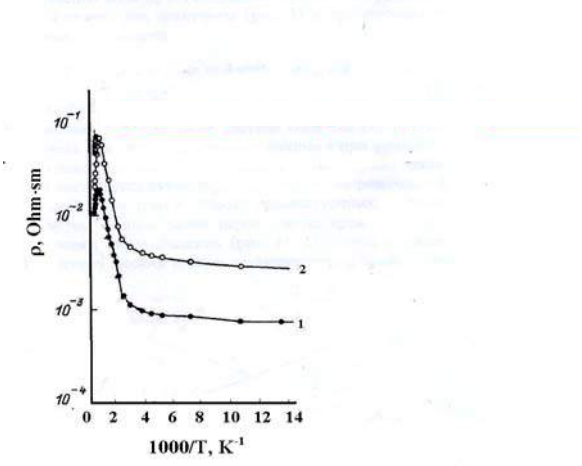

Fig.1. The temperature dependences of specific resistance, radiated by electrons ($\Phi=5\cdot10^{17}$cm^2),
1 - the sample before radiation;
2 – the sample after radiation.

It is established, that all investigated samples have firstly slow decrease, and after slow increase of specific resistance ρ at temperature 77K at radiation by electrons. Moreover, the more significant changes are character for the samples with lowest initial electron concentration.

The character of the dependencies ρ *(1/T)* of samples with high initial concentration of electrons after radiation doesn't change. The activative region, connected with own ionization of charge carrier appears in temperature region, which are close to the room one.

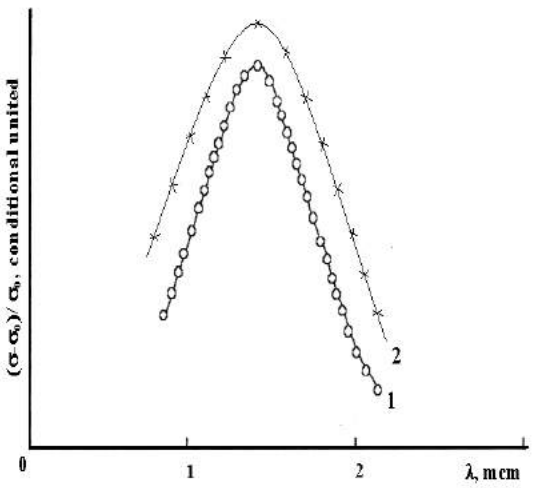

Fig.2. The spectrum of photoconductivity of films $Pb_{1-x}Mn_xTe$ (x=0,04) (x=0,04), fixed at temperature 77K
1 – the sample before radiation;
2 – the sample after radiation.

At the same time the experimental data, obtained [5,6] at the investigation of crystals of *p*-type don't allow to predict with accuracy the change character of melts' parameters of *n*-type at the radiation: in the dependence on the ratio of generation velocities of defects of donor and acceptor character, the radiation of crystals of *n*-type can lead as to the conversion of *p*-*n*-type ($dN_d/d\Phi<dN_a/d\Phi$) , so to the increase of electron concentration in conduction band till the stabilization of Fermi level on energetic level of defects of donor type ($dN_d/d\Phi>dN_a/d\Phi$). Besides, the question about energetic position of radiation level of donor type and character of reconstruction of energetic spectrum of radiated melts at the variation of the content of tin in the melts isn't clear.

That's why the investigation of deep radiation by electrons on electrophysic properties of unalloyed monocrystals $Pb_{1-x}Mn_xTe$ (x=0,04) with the aim of the definition of parameters of energetic spectrum of charge carriers for these materials, clearness of the change character of their properties and in particular, the possibility of the achievement of limit material characteristics in the result of the radiation was the common task of the given paper.

On the base of the treated mode the high-ohmic epitaxial films $Pb_{1-x}Mn_xTe$ of *n*- and *p*-type conductivity with *n*, ρ(77K)=$4\cdot10^{15}\div1.5\cdot10^{16}$cm^3 concentration and mobility of charge carriers μ (77K)=$2.5\div3\cdot10^4$cm^2/V·sec have been obtained. The films with different types of conductivity were obtained by the temperature change of main $Pb_{1-x}Mn_xTe$ and compensating source Te. It is established, that at the above mentioned conditions the epitaxial films are photosensitive at the temperature of liquid nitrogen (77K) (fig.2).

As it is seen from the picture the maximum of spectrum of photoconductivity of $Pb_{1-x}Mn_xTe$ films (x=0,04) is shifted to the side of more short waves in the comparison of the similar spectrums for other compositions of given solid solutions ($0\le x\le0,04$) given in the ref [7], that is explained by the increase of the width of prohibited band with increase of manganese quantity in investigated samples. From the fig.2 it is seen, that the samples were become more sensitive after the radiation.

[1] *F.F. Sizov*. Foreign electronic technique, 24, 1977, 14. (In Russian).

[2] *A.V. Matveenko, Yu.V. Medvedev, N.N. Bergenko*. Foreign electronic technique, 11, 1982, 54. (In Russian).

[3] *Z.F. Vasilyev, A.E.Klimov, N.I.Petikov, V.NShumsky*. Inorganic materials, 37, 2001, 123. (In Russian).

[4] *I.R. Nuriyev, S.S. Farzaliyev, A.M. Nazarov*. Izvetiya AN Azerb.Res., V.XXII, N 2, 2002, p.43-45. (In Russian).

[5] *E.P. Skipetrov, A.N. Nekraso*. FTP, v.31, N3, 1997, p.264-267. (In Russian).

[6] *Sh.M.Abbasov*. Effect of irradiation on electrophysical, optic and photoelectricproperties of solid solutions germanium-silicon. "Elm",Baku 2003. 208p. (In Russian).

[7] *I.R. Nuriyev, S.S. Farzaliyev, R.M. Sadikhov*. XVII International Scientific-technical conference on photoelectronics and PNV. ORION. Moscow 2002, p.42. (In Russian).

Ş.M. Abbasov, H.R. Nuriyev, G.T. Ağaverdiyeva, R.M. Sadıqov, T.İ. Kərimova

Pb_{1-x} Mn_x Te ƏSASLI NAZİK TƏBƏQƏNİN ELEKTROFİZİKİ VƏ OPTİK XASSƏLƏRİNƏ ELEKTRON ŞÜALARININ TƏSİRİ

Bu işdə molekulyar kondensasiya üsulu ilə BaF_2 altlıq üzərində alınmış Pb_{1-x} Mn_x Te (x= 0,04) nazik təbəqələrinin elektrofiziki və optik xassələrinə elektron şualanmasının təsiri tədqiq edilmişdir. Müəyyən olunmuşdur ki, şualanmadan sonra nümunələrin optik həssaslığı artır.

Ш.М. Аббасов, И.Р. Нуриев, Г.Т. Агавердиева, Р.М. Садыхов, Т.И. Керимова

ВЛИЯНИЕ ОБЛУЧЕНИЯ ЭЛЕКТРОНАМИ НА ЭЛЕКТРОФИЗИЧЕСКИЕ И ОПТИЧЕСКИЕ СВОЙСТВА ТОНКИХ МОНОКРИСТАЛЛИЧЕСКИХ ПЛЕНОК Pb_{1-x} Mn_xTe

В настоящей работе исследовано влияние облучения электронами на электрофизические и оптические свойства эпитиаксиалных пленок Pb_{1-x} Mn_x Te (x= 0,04) полученных методом конденсации молекулярных пучков на подложках BaF_2 (ÛÛÛ).

Установлено, что после облучения образцы становятся более фоточувствительными.

Received: 16.05.06

VALIDITY AND SAFETY OF BANK OF STATISTICAL DATA OF THE PASSIVE PHYSICAL EXPERIMENT

A. Z. MURADALIYEV, Y. Z. FARZALIYEV
ASRI of Power and Power Design,
Baku, Zardabi ave., 94

The methods of protection retrospective given are considered about reliability and efficiency Power Station Blocks as from full or partial destruction database, so and undeliberate mistake. In base of the system of the checking are found methods, using surplus information, logical methods, recommended matrix method

One of the basic directions to increase of efficiency of the automated information systems analysis and control of reliability of the equipment and devices of electro power systems is the increase of validity of the retrospective data. The information support of the personnel at the decision of operational tasks connected to a problem of reliability of the equipment should be objective. The infringement of objectivity of results of the analysis and control of reliability occurs as a result of complete or partial destruction of a database, and as a result of inadvertent mistakes.

In [1] was shown that the complete or partial destruction of a database occurs in case of submission of inadvertent, casual teams from the keyboard, fluctuation of a voltage in a network and failures in the COMPUTER. The prevention of destruction of a database, maintenance of its safety is achieved by creation of the duplicate of objects of a database with the closed access, automatic control of their integrity and restoration at failure. The special procedures of systematic updating of the duplicate objects of a database are developed. It is necessary to consider inadvertent mistakes at input of the information in a database not only possible, but also inevitable. The visual monitoring system of reliability at all efficiency is not capable to prevent all inadvertent mistakes and furthermore to protect a database deliberate distortions.

The description of technical methods of protection retrospective data on reliability and efficiency Power Station Blocks from possible mistakes is resulted below.

The data include: monthly importance of manufacture of the electric power (W), specific charge of fuel (b), charge of the electric power in system of own needs (W_{sc}), date both time of a beginning and end of non-working condition, kind of switching-off, type of a condition, type of the damage equipment, type of unit of the damage equipment, character of damage [2].

Let's remind, that as against system methods of the protection which is carried out within the framework of accepted DBASE (in our case, accepted, PARADOX), the technical methods should be developed and to be based on the account of interrelation of the separate data.

1. Control of mistakes at entering given about the basic productively parameters of power blocks.

The protection of these data is carried out by a method of input of the superfluous information, what the data on the basic production parameters Power Blocks are. It is obvious, that these parameters can be calculated on production parameters Power Blocks. Just in this sense it is considered superfluous. After input of this block of the data the automated monitoring system and elimination of mistakes carries out:

- the control of reliability of the data about manufacture of the electric power by a method of the control sums under the formula:

$$\left| 1 - \sum_{i=1}^{n} W_I \Big/ W_\Sigma \right| \le 10^{-3} \qquad (1)$$

where n - number PB; W_i - manufacture of the electric power i - st PB; W - manufacture of the electric power on POWER BLOCKS as a whole.

The accounts will be carried out with accuracy 0,1%, practically sufficient for the subsequent analysis of these data. If a condition is carried out, the control is transferred to the subsequent stage of the control. Otherwise system requests about an opportunity of correction of the statistical data. The user, by checking up conformity entered statistical given and data in the initial document, can correct a mistake.

If by the reason of input was the mistake in the initial document and the time for the analysis of these data is necessary for the User, he presses the appropriate key, the attribute of unauthenticated of the data is entered and the control is transferred to data input about non-working condition, having a place, power block;

- the control of reliability of the data about the specific charge of fuel and charge of the electric power in system of own needs will be carried out accordingly under the formulas:

$$\left| b_\Sigma - \sum_{i=1}^{n} b_i W_i \Big/ W_\Sigma \right| \le 0{,}5 \qquad (2)$$

$$\left| 1 - \sum_{i=1}^{n} W_{CH,i} \Big/ W_{CH,\Sigma} \right| \le 10^{-3} \qquad (3)$$

where b_i - specific charge of fuel i - in PB; b - specific charge of fuel on Power Station Blocks; W_{sc}, i - charge of the electric power in system of own needs i- in PB; W_{SCi}, - charge of the electric power of system of own needs Power Station Blocks

The algorithm of the control and elimination of mistakes of the data about bi and W_{SCI}, i with i = 1, n is similar to the considered above algorithm for W_i with i =1,n.

2. Control of reliability at data input about date both time of a beginning and end of a condition and its duration.

The algorithm includes consecutive input and control of reliability: dates (day, month, year) beginning j- st of a

condition *i*- st PB - $T_{i,j}^{H}$; dates of the end j- st of a condition *i*- in PB - $T_{i,j}^{K}$; time (hour, mines.) beginning *j*- st of a condition *i*- in PB - $t_{i,j}^{H}$; time (hour, mines.) end *j*- st of a condition *i*- st PB - $t_{i,j}^{K}$; duration *j*- st of a condition *i*- st PB - $\tau_{i,j}$.

The control of reliability of a beginning of a condition will be carried out by logic methods by a way:

– comparison to the moment of the end previous (m_i) of a condition *i*- st PB – ($T_{i,j-1}^{K}$). It is obvious, that $T_{i,j-1}^{K} \le T_{i,j}^{H}$. A case, when the data about are absent however $T_{i,j-1}^{K}$ is possible. For example, PB in one of the previous periods was deduced in emergency repair (in a reserve, or in scheduled repair), which was completed in current (in one of subsequent) accounting periods. On this marked comparison the check of presence of date precedes $T_{i,j-1}^{K}$. If the items of information about $T_{i,j-1}^{K}$ for any reason are absent, the User is notified on it and the opportunity of entering is requested $T_{i,j-1}^{K}$. If the answer positive (*Y*), on the screen of the monitor *j*-1 a condition *i*- st PB of the appropriate accounting period is allocated, is entered $T_{i,j-1}^{K}$ and further control is transferred to repeated input $T_{i,j}^{K}$. If PB still is in a condition of emergency repair (reserve or scheduled repair), or item of information about $T_{i,j-1}^{K}$ are absent, the User is notified on inadmissibility of data input about a technical condition it PB and opportunity of data input about the HARDWARE of the following PB. If there are items of $T_{i,j-1}^{K}$ information about, the condition is checked $T_{i,j-1}^{K} \le T_{i,j}^{H}$.

- comparison $T_{i,j}^{H}$ to dates started (T_{Π}^{H}) and end (T_{Π}^{K}) accounting period.

It is obvious, that the beginning of each of i=1,m of condition should be satisfied to conditions $T_{i,\mathrm{j}}^{H} \ge T_{\Pi}^{H}$ and $T_{i,j}^{H} \le T_{\Pi}^{K}$. It is uneasy to notice, that the entered control parities exclude an opportunity of mistakes in months and years and limit a mistake in days of a date started of a condition. Feature of the control of date of the end of a condition ($T_{i,j-1}^{K}$) is the opportunity of its absence and registration in the subsequent accounting periods.

The algorithm of the control of reliability of date of the end of a condition is reduced to the following to procedure:

- checks conformity to conditions $T_{i,j}^{K} \ge T_{i,j}^{H}$ (block 3) $T_{i,j}^{K} \ge T_{\Pi}^{H}$ and $T_{i,j}^{K} \le T_{\Pi}^{K}$.

On analogue with the control $T_{i,j}^{H}$ the entered control parities exclude an opportunity of mistakes in months and years of date and limit size of a possible mistake in days of date of the end of a condition. After input of time of a beginning of a condition the automatic control checks:

- $t_{час,i,j}^{H} \le 23$ not excess of number of hours (block 2);

- $t_{мин.i,j}^{H} \le 59$ not excess of number of minutes (block 3);

- $t_{i,j-1}^{K} \le t_{i,j}^{H}$ not excess of time of the end of a previous condition, where $t_{i,j}^{H} = t_{час,i,j}^{H} \cdot 60 + t_{мин.i,j}^{H}$ provided that $T_{i,j-1}^{K} = T_{i,j}^{H}$.

The control of reliability of time of the end a condition practically is similar to the control $t_{i,j}^{н}$, with that difference, that this information at the uncompleted condition will be absent. The control thus is transferred to the block of the control of presence of the data $T_{i,j}^{K}$. If the data about $T_{i,j}^{K}$ are absent, the User is warned about inadmissibility of data input $t_{i,j}^{H}$, the data are automatically erased also control is transferred on a route to the block of data input about a kind of switching-off.

As was perfectly above, the entered control parities allow definitely to prevent mistakes of data, input and as a matter of fact concern to a method using “internal reserves” of the data. The possible mistakes of the data describing year and month of occurrence and the termination of condition and partially - of the item of information on day and hour of month of year are completely eliminated. To ensure reliable protection of these data, the superfluous information on duration of a condition (in hours) is entered. A condition of the control is not the excess of unit of a difference of the duration, entered into a computer memory, of a condition $\tau_{i,j}$ and settlement size $\tau_{i,j}^{0}$. The size $\tau_{i,j}^{0}$ is calculated as a difference of the calendar moments of time of the end and beginning of a condition. And if this condition is not carried out, the management is transferred to algorithm of liquidation of a mistake, the principle of which action was considered earlier.

3. Experience of application of the automated monitoring system of reliability.

The monitoring system of reliability of the initial data was test on a database, which earlier repeatedly was used at the decision of many operational tasks [2]. As was marked [1], the mistakes of the data came to light and during the analysis of reliability power blocks. Thus, not only the concrete mistakes were corrected, but all statistical material was analyzed.

The opportunity of reception of erroneous results of the analysis required the labor-consuming visual control of reliability of the data, and the experience of work has learned more skeptically concerns to the first accounts and to the recommendations, following from these accounts. Therefore, the application of the monitoring system of the data has not revealed serious mistakes. However number of discrepancies was found out. They were caused, as by mistakes in primary carriers of the information, and at input of the information in the COMPUTER. Is noticed, that the mistakes most frequently arise in numbers containing many of marks (“manufacture of the electric power”, date started and end of

condition, charge of the electric power in system of own needs). The application of qualifiers of the textual information has allowed essentially to lower probability of mistakes, which were shown now in an inadvertent choice of adjacent codes. Not less probable the mistakes in carriers of the initial data improved have refused at the visual control or arisen at formalization and entering of the data in the special tables.

At entering the initial data and automated control of their reliability the deliberate attempts were automatically warned to deform the information, and the registration of admitted mistakes has allowed to open the basic reasons of their occurrence and to accept the appropriate measures. Essential result has appeared also protection of integrity of a database [1], which earlier repeatedly was broke and required significant efforts for the restoration.

Conclusions:

1. The system of automatic protection of the information, entered in THE COMPUTER, about reliability and efficiency Power Station Blocks is developed. In a basis of the monitoring system there are methods using the superfluous information, logic methods recommended matrix method. The matrixes of interrelation of versions of attributes essentially simplify algorithm of the control of occurrence of possible mistakes.

2. The practical approbation of the automated system of protection of integrity, safety and faultlessness of a database testifies to its high efficiency.

[1] *E.M. Farhadzadeh, A.Z. Muradaliyev, Y.Z. Farzaliyev* A problem of safety of a databank about reliability of Power Station Blocks. A problem of power, ¹ 1, 2006.

[2] *E.M. Farhadzadeh, T.Kh. Safarova, A.Z. Muradaliyev, T. K. Rafiyeva, Y.Z.Farzaliyev.* The automated system of the analysis of individual reliability and efficiency Power Station Blocks. M.: electrical stations, ¹ 11, 2005.

A.Z. Muradəliyev, Y.Z. Fərzəliyev

PASSİV FİZİKİ EKSPERİMENTİN STATİSTİK VERİLƏNLƏRİ BANKININ DÜRÜSTLÜYÜ VƏ TƏHLÜKƏSİZLİYİ

DRES-in enerji bloklarının etibarlığı və səmərəliliyinin baza verilənlərinin tam və ya qismən dağılmasından, həm də verilənlərdə təsadüfi səhvlərdən mühafizə üsullarına baxılmışdır. Nəzarət sistemi əsasında əlavə informasiyadan istifadə edən üsullar, məntiqi üsullar, təklif olunan matris üsulu tapılır.

А.З. Мурадалиев, Ю.З. Фарзалиев

ДОСТОВЕРНОСТЬ И БЕЗОПАСНОСТЬ БАНКА СТАТИСТИЧЕСКИХ ДАННЫХ ПАССИВНОГО ФИЗИЧЕСКОГО ЭКСПЕРИМЕНТА

Рассмотрены методы защиты базы данных о надежности и эффективности энергоблоков ГРЭС как от полного или частичного ее разрушения, так и непреднамеренных ошибок. В основе системы контроля находятся методы, использующие избыточную информацию, логические методы, рекомендуемый матричный метод.

Received: 15.03.06

THE INFLUENCE OF SEMICONDUCTOR PROPERTIES OF THE BASE ON LUMINESCENCE DAMPING KINETICS OF NEODYMIUM LEVEL $^4F_{3/2}$ IN THE CRYSTALS $\gamma - La_2S_3$, SULPHIDE, OXO-SULPHIDE AND SULPHIDE-OXIDE GLASSES

A.A. MAMEDOV
Institute of Physics of National Azerbaijan Academy of Sciences
Baku, Az-1143 H. Javid av., 33

The influence of semiconductor properties of the base on luminescence damping kinetics $^4F_{3/2}$ the neodymium level in the crystals $\gamma - La_2S_3$, sulphide, oxisulphide and sulphide-oxide glasses has been investigated**.**

The three-valency neodymium ion is the most spread activator of solid-state laser mediums [1]. This is connected with the its following peculiarities:

1) relatively intensive bands in visible region;
2) four-level generation scheme;
3) the generation wave length (λ≈1,06 и 1,35 mcm [2])which is comfortable for many practical applications;
4) the possibility to easy enough rule by the laser radiation as on the spectrum (harmony generation on nonlinear crystals), so in time (cavity damping).

The electron configuration of thrice-free ionized neodymium atom is $4f^3$. The electron number is odd one and *J* values are half-integral ones. The position of gravity centers of Nd^{3+} levels with definite *J* is close in different matrixes the same as all other three-valency rare-earth ions have. This is connected with weak interaction of 4*f* electrons with crystal field, in the comparison with spin-orbital one, as 4*f* membrane has been died and well screened by external membranes 5*s* and 5*p*. The electron transitions between membrane therms $4f^n$ are forbidden in the absence of the disturbing field. The influence of electric field of forbidden medium is partly taken and powers of oscillators of optical transitions have the order 10^{-7}. The interaction with crystal field is revealed also in Stark structure of spectrums, consisting from narrow discrete lines, which are obliged to transitions between Stark components of different therms. The number of Stark components is defined by *J* value and local symmetry of impurity center.

The metastable level $^4F_{3/2}$ is the upper laser level of neodymium, and $^4I_{11/2}$ or $^4I_{13/2}$ is lower level. In many laser crystals the degeneration taking down on the electric field is full. The $^4I_{9/2}, ^4I_{11/2}, ^4I_{13/2}, ^4I_{15/2}$ and $^4F_{3/2}$ levels are separated on 5,6,7,8 and 2Stark components correspondingly. Each Stark component stays doubly degenerate on magnetic field, i.e. is the Cramer's doublet. The main generation transition connects the $^4F_{3/2}$ and $^4I_{11/2}$ levels. The final laser level $^4I_{11/2}$ lies on 2000 cm^{-1} higher, than the main one, that causes the four-level generation scheme and laser work at the room temperature. In many laser mediums with neodymium, the relaxation speed from absorption bands into metastable state is the big enough one, anyway not less, than 10^8 cm^{-1} [3]. The bigger relaxation speed is proved by the many-phone non-radiation transitions in the result of the electron-phonon interaction. Thus, at the excitation of neodymium, the absorption bands are caused by the transitions on the superincumbent (in the comparison with $^4F_{3/2}$) levels, the absorbed energy minus the Stokes losses makes the occupancy the metastable state. Moreover, any replenishment of excited state, the velocity of which is equal to relaxation speed of metastable state is absent, thus that coming and going processes from metastable state are significantly separated in time and aren't cover the each other. The given conditions, as a rule, are carried out in known dielectric laser crystals and glasses, activated by Nd^{3+}. The situation was another one in semiconductor single crystals $\gamma - La_{2-2x}Nd_{2x}S_3$ and sulphide glasses, investigated by us. The experimental facts are:

Firstly, the non-exponentiality is observed at the activator low concentrations in crystals $\gamma - La_{2-2x}Nd_{2x}S_3$ at the excitation by the light, the wave length of which is λ=0,53 mcm on the initial region of decomposition curves of metasdtable level $^4F_{3/2}$ of neodymium.

Secondly, the neodymium deceleration takes place at the excitation of the samples $\gamma - La_{2-2x}Nd_{2x}S_3$ by the light, the wave length of which is λ=0,53 mcm on the far stages of the decomposition of metastable level $^4F_{3/2}$ of neodymium.

Thirdly, the time evolutions of population $^4F_{3/2}$ of neodymium in $\gamma - La_2S_3$ and sulphide glasses have strongly expressed maximums.

Firstly let's discuss the first two experimental facts. The crystal lattice $\gamma - La_2S_3$ is characterized by big quantity of structural vacancies, chaotically distributed (~$10^{21}$$cm^{-3}$), that leads to the quasi-amorphous lattice structure. Nowadays, it is established, that in many amorphous semiconductors, the electron states near band edges are localized, moreover, the continuous state density N(E) can take place, i.e. all states are localized in some energy interval. However, the some energy E_c, separating the localized and non-localized states, exists. From the defect crystal structure $\gamma - La_2S_3$ the quazi-continuous distribution of traps, the density maximum of which is situated on the depth 0,1-0,2 eV from conduction band bottom, takes place. In forbidden band of single crystals $\gamma - La_2S_3$, the levels with energies 1,3 and 2,6 eV below the bottom of the conduction band are revealed [4]. These levels in [4] are designated as level I and level II correspondingly.

In single crystals $\gamma - La_2S_3$ the photoluminescence band with maximum in region 1,6-1,7 eV is observed.

The luminescence spectrum at the excitation by the light, the wave length of which is 0,53 mcm, is presented on the fig.1. The spectrum consists from the one wide band.

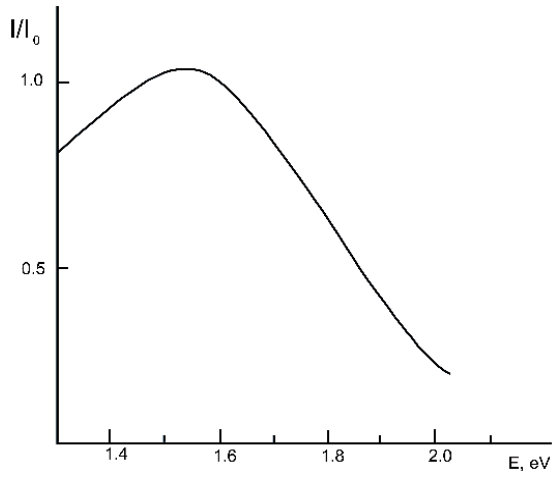

Fig.1. The luminescence spectrum of $\gamma - La_2S_3$ crystal at the excitation by the light with wave length λ=0,53 mcm (T=330K).

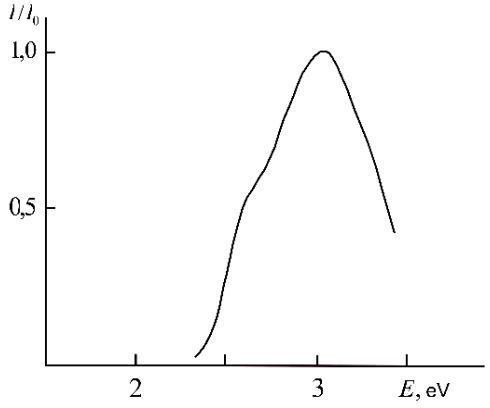

Fig.2. The luminescence excitation spectrum of $\gamma - La_2S_3$ crystal (T=300K).

The excitation spectrum of luminescence of non-doped crystal $\gamma - La_2S_3$ is given on the fig.2. It consists from wide non-elementary band, being the superposition at less of three excitation bands: the band situated in region 460-470 nm (2,6-2,7 eV), the band with maximum ~430 nm (~2,9 eV) and the band, situated in region 390-400 nm (3,1-3,2 eV), caused by the own excitation. The half-width of excitation spectrum is 0,5-0,8 eV. It is need to note, that the own luminescence $\gamma - La_2S_3$ is well excited by the light with wave length λ=0,53 mcm. Vice versa, the wideband radiation isn't observed at the crystal excitation $\gamma - La_2S_3$ by the light with wave length λ=0,6 mcm.

For the explanation of the luminescence in single crystals $\gamma - La_2S_3$ the next model is suggested. The luminescence in single crystals $\gamma - La_2S_3$ is caused by the recombination of donor-acceptor couples, differing not only by the distance between donor and acceptor, but by the energy of donor ionization. In the capacity of donor, the quasi-continuous set of traps near conduction band takes place, and the center, causing the appearance of level II with big cross-section of capture for holes is the acceptor. The luminescence excitation is carried out firstly, at the direct neglecting of electrons from valency band on level II (this transition corresponds to the energy 2,8-2,9 eV). Moreover, the luminescence excitation is carried out at the electron transition from II level into conduction band and at the followed their capture by the quazi-continuously distributed traps (transition from energies 2,6-2,7 eV). And finally, the luminescence is excited at the creation of electron-hole couples by the light from the region of own absorption $\gamma - La_2S_3$. The big half-width of spectrum is explained by the existence of quasi-continuous distribution of donors near bottom of conduction band. The damping velocity of own luminescence decreases with time – on far stages of decomposition it becomes the significantly less, than the decomposition velocity of excited state of neodymium $^4F_{3/2}$. It is character, that the own luminescence of matrix is significantly damps at the introduction of neodymium ions, moreover, the modulation of wideband matrix radiation Nd^{3+} and also the decrease of intensity of wideband radiation there, where Nd^{3+} doesn't observe, is observed. The decomposition law of excited state of neodymium at the excitation of the sample with radiation λ=0,53 mcm on far stages of decomposition is identical to damping law by own damped luminescence (fig.3). This is suggest the idea to fact, that the superposition of neodymium and matrix radiations takes place at the excitation of activated crystal by the radiation with λ=0,53 mcm in region of neodymium luminescence. However, the coincidence of the laws of damping of own luminescence and neodymium luminescence can be then, when the energy transformation from the traps to the impurity centers of neodymium takes place, if the velocity of this transformation is less, than the decomposition velocity of excited neodymium state [5]. That fact, that luminescence isn't observed, for example, in region 0,99mc, where neodymium doesn't radiate, and decomposition kinetics of excited state of neodymium, measured in region ~0,9 mcm (transition $^4F_{3/2} \rightarrow {}^4I_{9/2}$), coincides with decomposition energy, measured in region ~1,06 mcm (transition $^4F_{3/2} \rightarrow {}^4I_{9/2}$), evidences about second mechanism of decomposition retardation of excited state of neodymium at the excitation by the radiation with λ=0,53 mcm. Thus, the revealed first experimental fact is caused by the slow energy transition from the traps to neodymium ions. At the temperature increase the increase of decomposition velocity is observed, and at temperature decrease is vice versa. This is connected with fact that "retardation" of luminescence on transition $^4F_{3/2} \rightarrow {}^4I_J$ disappears with temperature increase, in the result of the increase of release rate of electrons, captured by traps.

The quantum output of luminescence from metastable state $^4F_{3/2}$ Nd^{3+} in crystal $\gamma - La_2S_3 - 0{,}9\% Nd^{3+}$, at the excitation by the light with wave length λ=0,812 mcm approaches to the unit [6], i.e. the measured life time τ_m corresponds to radiational one τ_0. Thus, the decomposition of excited state $^4F_{3/2}$ of Nd^{3+} level carries out on exponential

law and decomposition curves at the excitation of any level, situating higher, than ${}^4F_{3/2}$ of Nd^{3+} level should be direct ones. The other picture is observed. The decomposition curves of metastable state of neodymium ${}^4F_{3/2}$ are not direct ones at the excitation by the light with wave length λ=0,53 mcm (fig.3, curve a), not only in final, but in initial region.

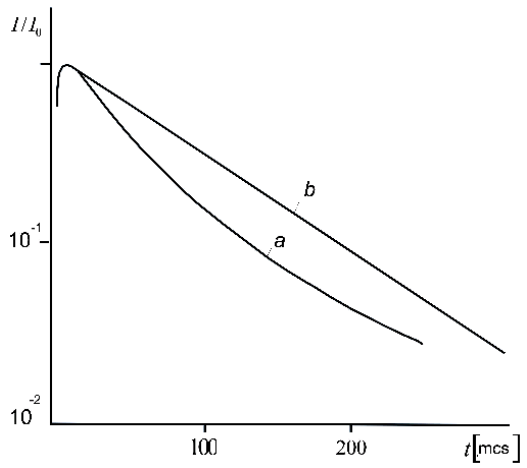

Fig.3. The decomposition curves of metastable state ${}^4F_{3/2}$ Nd^{3+} in crystal $\gamma - La_2S_3$ -0,9%Nd^{3+} at the excitation by the short impulse of the light λ=0,53 mcm (a), λ=0,6 mcm (b).

At the density increase of excited radiation (λ=0,53 mcm), the formula of decomposition curve ${}^4F_{3/2}$ of neodymium level didn't change. This evidences about the fact, that cooperative phenomena doesn't cause the observable anomaly. The exponential potential is observed at the light excitation with wave length λ=0,6 mcm, corresponding to ${}^4I_{9/2} \rightarrow {}^4G_{5/2} + {}^4G_{7/2}$ transition. The observable anomaly was explained by the following way. The Nd^{3+} ions are excited and electrons are taken from the II level to the quasi-continuous trap levels simultaneously, at crystal $\gamma - La_2S_3 - Nd^{3+}$ excitation by the light, the wave length of which is λ=0,53 mcm. In excited neodymium ions, the energy is transformed to the metastable state ${}^4F_{3/2}$. The energy, corresponding to the ${}^4F_{3/2} \rightarrow {}^4I_{13/2}$ transition (1,41 mcm or ~0,88 eV) of neodymium ions is transformed to the electrons in valency band. This energy is enough for the electron neglecting from the valency band on II level. Moreover, Nd^{3+} ions are in low excited states ${}^4I_{13/2}$. Thus, the energy transition from ${}^4F_{3/2}$ level is carried out. Because of this reason, the non-exponentiality is observed on initial stage of decomposition kinetics. The electron neglecting from the valency band on II level can only increase the life time of excited electrons in conduction band. Thus, in the difference from the wide-known dielectric matrixes, the conduction electrons interact with valency 4f-electrons in semiconductors.

Let's consider the third experimental fact. The observation of luminescence becoming flushed Nd^{3+} on ${}^4F_{3/2} \rightarrow {}^4I_J$ transitions in $\gamma - La_2S_3$ and sulphide glasses is the consequence of slow occupancy of upper laser level. In $\gamma - La_2S_3 - Nd^{3+}$ crystal and sulphide glasses at the light excitation with λ=0,53 mcm, the transition possibilities from absorption bands in metastable state were significantly less ($10^5 \div 10^6$ sec^{-1}), that in significant degree is caused by the relatively short spectrums of own oscillations of given bases. The luminescence coming flushed on ${}^4F_{3/2} \rightarrow {}^4I_J$ transitions wasn't observed in oxo-sulphide and sulphide-oxide glasses at Stokes excitation. The comparison of the spectrums of combination light scattering of $\gamma - La_2S_3$ crystal and oxo-sulphide and sulphide-oxide glass is revealed, that the more high-frequency oscillations are present in glass, than in crystal [7]. Besides, as the spectrum of combination scattering of glassy material reflects the distribution of density spectrums and its oscillation states that it is clear, that the density maximum is on the oscillation frequencies with high energy [8]. It is clear, that these obstacles in significant degree define the big velocity of non-reflecting relaxation energy from the excitation levels and its more effective accumulation on upper laser level Nd^{3+} in oxo-sulphide and sulphide-oxide glasses in the comparison with the crystal $\gamma - La_2S_3$.

[1] *A.A. Kaminskiy.* Lazernie kristalli. M., «Nauka», 1975.

[2] *A.A. Kaminskiy*. Dostidzheniya i problemi spektroskopii stimulirovannogo izlucheniya aktivirovannikh kristallov. V sbornike «Spektroskopiya kristallov» M., «Nauka», 1975, s. 92-122.

[3] *A.A. Zlenko, A.M. Proxorov, V.A. Sichugov, G.P. Shipulo.* JETF, 1970,t.59, s.785-793.

[4] *A.N. Georgobiani, M.V. Glushkov, A.A. Kamarzin, E.S. Logozinskaya, Yu.N. Malovitskiy, J.A. Puxliy, V.V. Sokolov, I.M. Tiginyanu, İ.A. Sherbakov.* Kvantovaya elektronika 9, №7,(1982), 1515-1517.

[5] *A.G.Avanesov, B.I.Denker, V.V.Osiko, V.G. Ostroumov, V.P. Sakun, V.A. Smirnov, I.A. Sherbakov.* Kvantovaya elektronika 9, №4,(1982), 681-688.

[6] *A.A. Mamedov.* Avtoreferat kand. Diss.-Moskva, IOFAN SSSR 1984.

[7] *A.A. Kamarzin, A.A. Mamedov, V.A. Smirnov, A.A. Sobol, V.V. Sokolov, I.A. Sherbakov.* Kvantovaya elektronika 10, №8,(1983), 1560-1564.

[8] *K. Shuker, R. Gammon.* Phys. Rew. Lett.(1970), v.25, Num.4, 222-225.

A.A. MAMEDOV

A. Ə. Məmmədov

$\gamma - La_2S_3$ KRİSTALLARINDA SULFİD, OKSOSULFİD VƏ SULFİDOOKSİD ŞÜŞƏLƏRİNDƏ MATERİALIN YARIMKEÇİRİCİ XASSƏLƏRİNİN NEODİMİN $^4F_{3/2}$ SƏVİYYƏSİNDƏN LYUMİNESSENSİYANIN SÖNMƏ KİNETİKASINA TƏSİRİ

$\gamma - La_2S_3$ kristallarında, sulfid, oksosulfid və sulfidooksid şüşələrində materialın yarımkeçirici xassələrinin neodimin $^4F_{3/2}$ səviyyəsindən lyuminessensiyanın sönmə kinetikasına təsiri tədqiq edilmişdir.

А.А.Мамедов

ВЛИЯНИЕ ПОЛУПРОВОДНИКОВЫХ СВОЙСТВ ОСНОВЫ НА КИНЕТИКУ ЗАТУХАНИЯ ЛЮМИНЕСЦЕНЦИИ УРОВНЯ $^4F_{3/2}$ НЕОДИМА В КРИСТАЛЛАХ $\gamma - La_2S_3$, СУЛЬФИДНЫХ, ОКСОСУЛЬФИДНЫХ И СУЛЬФИДООКСИДНЫХ СТЕКЛАХ

Исследовано влияние полупроводниковых свойств основы на кинетику затухания люминесценции уровня $^4F_{3/2}$ неодима в кристаллах $\gamma - La_2S_3$, сульфидных, оксосульфидных и сульфидооксидных стеклах.

Received: 15.01.06